University of Stavanger

FACULTY OF SCIENCE AND TECHNOLOGY

MASTER THESIS

Study program/Specialization: Marine and Offshore Technology	Spring semester, 2023 Open
Author: Aleksandr Volkov	…………………………………… (Author signature)
Supervisor: Ove Tobias Gudmestad	
Master thesis title:	Design basis for development of offshore oil and gas fields in the Sea of Okhotsk
Keywords: offshore field development, Okhotsk Sea, Sakhalin 3, Ayashskaya license area, Bautinskaya structure, concept selection, subsea production system, reservoir engineering, production profile.	Number of pages: 148 + appendices/other: 4 Stavanger, 15.06.2023 date/year

Abstract

Keywords: offshore field development, Okhotsk Sea, Sakhalin 3, Ayashskaya license area, Bautinskaya structure, concept selection, subsea production system, reservoir engineering, production profile.

Scope of work

Much attention is now being paid to the development of offshore oil and gas fields. Fields located on the continental shelf of the Sea of Okhotsk are of great value as they contain significant volumes of oil and gas. In addition to maintaining production from existing offshore fields on the Russian continental shelf, it is important to engage in the development of unexplored or poorly explored areas. The Sakhalin 1 and Sakhalin 2 projects have been in production for some time. Oil and gas production from these projects continues to this day. The Sakhalin 3 project is developing the Yuzhno-Kirinskoye gas condensate field, which was discovered in 2010. In 2017 and 2018, exploration work led to the discovery of two oil fields, Neptun and Triton, with total reserves estimated at 500 million tonnes. The Triton field was among the top 3 largest fields discovered worldwide in 2018. Today, oil and gas companies strive to develop fields in the safest, most technologically efficient, and environmentally friendly way. Therefore, the assessment of the field potential, the proposal of the field development option and the preliminary version of the production profile calculation is an important task, which can later be used as the basis for selecting the field development option when specifying the field data.

The purpose of this master's thesis is to identify a technical feasible option of developing the Triton field. In Chapter 1 a review of the different phases of an offshore field development is described. The master's thesis includes in Chapter 2 a description and analysis of the natural, climatic, and geographical conditions in which the field is located. In addition, in Chapter 3, the geology of the Triton field reservoir is described. An estimate calculation using Python

programming language of potential geological reserves are made in accordance with the data obtained seismic exploration was performed, and the first well was drilled. Based on data from neighbouring fields and relative phase permeability curves, an approximate value of the oil recovery factor that can be achieved by implementing existing technologies is hand-calculated in Chapter 4. Also, in this Chapter excel calculations were conducted to calculate and plot production profiles for V-0, V1-1, and V1-2 layers (production profiles for layers V1-2 and V-0 are provided in Appendix 2).

Next, Chapter 5, screening of existing concepts for the development of offshore fields on the shelf of Sakhalin and Norway is carried out. A comparative analysis of different field development options is done, and each concept is evaluated. A subsea production system with pipeline fluid transfer to the Moliqpaq platform with further transportation to onshore processing facility is suggested as a result of the concept’s analysis. Finally, in Appendix 4 the maximum allowable wire tension during the lifting operations of subsea template is estimated. A summary is prepared, and an extensive list of references is enclosed.

This master's thesis does not include an economic analysis due to the volatility of oil prices and the prevailing economic uncertainty. The absence of a specific investment date further hinders the ability to conduct a comprehensive economic analysis to estimate prices for oil products leading up to the investment date. The economic can be calculated once the approximate start date of the project has been established, in order to assess whether the project will be economically viable to implement.

Acknowledgements

I would like to express my sincere gratitude to the administration of the University of Stavanger and my professors for their assistance during these challenging times. Your support has been invaluable throughout my academic journey.

I am especially grateful to Professor Ove-Tobias Gudmestad for his unwavering support, knowledge, guidance, and invaluable assistance in the completion of my Master's thesis. Your expertise and mentorship have greatly contributed to the success of this work.

I would also like to extend my heartfelt appreciation to Professor Vladimir Pavlovich Balitsky for his support, belief, and assistance throughout the entire program. Your encouragement and guidance have been instrumental in shaping my academic path.

I would like to take this opportunity to express my deepest gratitude and appreciation to the late Anatoly Zolotukhin, whose untimely passing has left a profound void in our hearts. Anatoly's invaluable contributions to the joint Master's program will forever be cherished and remembered. Having been Anatoly Zolotukhin's student is a tremendous honor—one that all his students and I will forever treasure.

To my family, including my parents, sister, grandparents, and my future wife, Eline, I am deeply grateful for their unwavering support throughout this challenging journey. Your constant encouragement has been a source of strength and motivation.

Lastly, I would like to acknowledge all the dear people who have played a role in the achievement of this milestone. Your contribution and support are deeply appreciated.

Thank you all for being a part of this important chapter of my academic and personal life.

Table of Contents

List of Figures

List of tables

List of acronyms

ALA – Ayashsky license area;

AP – approval point;

CAPEX – capital expenditures;

CIDS – concrete island drilling system;

DST – drill stem test;

DG – decision gate ;

FPSO – floating, production, storage and offloading vessel;

HMS – hydrometeorological station; HC – hydrocarbons;

HSE – health, safety and environment;

HXT – horizontal x-mas tree;

LNG – liquefied natural gas;

MDT – modular dynamics tester;

MODU - mobile drilling offshore;

OGC – oil and gas bearing complexes;

OPF – onshore processing facility;

ORF – oil recovery factor;

PI – productivity index;

POS – probability of success;

R&D – research and development;

RF – recovery factor;

SPE – society of Petroleum Engineers;

SPS – subsea production system;

SPO – single point outlet;

STOIIP – Stock Tank Oil Initially In Place;

TAML – technology advancement for multi-laterals;

WS – weather station.

1. Field development project phases

According to [1] project development phases can be represented as it is shown in figure 1.

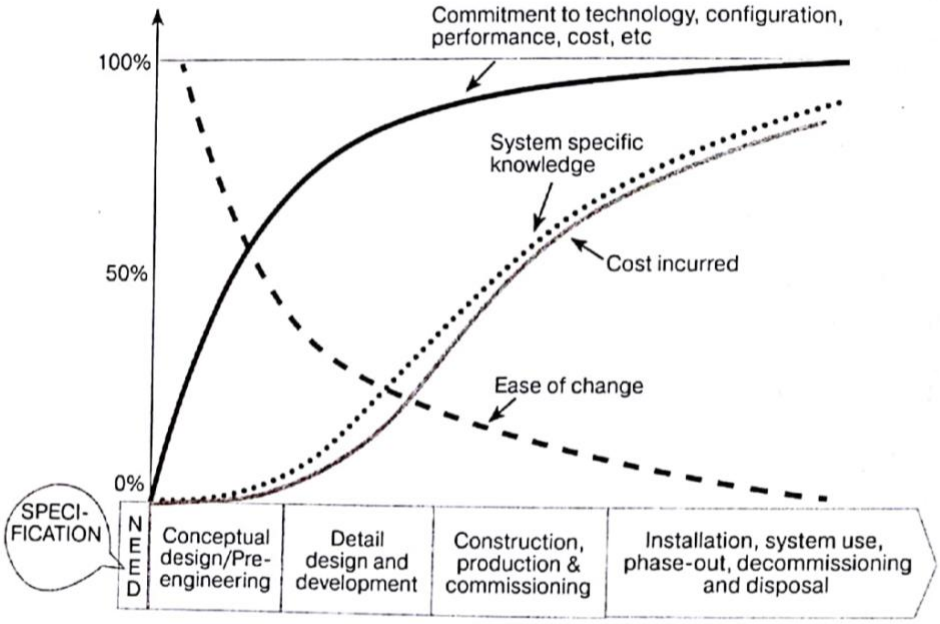

Figure 1 Project phases and commitment to costs and technical issues [1]

From figure 1 it can be observed that specifications are typically consist of:

- Conceptual design/pre-engineering;
- Detail design and development;
- Construction, production and commissioning;
- Installation, system use, phase-out, decommissioning and disposal.

This part of the work is devoted to defining the main stages of project development and phases of the project are addressed in this work are discussed. No economics has

1.1 Project development model

The development of offshore oil and gas fields is a costly process, which is associated with a lot of risks and uncertainties. Oil and gas companies strive to extract hydrocarbons technically feasible at the lowest possible cost. At the same time, it is important to maintain the quality of used techniques, technologies and equipment, personnel and the environment safety. It is equally important to properly abandon all wells and decommission equipment after field was development. All these requirements are a driver of industry development. Ultimately, this leads to an increase in the stages in the project planning of field development. Figure 2 shows the main components of the project development model.

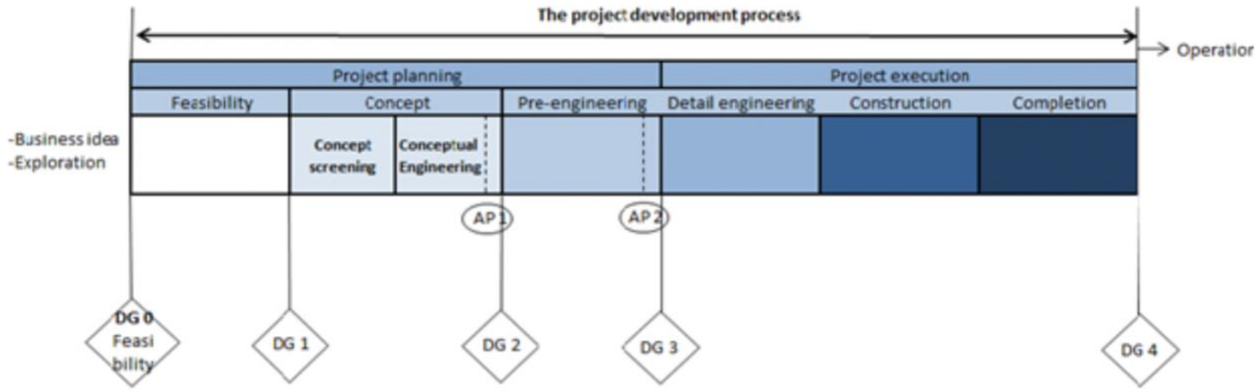

Figure 2 Project development model for the investment projects with phases and decision gates [1]

According to figure 2 there are two stages in the investment project:

1) Project planning;
2) Project execution.

Planning period leads to a decision to start project execution and the execution period leads to start-up the facility. The entire project plan is divided into decision gates (DG), during which the project is evaluated and a decision on its future fate is made. For the same purpose approval points (AP) are used.

1.2 The planning period

The planning period covers the feasibility, concept, and pre-engineering phases.

The main objective of the planning period is to examine in depth the vast majority of concepts to judge if a field can be developed that meets the requirements of cost-effectiveness, HSE and technical feasibility within certain limits of uncertainty. It is also important at this stage to make sure that all uncertainties in the technical concept are resolved. [1]

1.3 The feasibility phase

The main appointment of the feasibility phase is to establish and document whether a business opportunity discovered, or a hydrocarbon find is technically feasible to develop and has an economic potential in accordance with the corporate business plan to justify further development. The feasibility phase leads to decision gate DG 1, «Decision to start concept development»

The DG1 approval is an authorization by the Company and partners to continue developing the project through the concept phase towards DG2 in accordance with the approved plans and budgets.

When it is likely that the business concept is profitable, technically feasible and consistent with the corporate business plan, DG1 can be passed. [1]

1.4 The concept phase

The purpose of the concept phase is to provide a firm determination of the design (resource and product) basis solution and to identify all relevant and feasible technical and commercial concepts. Then evaluate and define the selected alternative (preferably one) and confirm that the profitability and feasibility of the business opportunity will meet corporate requirements and business plans. The concept development phase results in the selection of a concept for further development up to the " Provisional project sanction " decision gate (DG2). [1]

1.5 Approval point 1 “Concept selection”

The approval point «Concept selection», AP1, marks that one or limited number of concepts have been chosen for further detailing towards DG2 «Provisional project sanction».

Approval point 1 shall be the result of a screening process all concepts under consideration that have been elaborated and found and identified as potential for the development of a business opportunity. The concept selection should be based on documentation that establishes the criteria for concept definition with emphasis on:

1) Design basis;
2) Concept alternatives and variants;
3) Screening parameters and weighting;
4) Description of and justification for both the selected concept and the rejected option;
5) Technology qualification program. [1]

1.6 Decision gate 2 “Provisional project sanction”

Approval of the provisional project sanction is an authorization by company and the partners to continue developing the project through the pre-engineering phase towards decision gate 3 - «Project sanction» in accordance with the approved project plans and budgets. The approval includes a decision to develop the necessary applications to the authorities.

DG2 may be passed at the moment when it is documented that the business concept is economically viable, technically feasible, and met the company's business requirements.

The provisional project sanction – DG2 documentation shall include an assessment of the availability of qualified human resources and capacity in the relevant supplier industry. [1]

1.7 Pre-engineering phase

The purpose of the pre-engineering phase is to further develop and document the business opportunity based on the selected concept to such a level that a final project sanction can be made, application to authorities can be sent and contracts can be entered into. The pre-engineering phase leads to approval point 2 (AP2), «Application to the authorities», and to decision gate 3 (DG3) «Project sanction». [1]

1.8 Approval point 2 “Application to the authorities”

The project shall compile and prepare for submittal of the necessary application for approval of the facility development in accordance with the relevant laws and regulations. It is particularly important to have undertaken an analysis to determine which requirements apply. [1]

1.9 Decision gate 3 “Project sanction”

The DG3 approval is an authorization by company and the partners to continue developing the project through the execution period in accordance with the approved project plans and budgets. When business concept has been developed to a level where it has been documented that it meets the established requirements with regard to profitability, HSE, technical definition, cost estimate accuracy and project execution uncertainty, the DG3 may be passed. [1]

Chapter summary

The result of studying the main stages of offshore field design shows that this Master thesis refers to the phase of project planning and includes a screening of existing concepts of field development, determining the required number of production and injection wells, the rate of wells drilling, as well as a technical study.

2. Climatic conditions of the region, the soil characteristics of the seabed and sea parameters during the installation process.

2.1 The area climate

The field is located within the Ayashsky license area (ALA) near the northeastern coast of Sakhalin Island. The settlement of Nogliki is the closest to the field, so we will rely on climatic data accumulated for this settlement (is shown in figure 2). The Ayashsky license area is part of the Sakhalin-3 project and is located near the Sakhalin-1 and Sakhalin-2 fields. The field was discovered by drilling and testing an appraisal well. The field is located offshore the north-eastern part of Sakhalin Island, 55 km from the coastline and 500 km from Yuzhno-Sakhalinsk. Neighboring blocks are Veninsky, Kirinsky, and Vostochno-Odoptinsky.

Figure 2 Map of the seven officially recognised areas of traditional indigenous settlement on the Sakhalin island [2]

The main parameters that characterize the conditions of Sakhalin Island and its current state are analyzed from freely available instrumental observation series. Sakhalin Island area is characterized by short, cool summers and cold, long winters. July is the warmest month, and January is the coldest. August is the warmest month, and January is the coldest. Usually, the first frosts in the north of the island are observed in late September and the last in early June. On the north-east coast there are about 100 days a year without frosts, the duration of the period with positive temperatures is 160-180 days. The seasonality of climate change and ice conditions allow exploration drilling from June to November. The average duration of the ice period is about 180-190 days. Table 1 contains the minimum, average, maximum, and standard deviation of the average air temperature from data collected at WS Nogliki and in figure 3 graphical representation of the data from table 1 is shown. [3]

Table 1 Thermal regime basing on monthly average data of weather station (WS) "Nogliki" for 1930–2022. [3]

Data	Air temperature, C											
	Jan	Feb	Mar	Apr	May	Jun	Jul	Aug	Sep	Oct	Nov	Dec
Min	-28,3	-24,6	-15,4	-5,7	0,4	5,1	9,4	11,6	8,4	0,5	-13,5	-23,0
Mean	-18,5	-16,2	-10,0	-1,9	3,4	9,0	13,3	14,5	10,8	3,2	-7,1	-15,5
Max	-9,8	-9,9	-4,3	1,1	8,5	14,3	19,4	17,7	13,0	6,1	-2,2	-8,4
StdD	3,4	2,6	2,3	1,4	1,5	1,7	1,8	1,5	1,0	1,3	2,2	2,8

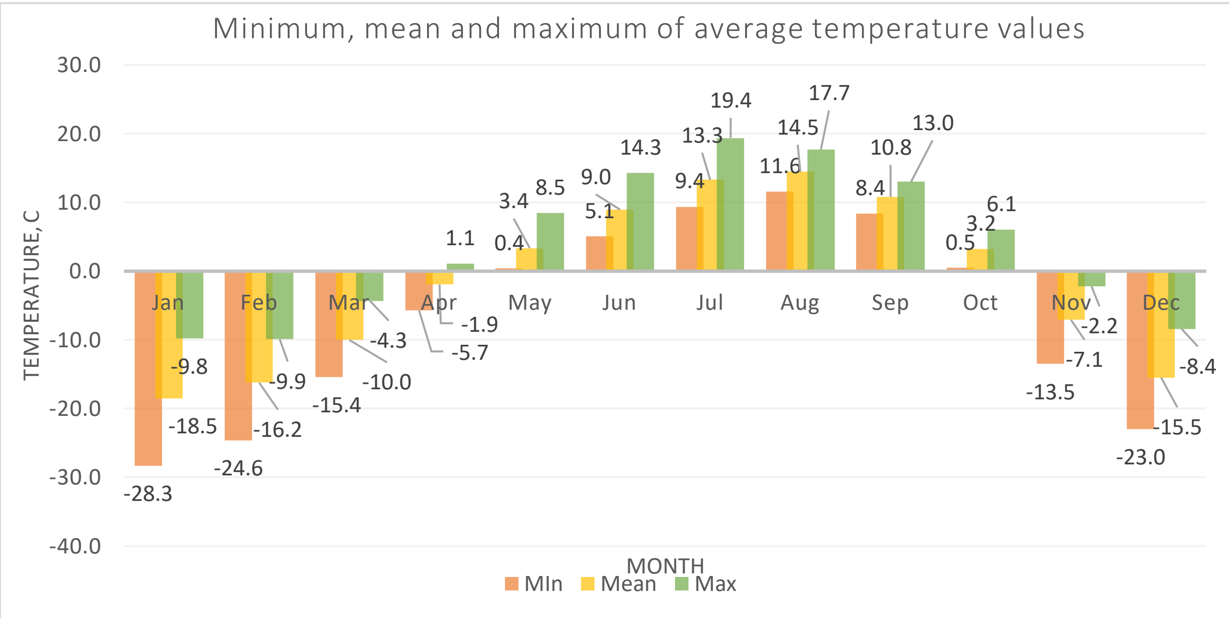

Figure 3 Mean, minimum and maximum average monthly temperature for period 1930 – 2023. [3]

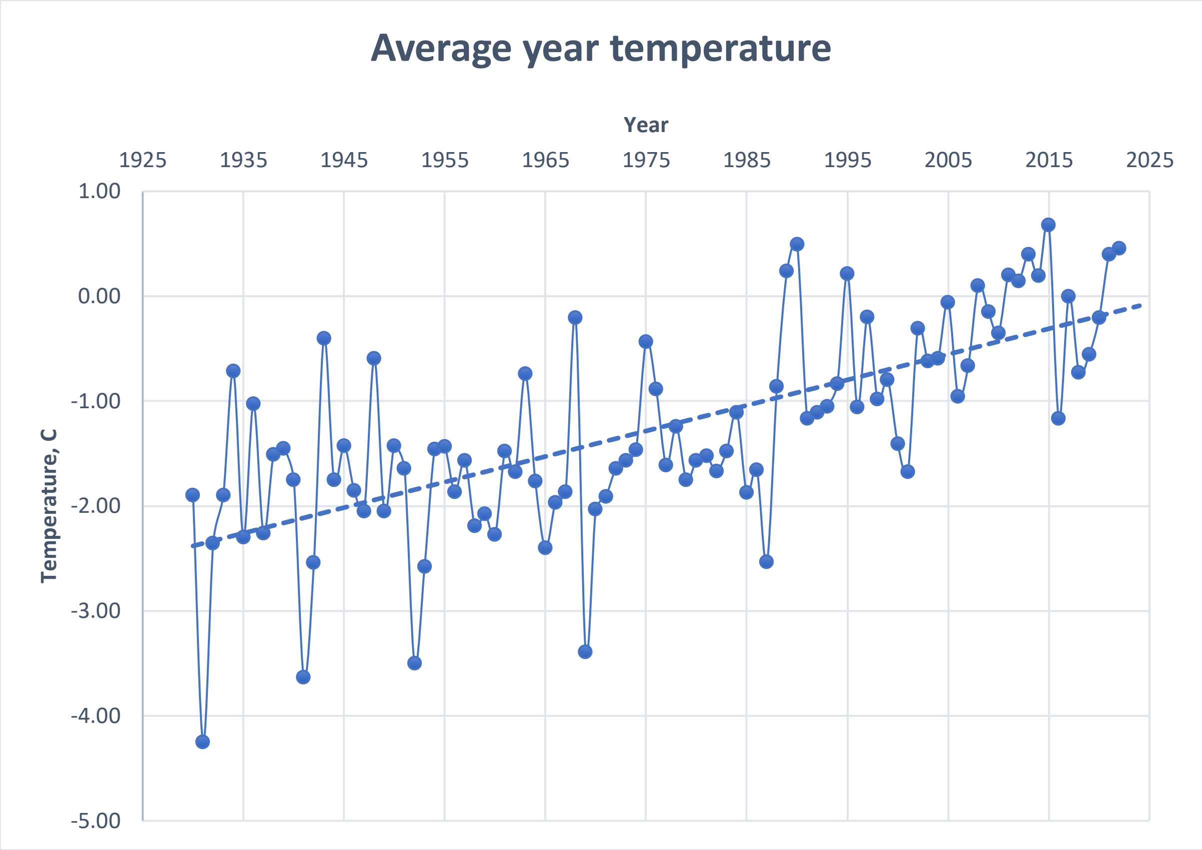

Figure 4 Average year temperature from year 1930 to 2022 (dotted line – linear trend). [3]

The average annual air temperature in the area varies from -3 to +6 °C (is shown in figure 4). From the chart it can be concluded that there is an increasing trend in the average year temperature increasing. [3]

2.2 Precipitation

There is a division of the seasons into two groups: a warm period (from April to October) and a cold period (from November to March). [4] Precipitation in winter is quite frequent: in January there are 10 to 25 days with precipitation, but their intensity is low. In some winters there may be heavy precipitation, however. Winter on Sakhalin is characterized by a long and stable snow cover. Snow cover reaches its maximum height in March, averaging 500 mm to 700 mm. During the warm period, the amount of precipitation can reach 300-650 mm. The maximum amount of precipitation associated with the intensification of cyclonic activity over the ocean is observed in August-September. The total number of days with precipitation in summer, as a rule, decreases, but precipitation is characterized by great intensity. The number of days with heavy rainfall especially increases. From October, the total amount of precipitation begins to decrease. This is due to a decrease in the number of days with heavy rainfall. Figure 4 shows the dynamics of changes in the average annual precipitation. [4]

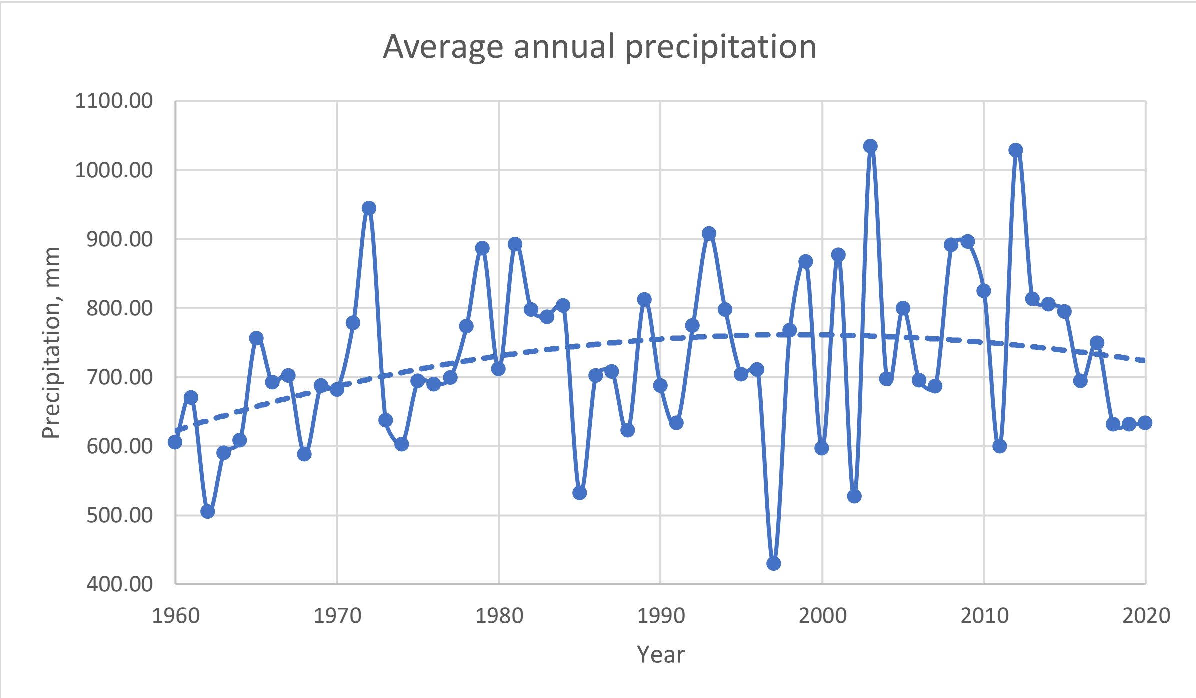

Figure 5 Average annual precipitation according by WS "Nogliki" for 1960–2020 (dotted line – polynomial trend). [4]

In certain years there have been a sharp decline in precipitation volume, and in some years, there was a rapid growth. The polynomial trend line shows the absence of an increasing or decreasing trend in annual average precipitation.

Hail and thunderstorms in the studied water area are extremely rare and short-lived. The frequency of thunderstorms, on average, is 4 days per year, while hail occurs 3 days per 10 years. The duration of these phenomena usually does not exceed 1-2 hours. [4]

2.3 Winds

Strong winds 15 m/s are the most frequent dangerous weather phenomenon on Sakhalin territory, especially in the cold half of the year. Wind intensification is influenced by the configuration of the coastline, atmospheric circulation activity, mesoscale movements in the lower atmospheric layer also make a great contribution. The repeatability of strong winds in Sakhalin reaches 20-40% in some months of the cold half of the year. Often strong winds are accompanied by low negative air temperatures (down to -15 °C and below), which makes it difficult to carry out production work outdoors and makes negative adjustments to planned activities. Strong winds are an extremely important factor determining the operation of seaports. [5] Average annual wind speed distribution based on [6] is shown in figure 6.

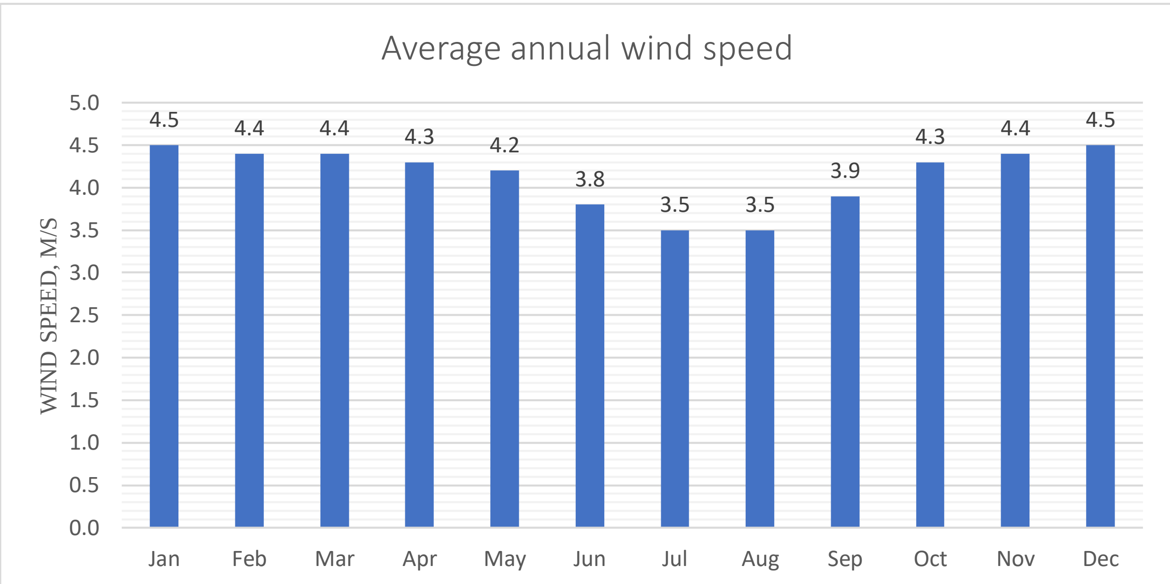

Figure 6 Average monthly and annual wind speed in m/s. [6]

On land, the average annual wind speed on the Sakhalin coast varies between 4.3-5.4 m/s. In the offshore zone, the average annual wind speeds increase by 10-20%. The highest average monthly velocities are observed in the cold season, most often in December and January, and amount to 4.2-7.1 m/s; in summer, the average monthly velocity is 3.0-4.9 m/s. Also, the territorial location of Odoptu favors storm winds up to 34-38 m/s. [6]

A characteristic feature of the wind regime in the Nogliki district is the prevalence of northwestern and western winds throughout the year. Winds of the northeastern and eastern directions are characterized by the lowest annual average repeatability. In summer, the prevailing directions are south and south-east quarter winds - 40-49% of the total number of cases. Calm sea is relatively rare throughout the year, but in summer they are more probable (about 6-9% of cases), in winter season their number is a little more than 1%. [6]

From October, when the winds change to winter mode, the prevailing winds are from the continent - north-west and west (table 2), about 77-82% in total. The distribution of winds probability by directions and speeds shows their connection with atmospheric processes. [4]

Table 2 Repeatability of wind directions. [4]

Month	N	NE	E	SE	S	SW	W	NW	Calm
Jan	5,5	2,2	1,7	0,9	2,4	6,4	51,3	29,8	0,9
Feb	9,1	4,6	1,9	1,8	1,8	3,3	43,5	34,1	1,5
Mar	13	7	8,1	8,1	5,6	4,7	29,2	24,6	5,1
Apr	13,6	10,1	13,8	17,2	9,3	6	16,6	13,7	3,9
May	10,3	10,1	15,7	23,8	10	8,8	13,2	8,3	5,5
Jun	6,4	7,9	15,9	33,2	12,9	8,6	10,8	4,5	6,1
Jul	4,7	6,8	15	34,8	12,6	10,6	11,3	4,4	7,6
Aug	6,3	6	13	25,9	12,2	12,7	15,7	8,3	8,6
Sep	8,4	6,4	9,6	18,7	13	12	19,7	12,5	5,7
Oct	9,3	4,4	4,5	7,3	8,5	13,5	34,2	18,5	4,1
Nov	5,3	3,3	2,8	2,4	6	12,4	51,7	16,3	2,8
Dec	6,9	2,9	2	1,7	2,4	5,3	53,2	25,9	1,7

2.5 Storms

An average of about 100 cyclones accompanied by strong winds, cloudiness and precipitation are observed in the Sakhalin region. Tropical cyclones (typhoons) born in the equatorial zone may be observed in late summer and early autumn. Their arrival is associated with heavy rains and destructive winds, which can reach speeds of up to 40 m/s. However, it should be noted that the vast majority of typhoons pass over the territory of the island to the south of Terpeniya Bay and do not have a significant impact on the eastern shelf of Sakhalin. [6]

2.6 Fog

The distribution of fogs is related to circulation features and a variety of physical and geographic conditions. The highest annual number of days with fog is observed on the eastern coast and varies from 70 days to 87 days in Odoptu. Sakhalin fog is formed when warm air masses move over the surface of cold currents and are carried over the island. Radiative fog occurs only in inner valleys and are observed comparatively rarely. [6]

Fog is observed mainly from April to September. During this period, fog most often forms early in the morning. The greatest number of days with fog is in June-July and amounts to 15-20 days. Most often fog is observed from May to September. [6]

Fog can last from several hours to several days in a row. Average duration of one case of fog for coastal stations in warm period of the year is about 8 hours, in cold period of the year - about 4 hours. The frequency and duration of fog during the summer months increases significantly with distance to the sea. The average duration of one case of fog for the navigation period reaches 18 hours. In winter, fog is extremely rare and short-lived. [6]

2.7 Water temperature and salinity

Horizontal distributions of water temperature and salinity in the Piltun Astokhskaya area are formed under the influence of heat and moisture fluxes across the sea surface, as well as heat and salt transport by non-periodic and tidal currents [7].

At the water depth horizons under consideration in the Piltun-Astokhskoye field, spring temperatures are uniform along the shore, and slightly increase with distance from the shore: at the 0 m horizon, from 3.5°C to 5.0°C, at the 20 m horizon, from minus 0.5°C to 1.0°C. In the deepest (50 to 100 m) eastern part of the area under consideration, the near-bottom temperature also increases in the seaward direction from minus 1.5 °C to minus 1.0 °C. In the Piltun-Astokh area, August surface temperature increases from southwest to northeast from 9.5°C to 12.5°C and reaches its maximum. [7]

2.8 Currents

A constant circular current of the Sea of Okhotsk, directed counterclockwise, is noted. The mean speed of the current along the northern coast of Sakhalin is 0.5 knots, which is equivalent to about 0.26 m/s. This current is responsible for a significant severity of climatic conditions of the work area at all times of the year. [8]

The vertical structure of currents in the study area is very homogeneous and is characterized by a smooth decrease in flow velocity from the surface to the bottom and a counterclockwise turn of the main axis of transport.

Tidal currents. Tidal currents in the field area are very dynamic. The influence of tidal currents on the overall flow pattern of the study area is significant. The speed of tidal currents is rather high here. [8].

In the coastal strip off the eastern coast of Sakhalin Island, the amplitude of the total tidal currents is rather high. The amplitude of the total tidal current is 70 cm/s. At the same time, the maximum tidal velocity in this area is 100-110 cm/s. The tidal current velocity decreases with increasing water depth. [9]

2.9 Waves

Waves in the area in question can be observed during the ice-free period. In winter, wind and swell in the Sea of Okhotsk predominantly spread from the north; in summer, they spread from the southern direction. The strongest waves are from October to March. During this period, waves can reach maximum heights of 13 m in some parts of the sea, and in coastal waters they exceed 11 m approximately once every five years. Repeatability of waves of 6 m in the central part of the sea is 2-3 % and about 1 % in other regions. The prevailing direction of waves is northward. Rather frequent are ripples, especially in the south of the sea. [10]

Wave heights of less than 2 m prevail. Waves with heights below this value occur with a probability of 85-87% as seen in figure 7. That means there is a 13-15% chance to meet waves with heights higher than 2m. Wave periods of 80-90% are less than 9 s, the most frequent periods are 3-7 s with a probability of 60-70%. The probability of waves with periods of 17 s and higher does not exceed 0.3%. In many coastal areas, the process of wave development is significantly influenced by local factors. When cyclones pass through, storm waves up to 11 m high in the south and 8-9 m high in the rest of the sea can occur. [10]

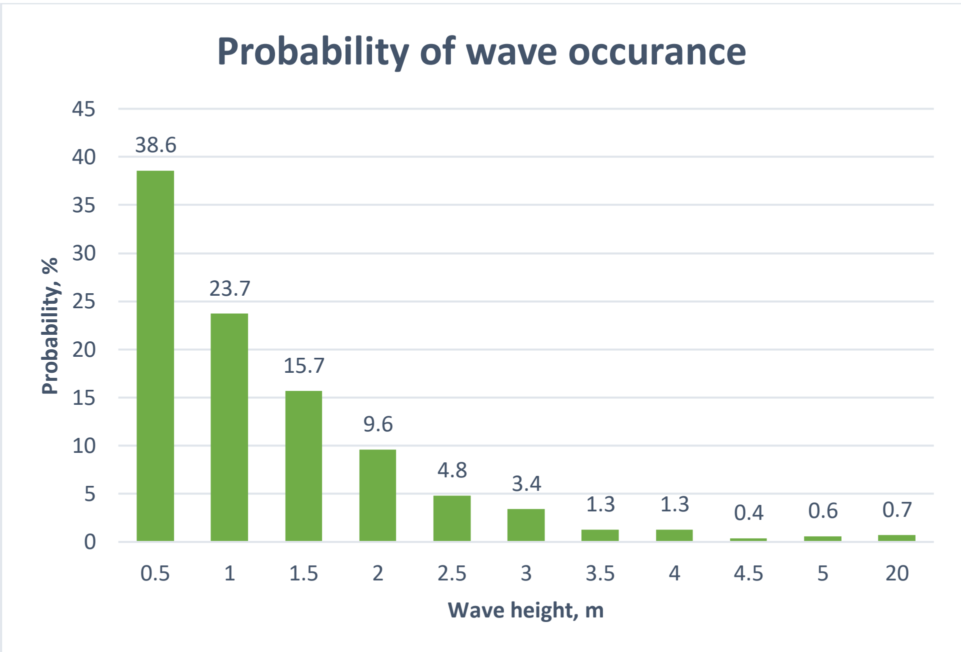

Figure 7 Wave occurrence probability for the sea of Okhotsk [11]

2.10 Tsunami

The open boundary of the Sea of Okhotsk runs along the Kuril Islands close to one of the main tsunami generation zones in the Pacific Ocean, the Kurilo-Kamchatka trench. The Kuril Islands are one of the most seismically active regions in the world, and the north-east coast of Sakhalin Island is potentially subject to tsunami waves passing through the Kuril Straits. However, most of the energy of tsunami waves generated in the ocean is absorbed by the Pacific coast of the Kuril Islands. Tsunamis passing into the Sea of Okhotsk are significantly attenuated by the time they reach the northeastern shores of Sakhalin Island. Sakhalin Island. The possibility of significant tsunamigenic small-focus earthquakes is unlikely here. [6]

The ice conditions in the study area are quite complicated. The first ice appears in the middle of November and holds until the middle of June. A land fast ice band is formed along the shore. Breaking of land fast ice usually occurs in April. Along the northern part of the eastern shore of Sakhalin Island, drifting ice forms. Drifting ice can be encountered until the last decade of June. [6]

2.11 Ice conditions

Ice formation on the shelf area of the northern coast of Sakhalin Island. Ice formation usually begins during the third decade of November with the appearance of the initial ice types. Stable appearance of the ice cover is noted in the third decade of December. Ice thicker than 0.3 m appears in January. The average duration of the ice period is 170 days. In late December, drifting gray-white and thin single-year ice of 8-10 grades (80 to 100%) fills the top of Sakhalin Bay and the North Bay, and in January, this ice is carried as a band to the shelf area of the northeast coast of Sakhalin Island. In January this ice is transported as a strip off the shelf of the northeastern coast of Sakhalin, and the prevailing northwestern winds carry it 40-50 km from the coast. The formation of local ice, represented first by gray ice and later by gray-white and thin annual ice, continues in January in the ice hole that has formed. During the period of cyclones passing over the area, the southern direction of the total ice drift changes to the northwestern and western ones, which causes the entire massif to move westward towards the coast. [12]

According to [12], in the course of the work, the characteristics of ice in the Yuzhno-Kirinskoye field were studied. Many ice objects on satellite images and on the images taken from a helicopter at a height of 200 m were preliminary identified as flat one-year ice of 70-80 cm thickness. However, on closer examination, from 10-30 m and less, it turned out that the ice blocks were structurally composed of 4-5 layers of layered one-year ice, and their total thickness exceeded 3 m. Examination of these ice fields clearly showed that their mass is at least 3-4 times greater than the mass of ice fields of similar horizontal dimensions of flat undeformed one-year ice. Such ice fields can potentially be decisive in terms of design situations, considered when designing the facilities. [12].

In March and early April, the ice situation reaches its greatest complexity. The density of drifting ice is 9-10 points. An important factor of the ice conditions in late April and early May that is the land fast ice retreats from the shore and the formation, because of this of large and extensive strongly disturbed ice fields, drifts along the shelf boundary. During the first and second ten-day periods of May in some years, the ice situation can be comparable with that of March, although the process of ice destruction and melting is under way everywhere. In the second half of May, there is a decrease in coverage to 4-5 points. In some years, drifting ice can be observed in June and even in early July. [12]

In April-May, ice in 54% of cases is 0.7-1.2 m thick, in 18% - more than 1.2 m, and in 26% - 0.3-0.7 m. The average thickness of smooth ice for a season considering the recurrence data is 0.65 m. Estimation of the maximum thickness of smooth ice according to data of the hydrometeorological station (HMS) of the northern part of the Sea of Okhotsk leads to a value of approximately 1.5 m. Ice formations with a constant thickness of more than 1.5 m in Sakhalin conditions are formed as a result of layering. [12]

Mechanical increase in ice thickness, e.g., because of ice layering, plays an important role. Ice stratification is possible if the ice is several tens of meters long. Ice formations more than 2.0 m thick can be formed from debris with a relatively flat bottom. The average seasonal thickness of ice formations is approximately 1.90 m. [6].

2.12 Icing

During the winter months, icing is the most common event, with ice also occurring in April-May. Even though the maximum frequency of ice and frost deposits occurs in winter, they are most dangerous in November-December and April-May and are associated with the occurrence of ice and wet snowfall. [13]

Icing of vessels and hydraulic structures in the work area, as well as in nearby areas of the Sea of Okhotsk, including shipping lanes, is observed during the entire cold season (November to May), with some cases of icing possible in September, October, and June. The main hydrometeorological parameters influencing icing of structures and vessels are air and water temperature, wind speed and direction, roughness (wave height and direction), and intensity of changes in weather characteristics. [13]

In the Sea of Okhotsk as a whole, the area off the eastern coast of Sakhalin belongs to the areas with the highest frequency and intensity of icing. The absolute majority of vessel icing cases were caused by sea spray, 89%. [13]

Chapter summary

Weather conditions in the Sea of Okhotsk is an important factor influencing the selection of the Triton field development option. For example, the presence of high winds, storms, tsunamis, and ice can destroy or damage oil platforms and hamper the operation of oil production vessels.

According to studies, the Sea of Okhotsk frequently experiences storms with waves up to 10 meters high and wind speeds of up to 25 m/s. This can lead to strong platform oscillations and hamper well drilling operations, installation of the subsea production elements or the operation of the offshore platform.

Ice conditions are one of the main factors influencing the choice of oil field development on the Sea of Okhotsk shelf. During the winter months, ice density in the sea reaches 9-10 points on the Landau-Obukhov scale, which makes access to the platforms very difficult.

In addition, currents and winds can have a significant impact on the spread of oil contamination in the event of an oil platform accident. For example, winds with high velocity can carry oil over long distances and currents can carry it to shorelines and coastal waters.

Thus, selecting an oil field development option offshore the Sea of Okhotsk must consider all natural and climatic conditions, including winds, storms, tsunamis, ice conditions, currents, and waves, to ensure safe oil production and minimize risks to the environment, personnel and company assets.

3. Geological formation description

3.1 Knowledge about the area

Systematic geological and geophysical studies of the Far Eastern seas began in 1957 and over the past forty years extensive geological and geophysical information on the structure of the sedimentary cover and basement, tectonics and oil and gas content of the Okhotsk region, including its water area, has been obtained. [14]

The Ayashsky license area is well studied by geophysical surveys. Comprehensive prospecting surveys, including seismic, gravity, magnetic and geochemical surveys, and detailed seismic surveys have been carried out within its boundaries. Also, 2D imaging was carried out in some areas. [14]

Two oil and gas condensate fields were discovered within the boundaries of the Ayashsky license area: Arkutun-Daginskoye and Chaivo. Large oil and gas condensate fields Odoptinskoye and Piltun-Astokhskoye as well as Veninskoye gas field were discovered in proximity. [14]

In 1977 in the vault of the northern dome of Odoptin offshore structure the first prospecting well discovered a multilayer oil-gas-condensate field with deposits in sandy reservoirs of Lower Nautovsky subhorizon, in the depth interval of 1373-2158 meters. When testing the well, the maximum oil flow rate of 308.5 m^3/day was obtained. Exploration of the Odoptinskoye field lasted from 1977 to 1983. Three prospecting and 12 exploratory wells were drilled during this period. [14]

In 1978, exploratory drilling began at the Veninskaya, Chayvinskaya and Daginskaya structures. Drilling of wells 2,500 meters deep at the Veninskaya structure resulted in discovery of a gas reservoir in the Daginskiy horizon. Drilling and testing of a well of 3978 m at the Chayvo structure resulted in the discovery of a multibed oil and gas condensate field. Well testing resulted in gas flow rate of 424,400 m^3/day, and condensate flow rate of 57.5 tonnes per day at 19mm choke. One prospecting and four exploratory wells were drilled in the period of exploration of the Chayvo field. Drilling at the Daginskaya structure resulted in the discovery of the Lower Nautical deposits, which are the main productive strata in the area, that are clayed in the vault and on the eastern flank of the structure. [14]

In 1986, exploratory drilling started on the Piltun-Astokh structure. As a result, a multilayer oil, gas, and condensate field was discovered in sediments of the Lower Nenets subhorizon. Oil flow rate was up to 472 m^3/day, gas flow rate was 370,000 m^3/day, and condensate flow rate was 67 m^3/day through a 19 mm choke. The Piltun-Astokhskoye field was explored from 1986 to 1990. Fourteen wells were drilled. [14]

In 1989, the Arkutunskaya structure located south of the Piltun-Astokhskoye field was drilled, and in 1990, the Daginskoye structure located further south. Drilling of exploration wells within the limits of the Arkutun and Daginsk structures resulted in the presence of a single large multilayer oil, gas and condensate field. Oil flow rate is up to 212.3 m^3/day, gas flow rate is up to 305.4 thousand m^3/day, and condensate flow rate is 65 m^3/day. Oil and gas deposits are confined to formations of the Lower Nautovsky subhorizon. [14]

The Ayashskaya anticlinal structure was first identified by regional seismic surveys in 1977. In 1989, the seismic work detailed the structure of the Ayashskaya anticline and identified the South Ayashskaya, West Ayashskaya, Osenginskaya and Ulvinskaya anticlinal structures of small size. In addition, the characteristics of isolated non-anticlinal traps in the lower part of the Nutovskaya Formation - Ayashskaya, Zapadno-Ayashskaya, and Severo-Veninskaya were refined. [14]

A scheme of geophysical exploration of the area by prospecting in 1989 and 1992 is shown in Figure 8. [15]

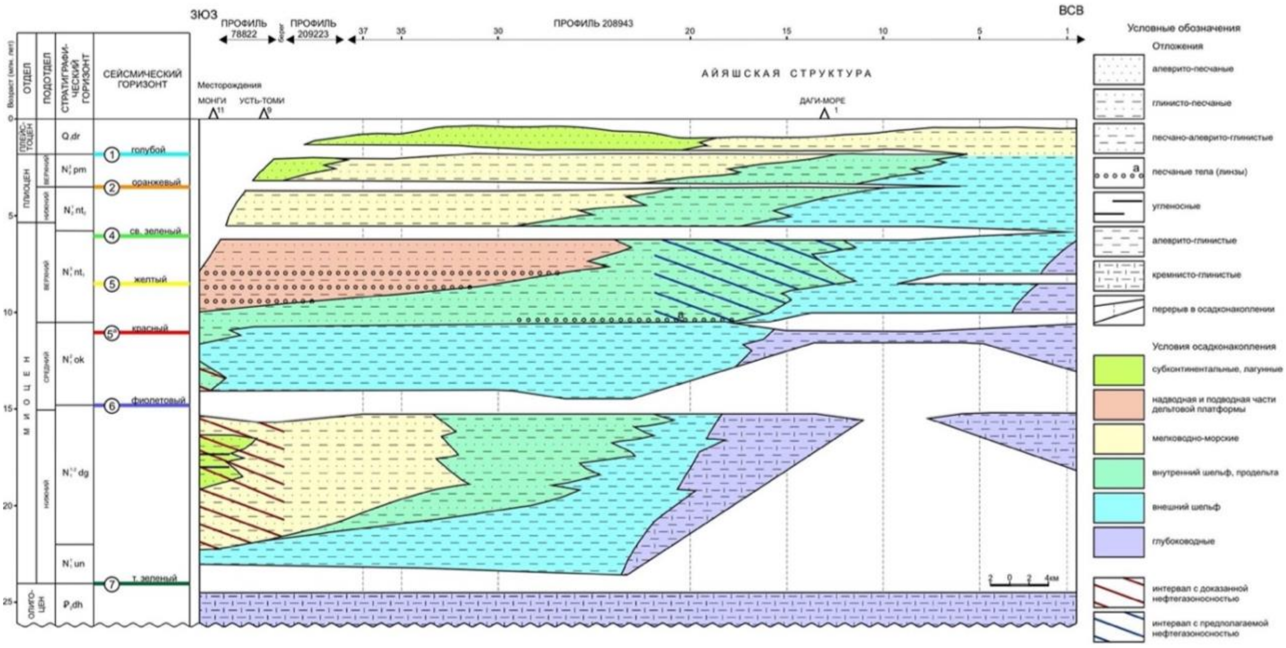

Figure 8 Chronostratigraphic scheme of the Neogene system. [15]

In 2009 the license for geological study, exploration, and production of hydrocarbons within the Ayashsky subsoil area was issued to Gazprom. The subsoil area is given by the status of a geological allotment without depth limitation for the period of geological exploration. Areas of the allocated subsoil findings (the Arkutun-Dagi and Chayvo fields) and the "Northern tip of the Chayvo-Sea field" are excluded from the area of the Ayashsky plot. [14]

In 2010-2011 processing and interpretation of 600 km2 of new 3D seismic data was carried out within the Ayashsky area. As a result, the geological model of the Ayashsky area was refined, and a forecast of the presence of reservoirs and the probability of their gas and oil saturation was made. The geological hydrocarbon resources of the group of Ayashsky structural-lithological traps, mapped in commercially promising Upper-Nizhnyutovsky sediments were estimated. Based on the results of works the location was determined and recommendations for drilling of prospecting well A-1 were given. [14]

3.2 Tectonics

The Ayashsky license area is in the central part of the North Sakhalin Cenozoic trough, which occupies almost the entire territory of Northern Sakhalin and the water area of the adjacent shelf. The depth of the basement in the troughs is 5-12 km, on the internal elevations - 1.5-3.0 km. The depth of the acoustic basement within the study area according to seismic survey data is estimated from - 8600 m in the most submerged part to - 3400 m in the vault of the Ayashsky structure. [14]

The tectonic structure of the sedimentary sequence of the North Sakhalin Basin is due to the Paleogene-Early Miocene riftogenic destruction of the Mesozoic partially consolidated basement. In the late Neogene, intensification of tectonic movements in the fault zones resulted in their transformation into a folded area, the northern link of the Hokkaido-Sakhalin folded system.

During the early to middle Miocene, the previously formed trough was filled with terrigenous-clastic sediments of the Uinin-Dagin complex. The main volume of terrigenous sediments was accumulated at the site of the present-day Venninsk anticlinal zone. Deposits of Uyninsko-Daginsky complex did not accumulate within Daginskaya anticlinal zone. [14]

At the end of the stage, ancient faults reactivated under compression conditions and block movements took place. The spread of folded movements reached 150-200 m. The fold-block forms of the Uinin-Dagi Complex formed a series of structural lines of northwestern strike, confined to "hidden" basement faults. [14]

The Middle Miocene to Late Pliocene period is characterized by quiet deltaic sedimentation. At this time, sandy-clay and clay-sandy Okobikai-Nutov deposits up to 5km thick are deposited that constitute a significant part of the volume of the North Sakhalin sedimentary basin. [14]

The Pliocene sedimentation was terminated by intense tectonic movements of the Sakhalin folding phase of great magnitude, which took place under compression conditions. [14]

There has been reactivation of thrusts in the basement. Large anticlines were formed in the Okobykai-Nutovo period. [14]

Due to riftogenesis and subsequent strike-slip faulting, the North Sakhalin Trough is complicated by large synclinal zones as well as anticlines (Figure 9). Anticlinal zones are complex folded structures 50 to 100-120 km long and 15 to 30 km wide, separated by regional and zonal faults into a series of structurally autonomous blocks. The synclines and synclinal zones are relatively simply built and composed of late Eocene sediments up to 10-12 km thick. [14]

The dominant role in the formation of the modern structure of the sedimentary cover of the area during the Cenozoic history was played by faulting (Figs. 10, 11). Three main systems of regional faulting are distinguished in the study area - submeridional, northwestern and northeastern directions. The most active influence on the formation of sedimentary cover structure was exerted by regional strike-slip, strike-slip, and associated strike-slip faults during the Sakhalin tectogenesis phase, resulting in the formation of all post-sedimentary anticlinal zones. The length of these faults is hundreds of kilometers, and the amplitude of horizontal displacement of blocks along them reaches 5-10 km. Miocene strike-slip faults and faults were most developed in middle Miocene time. As a result of their activity buried conditional anticlinal zones were formed. [14]

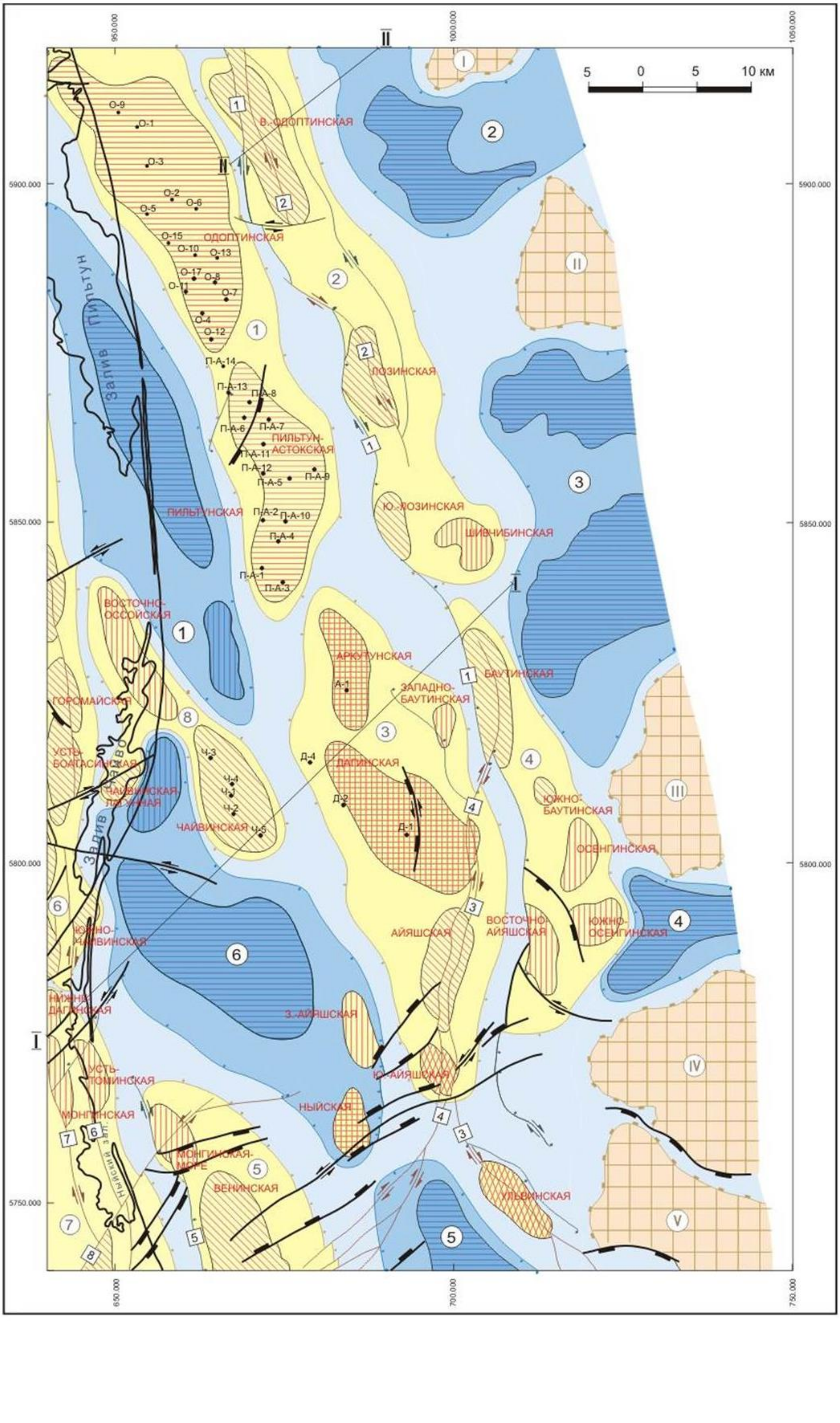
5 0 5 10 км
950.000
1000.000
1050.000
5900.000
5850.000
5800.000
5750.000
650.000
700.000
750.000
В.-ОДОПТИНСКАЯ
ОДОПТИНСКАЯ
Залив Пильтун
ЛОЗИНСКАЯ
ПИЛЬТУН-АСТОКСКАЯ
ПИЛЬТУНСКАЯ
Ю.-ЛОЗИНСКАЯ
ШИВЧИБИНСКАЯ
ВОСТОЧНО-ОССОЙСКАЯ
АРКУТУНСКАЯ
ЗАПАДНО-БАУТИНСКАЯ
БАУТИНСКАЯ
ГОРОМАЙСКАЯ
УСТЬ-БОАТАСИНСКАЯ
ЧАЙВИНСКАЯ-ЛАГУННАЯ
ЧАЙВИНСКАЯ
ДАГИНСКАЯ
ЮЖНО-БАУТИНСКАЯ
ОСЕНГИНСКАЯ
ЮЖНО-ЧАЙВИНСКАЯ
АЙЯШСКАЯ
ВОСТОЧНО-АЙЯШСКАЯ
ЮЖНО-ОСЕНГИНСКАЯ
НИЖНЕ-ДАГИНСКАЯ
З.-АЙЯШСКАЯ
УСТЬ-ТОМИНСКАЯ
Ю.-АЙЯШСКАЯ
МОНГИНСКАЯ
НЫЙСКАЯ
МОНГИНСКАЯ-МОРЕ
ВЕНИНСКАЯ
УЛЬВИНСКАЯ
Залив Чайво

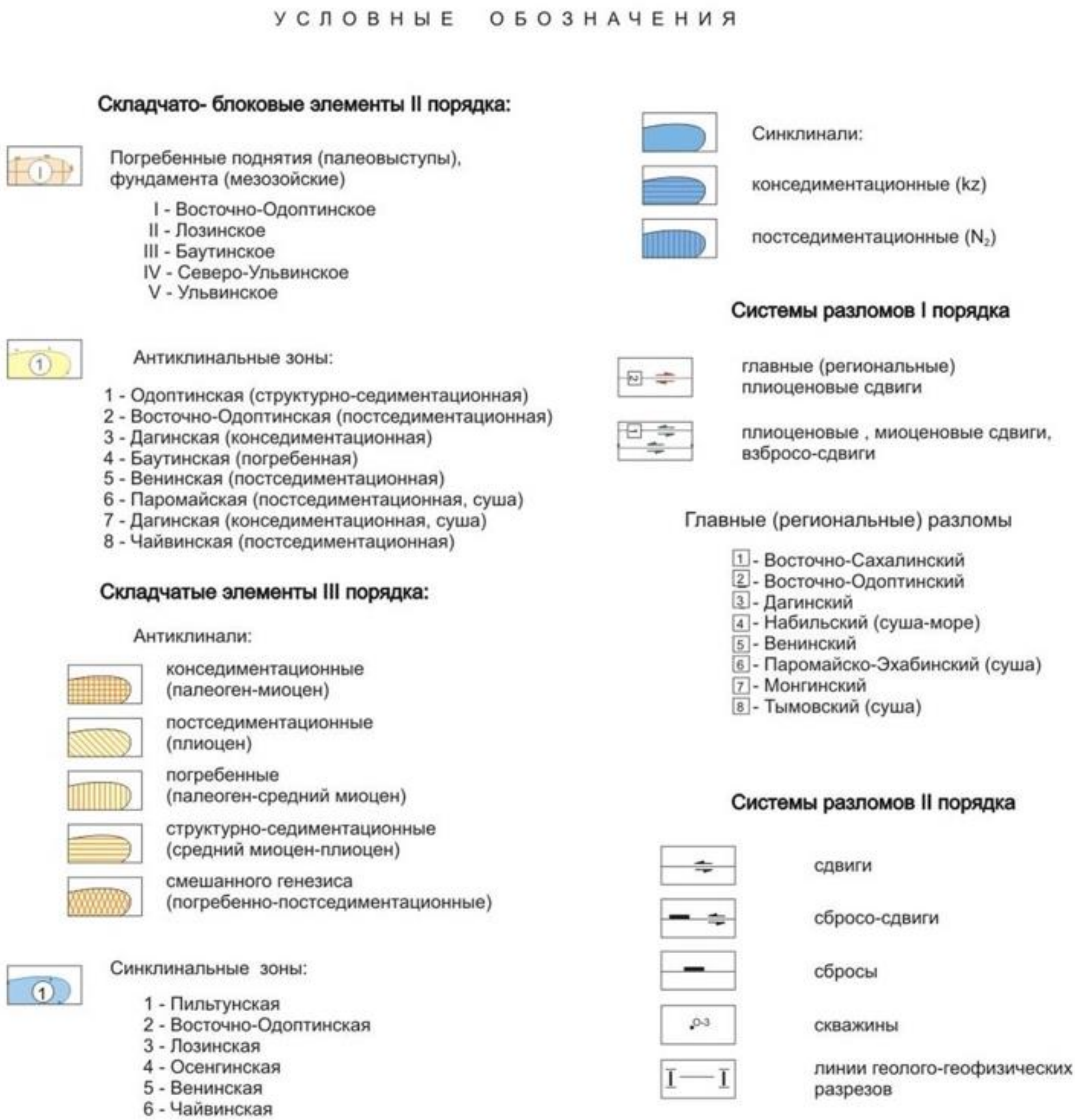

Figure 9 structural and tectonical scheme [14]

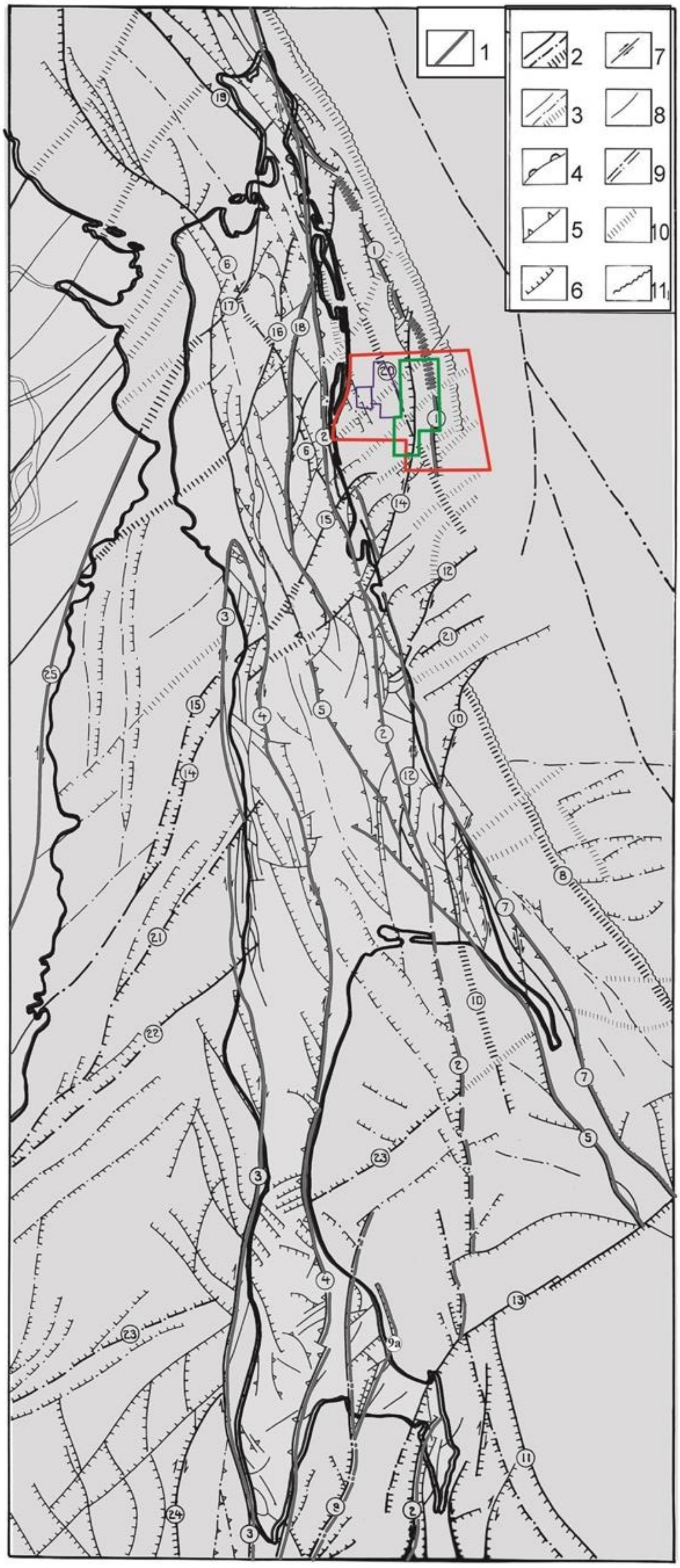

Figure 10 Fault map of Sakhalin and the Sakhalin shelf [14]

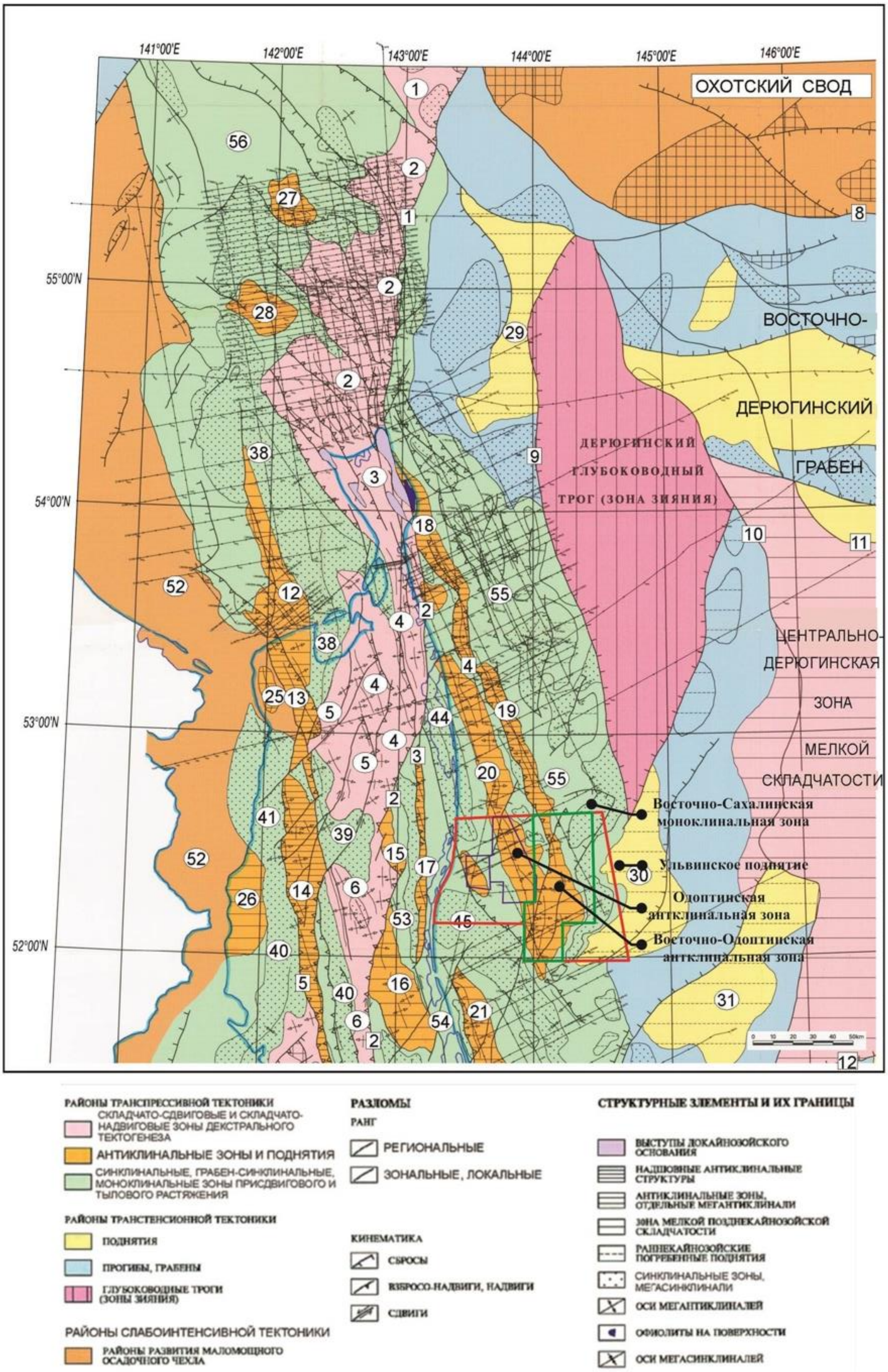

Figure 11 Fragment of the tectonic map of north-eastern Sakhalin Island [16]

3.3 Lithological and stratigraphic characteristics of the section

By analyzing the current understanding of the geology of the region and the information provided by the first exploration and evaluation well 1 Ayashskaya, we can conclude that the history of geodynamic development and formation of the maternal and sedimentary strata of the region is very complex. The main event in the formation of the strata in question was the change of conditions of passive continental margins to those of active zones during Mesozoic and Cenozoic times. The sediments of the Northeastern Sakhalin Basin were formed as a result of Oligocene-Early Miocene riftogenic destruction (P3-N1) of the Late Paleozoic-Early Mesozoic accretionary basement and Middle Miocene (N1-N2) post-rift depression sedimentation (Fig. 12.). The consequences of changing geodynamic regimes can be seen in the core from well 1 Ayashskaya. [17]

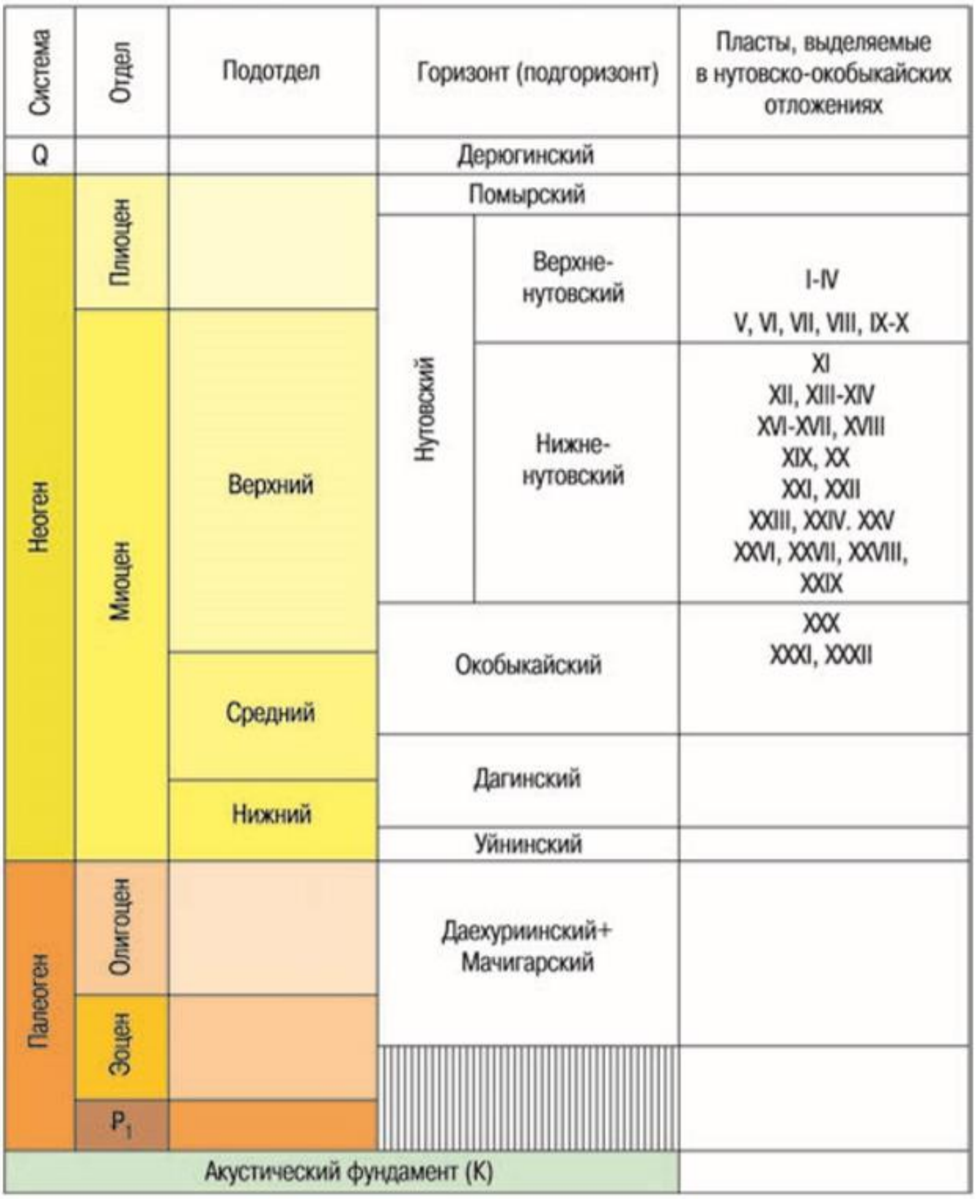

Figure 12 Stratigraphic scale of the North Sakhalin oil and gas bearing area [17]

The lithologic and stratigraphic characterization of the section is based on deep drilling data from the northeastern Sakhalin Island offshore fields (Fig. 12). The lithological and stratigraphic characteristic of the section is based on deep drilling data from the northeast Sakhalin shelf (Fig. 12) and the adjacent onshore area, using past geophysical survey results.

Two reservoir nomenclatures of the target Nuton complex, proposed in different years by SMNG and ExxonMobil, have been adopted during the study of this area. The ExxonMobil variant of the indexation is used in this paper but converting it to SMNG nomenclature is not difficult; in most cases, 10 (X) must be added. The correlation table (Table 3) for the reservoir indices is shown below. [14]

Table 3 Correlation table of reservoir indices [14]

CMNG LAYERS NOMENCLATURE	ExxonMobil's LAYERS NOMENCLATURE
Daginskiy subdivision	
XIX	X-TU
XX	X-L
XXI	XI
XXII	XI-L/XII
XXIII	XIII-TU
$XXIII_1$	XIII-L1
$XXIII_2$	XIII-L2
$XXIV_1$	XIV-T
$XXIV_2$	XIV-S1
XXV	XIV-S2
XXVI	XIV-F
XXVII	XVII-F
XXVIII	XVIII-F
Arkutunsky subdivision	
XXI_{1-2}	XI-UA
XXIII	XIII-S

Regionally, the Ayashsky area is located within the North Sakhalin sedimentary basin. The geological structure of the area of operations involves two structural layers: a basement composed of intensely dislocated and consolidated volcanogenic-sedimentary rocks of Mesozoic age, and a sedimentary cover represented by Cenozoic terrigenous sediments. [14]

3.4 Oil and gas potential of the area

The Triton field is located within the North Sakhalin oil and gas bearing area.

The main oil and gas bearing horizons in the region are the Daginsky, Okobikai and Nutovsky. The latter is subdivided into upper and lower sub-horizons. Prior to the drilling of the first prospecting and appraisal well, Ayashskaya well 1, the Upper Nutovsky had not been proven to be oil and gas bearing in the region. In the field, three horizons of this part of the section were tested in the open hole and two in the casing. Commercial inflows of water-free oil with good properties were obtained. It should also be noted that the Ayashsky structure confirmed the productivity of the target Lower Nutovsky sediments, the oil and gas content of which has been proven in neighboring fields. A total of 162m of core with direct evidence of oil saturation was recovered from these reservoirs and water-free oil inflows were obtained from modular formation dynamics tester (MDT) and drill stem test (DST) reservoir testers.

The North Sakhalin oil and gas bearing basin is characterized by the highest hydrocarbons (HC) concentrations in the Okhotsk region. More than 70 fields have been discovered in this basin: 20 oil fields with over 90% reserves, 11 gas fields, 18 gas-oil fields, 7 gas-condensate fields and 13 oil and gas-condensate fields. Among them there are 5 large, 10 medium and 55 small reserves in terms of total recoverable reserves. [14]

Within the North-Sakhalin oil and gas bearing basin, deposits of the Miocene - Lower-Okobikai (Middle to Upper Miocene) and Daginsko-Uininsky (Lower-Middle Miocene) horizons are commercially oil and gas bearing. The Lower Uyutian-Okobylian horizons contain 90% of the basin's initial HC resources. The northeastern coastal part of the island is the most saturated with productive structures. Many developed oil and oil and gas fields with varying amounts of HC reserves are located here. [14]

The study area is located within the Odoptinskaya oil and gas bearing area of the North Sakhalin Industrial Oil and Gas Basin. [14]

The main oil and gas bearing complexes (OGC) of Northeast Sakhalin and the adjacent shelf are the Uininsko-Daginsky and Okobykaysko-lower-

Nutovsky, with significant prospects also associated with the fractured reservoirs of the Daekhurian complex.

The largest oil reserves are in the XXI1-2 and XXIII reservoirs. [14]

3.5 Reservoir characteristic

The Triton field was discovered in a very short time: the main work was carried out within a year and a half. Over the next three years, plans include additional exploration of the deposit, drilling at least three more exploration wells and carrying out a wide-azimuth seismic survey. The goal is to find quality zones from which development can be started. At the same time, the neighboring Bautinskaya structure, also very promising, is being explored.

The Uyninsko-Daginsky OGC is composed of clay-sand and sediments with sandy-silty rocks predominating. The lower part of the complex is characterized by a reservoir type with a gradual upward change in the ratio between reservoirs and fluids from predominance of fluids to predominance of reservoirs. The upper part of the complex combines with the subregional Okobikai clayey sequence to form a massive reservoir with a high accumulation potential.

The reservoir beds are mainly composed of fine- to medium-grained sandstones and coarse-grained siltstones. The thickness of sand layers in the strata varies from the first meters to 50 meters. The porosity is 12 - 25%, and permeability is 0.0001-1 μm^2.

Reservoirs and massive reservoirs with pore-type reservoirs contain commercial deposits of hydrocarbons in offshore fields: Lunskoye, Veninskoye, Kirinskoye, and adjacent onshore fields - Mongi, Mirzoeva, Ust-Tomi, Ust-Evayskoye and others.

The Okobykai-lower- Nutovsky petrochemical complex is productive in most of the fields discovered on the Sakhalin shelf.

The complex is characterized by significant changes in lithofacies composition along the section and laterally.

The Okobikai reservoirs are developed mainly onshore and contain more than 45 % of oil reserves and about 48 % of gas reserves. Strongly clayey siltstones and sandstones are found in the tops of the Okobykai horizon in the Odoptinskoye field.

The Lower Nutovsky reservoirs are of major importance offshore, containing up to 42% of gas and up to 90% of oil. HC reservoirs in Lower Nuton sediments are found in all of the fields located in close proximity to the Nutovsky area: the Arkutun-Daginskoye, Chaivo, Odoptinskoye and Piltun-Astokhskoye fields.

The Arkutun-Daginskoye oil and gas condensate field is located within the southern part of the Odoptinskoye oil and gas bearing zone. In terms of geological complexity, it is classified as a field of very complex structure. Oil, gas and gas condensate deposits have been found in sandy and sandy-siltstone reservoirs of porous type of the Lower Nutovsky subhorizon at depths of 1680-2800 m. Filtration and permeability properties of reservoirs vary within a wide range: porosity - 16-30 %, permeability - 0,021-0,84 μm^2, clay content - 9-20 %. The total thickness of reservoir beds also varies widely, from 14.2 to 47.7 m.

3.6 Triton field Oil reserves estimation

It is common practice in field perspectivity assessment to perform two tasks: reserve estimation and risk calculation. [19]

There are 2 main approaches on reservoir estimation: material balance and volumetric method. [20]

The size of potential reserves is meaningful only if a hydrocarbon accumulation exists. The chance of that happening is the probability of success (POS). It is determined by reviewing the critical geologic risk factors and assessing their probabilities. [20]

In the probabilistic approach, each parameter involved in the formula for estimating reserves is treated as a random variable, and the value of reserves is treated as a function of these random parameters. The main difference between the probabilistic model and the deterministic model is that the deterministic approach produces a single ("point") estimate of reserves, while the probabilistic approach produces a range (interval) of possible values of the target reserves. [21]

In 1991 methods used in reservoir evaluation were classified in three principal categories: analogy, volumetric and performance analysis. It was stated that these three classes of hydrocarbon reserves evaluation methods can be used for either deterministic or probabilistic analysis, noting that when uncertainty is high, the applicability of probabilistic methods seems to be more viable compared to the deterministic methods. [22]

Monte Carlo simulation can be used for propagating the uncertainty of individual parameters to reserves. Parameter values are drawn randomly from their respective distributions and multiplied to produce a histogram of reserves. This approach has maximum flexibility, and can handle correlation among inputs, but it requires the specification of a distribution model for each individual parameter. [20]

Probability models can be used to estimate oil and gas reserves. According to the US classification of SPE (Society of Petroleum Engineers) reserves are subdivided:

P90 – are those quantities of oil that, from analysis of geological and engineering data, can be estimated with 90% probability to be commercially recoverable to date from known fields;

P50 – are those unproved reserves that geological and engineering data suggest have a 50% chance of being recoverable;

P10 – are those unproved reserves that should be at least 10% likely to be recoverable. [20]

The Monte Carlo method is a method in mathematics for studying random processes. Random is when something happens in an unpredictable way (for example, we cannot say exactly how thick a reservoir will be, so we cannot say what the oil and gas reserves will be).

In the probabilistic approach, each parameter involved in a hydrocarbons volume calculation formula is treated as a random variable, and the value of the hydrocarbons volume is treated as a function of these random parameters. [21]

Consider the probability distributions that can be used:

Normal distribution. The normal probability distribution is used mainly in statistics. It is a good model for real world phenomena. It gives the mean and the standard deviation. Such a distribution can be used for porosity, saturation, and conversion factor.

A uniform distribution is useful when describing variables where each value is equally likely to be in the interval [a;b]. A minimum and maximum value is required. The uniform distribution is suitable for the parameters: area, density, conversion factor.

Triangular distribution. The minimum, best fit and maximum values must be determined for the calculation. This distribution can be used for any parameter.

The exponential distribution is often used to describe intervals between successive random events, which in ordinary language might be called rare. [23]

The Monte Carlo method (statistical testing method) involves the following steps:

Constructing a mathematical model of the system that describes the dependence of modelled characteristics on the values of the stochastic variables.

Establishing probability distributions for stochastic variables.

Determine a random number interval for each stochastic variable and generate random numbers.

Simulate system behavior by performing multiple trials and obtaining an estimate of modelled system performance for fixed values of control parameters. Evaluation of the accuracy of the result. [24]

After conducting Monte Carlo simulations with a given number of iterations, a curve of reserves distribution of the Triton field is constructed. Typical distribution is shown in figure 13. The following take aways can be made basing on this distribution:

Proven Reserve (P90) = 2 mln tonnes. Reserves are equal or more than 2.0 M tonnes, with confidence 90%.

Proven and Possible Reserves (P50) = 3.7 mln tonnes. Reserves are at least 3.7 M tonnes, with confidence 50%.

Proven, Possible and Probable Reserves (P10) = 7 mln tonnes. Reserves are at least 7.0 mln tonnes, with confidence 10%. [24]

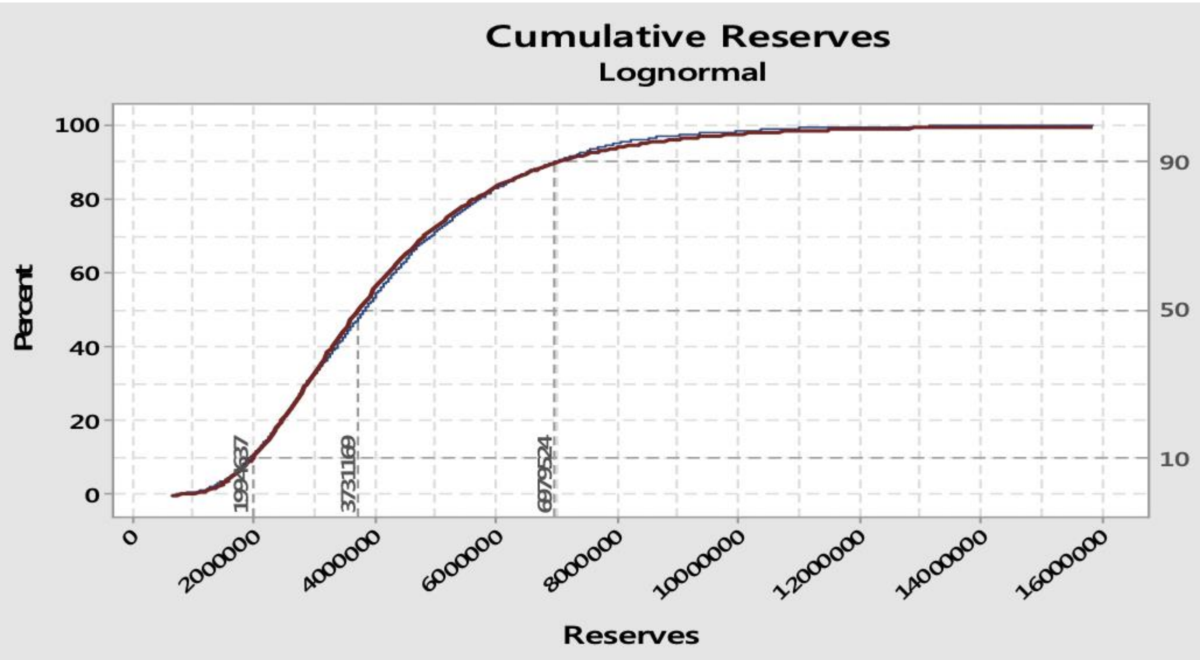

Figure 13 Cumulative reserves (tonnes) and P10, P50 and P90 estimates. [24]

Oil and gas reserve estimation methods are broadly divided into analogy, volumetric and performance methods. Volumetric and performance methods are the more complex methods, and the main difference between them lies in the type of pre- and post-production data used.

Volumetric Method: As the name suggests, this method requires the volume of the reservoir to be calculated through maps and petrophysical data of the drilled wells. This method is carried out in the early phases of exploration to find the amount of Oil and Gas in place and the likely corresponding reserves.

Material Balance Method: This method is applied in the intermediate stages of exploration and thus estimates oil and gas production.

Decline Curve Analysis: This method is applied in the late stages of a field operation when most of the oil and gas have already been extracted and the production rate in the field is declining. A forecast of future production is given by the reserves. [25]

In this analysis we will focus on volumetric method.

$$STOIIP = \frac{A * h_0 * \phi * (1 - S_{wi}) * \rho}{B_0} \tag{1}$$

Where:

$\text{STOIIP} - \text{Stock Tank Oil Initially In Place } [\text{tonnes} * 10^3];$

$A - \text{the area of oil saturated formations } [\text{m}^2];$

$h_0 - thickness\ of\ oil\ saturated\ interval\ [m];$

$\phi - reservoir\ porosity;$

$S_{wi} - initial\ water\ saturation;$

$\rho - oil\ density\ \left[\frac{kg}{m^3}\right];$

$B_0 - a\ conversion\ factor\ to\ account\ for\ the\ shrinkage\ of\ oil;$

Geological reserves are calculated using Monte-Carlo method - probabilistic approach. All input data for the calculations is taken from the table 4.

Table 4 Collected data for reserves volume calculation [26]

Parameter	Dimension	Layer V-0		Layer V-1		Layer V-2		Layer V-3		Layer V-4		Layer V1-1		Layer V1-2	
		Mean	St. deviation	Mean	St. deviation	Mean	St. deviation	Mean	St. deviation	Mean	St. deviation	Mean	St. deviation	Mean	St. deviation
Area	$10^3 m^2$	25134	3000	8075	500	9543	400	10961	367	1898	360	58461	700	23029	542
Thickness	m	13,4	1	1,76	0,4	8,85	0,3	7,07	0,2	1,18	0,2	11,09	0,1	7,36	0,1
Porosity	-	0,36	0,03	0,36	0,02	0,3	0,01	0,31	0,01	0,31	0,01	0,3	0,01	0,29	0,01

Initial water saturation	-	0,49	-	0,47	-	0,58	-	0,47	-	0,47	-	0,47	-	0,47	-
density	kg/ m^3	818	-	817	-	817	-	817	-	822	-	822	-	822	-
Conversion factor	-	1,144	-	1,176	-	1,176	-	1,176	-	1,190	-	1,190	-	1,205	-

It is assumed that the area, thickness, and porosity parameters are normally distributed. Initial water saturation, density and conversion factor are constant.

The Monte Carlo simulation of the reserve calculation was carried out using the Python programming language. The code is presented in Appendix 1. The following results were obtained:

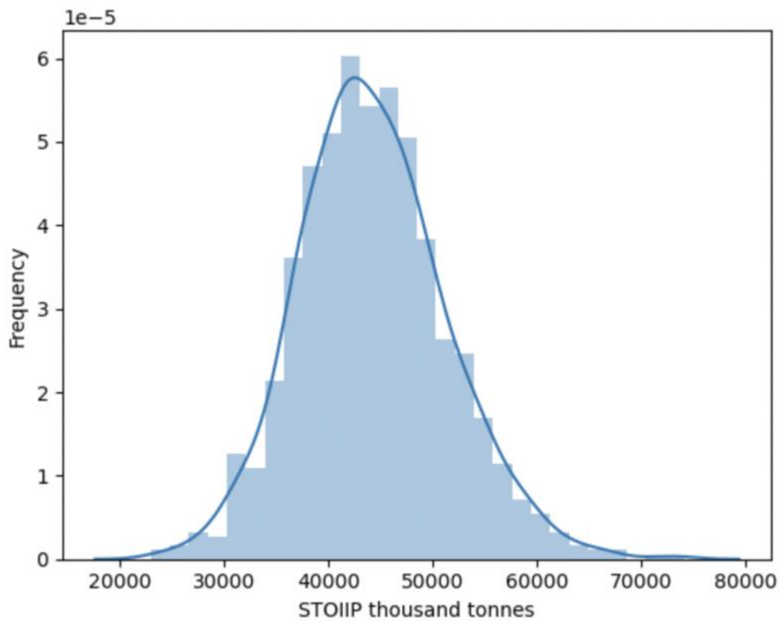

Figure 14 STOIIP distribution for 1000 iterations of Monte-Carlo simulation for the V-0 layer

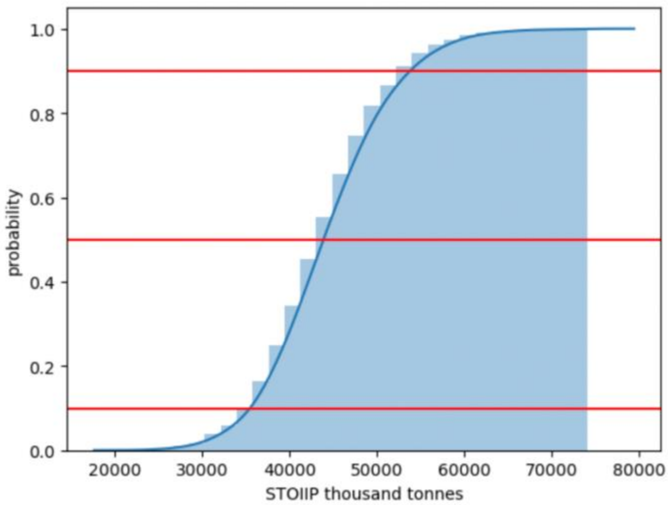

Figure 15 Probability to have volume less than specified for the V-0 layer

As it can be seen on figure 14 that the STOIIP has a normal distribution. Figure 15 shows the probability to observe volumes less than specified. So, with 10% probability we will observe 53,7 mln tonnes of oil (P10), with 50% probability 43,7 mln tonnes of oil can be observed (P50), and, finally, the probability of prove 35,9 mln thousand tonnes of oil is 90% (P90). As it was described above, reserves with 90% confidence are proven. So, for layer V-0, 35,9 mln tonnes of oil are considered as proven reserves. The same steps were performed for the other layers and the results are presented in table 5.

Table 5 P10, P50 and P90 geological reserves

Parametr	P10 volume of reserves, thousand tonnes	P50 volume of reserves, thousand tonnes	P90 volume of reserves, thousand tonnes
V-0	53683,12	43717,86	35946,03
V-1	2235,06	1711,68	1224,09
V-2	8030,3	7412,91	6829,14
V-3	9470,15	8828,63	8263,41
V-4	1951,08	1593,00	1225,92
V1-1	80250,47	7133,36	62455,68
V1-2	20979,11	17664,56	14593,88
Sum			130538,15

There are a total of 130,538 thousand tonnes of proven geological oil reserves in the seven layers.

Document [27] establishes the classification of petroleum reserves and inferred resources according to the number of recoverable reserves:

Unique - more than 300 million tonnes of oil or 300 bcm (billion cubic metres) of gas;

Major - 30 to 300 million tonnes of oil or 30 to 300 bcm of gas;

Medium - 5 to 30 million tonnes of oil or 5 to 30 bcm of gas;

Small - 1 to 5 million tonnes of oil or 1 to 5 bcm of gas;

Very small - less than 1 million tonnes of oil, less than 1 bcm of gas

According to this classification, the deposit under consideration belongs to the category of major deposits.

Chapter summary

In this chapter the geological characteristics of the Triton field in the Sea of Okhotsk were described. The main geological processes determining the formation and accumulation of hydrocarbons were discussed, and the estimation of geological oil and gas reserves was assessed.

Modern reserve estimation methods, including a probabilistic Monte Carlo simulation approach, were used during the study. This allowed reliable results to be obtained and the probability of reserve accumulation in the Triton field to be assessed.

The reserve distribution analysis determined the reliability of the reservoir distribution. Proved oil reserves in reservoirs V-0, V1-1 and V1-2 total 113 thousand tonnes, which is 86.5% of Triton's total geological volumes. In addition, the total proven geological oil reserves in seven reservoirs amount to 130.5 thousand tonnes.

Based on the classification of oil reserves, Triton belongs to the category of large fields, which confirms its significance and potential for development.

Thus, the results of the geological assessment and evaluation of geological reserves lead to the conclusion that the development of the Triton oil field in the Sea of Okhotsk is promising and feasible. These data are the basis for making informed decisions on planning and implementation of the field development project

4. Reservoir development planning

4.1 Oil recovery factor estimation

The Triton field is at an early stage of exploration and is represented by limited data from the drilling of the first prospecting well.

The development system is a set of technical, technological, and organizational interconnected engineering solutions for displacing oil (gas) in productive layers to the bottom hole zone of producing wells. The development system includes the sequence and rate of drilling; the number, ratio, mutual arrangement of injection, production, special (control, etc.) wells, the sequence of their introduction; measures and methods of reservoir simulation to achieve a given rate of hydrocarbon recovery; measures to control and regulate the development of deposits. [28]

The development of an oil field should follow a system that makes the best use of the natural properties of the oil reservoir, its production regime, technology and well exploitation techniques. [28]

Not all oil or natural gas reserves can be recovered from reservoirs with existing production technologies. For example, much of the oil is not displaced from capillary and even less so from subcapillary channels (pores). The recoverable oil reserves are determined by the following expression:

$$Recoverable\ reserves = STOIIP * RF \tag{2}$$

Where:

RF – recovery factor ;

In general, oil recovery factor depends on three groups of factors:

- geological and physical characteristics of reservoirs, including reservoir structure and reservoir parameters (reservoir type, permeability, thickness, reservoir heterogeneity, oil viscosity, etc.);

- technological factors - implemented reservoir development system of a particular reservoir, where systems may be applied during development, from natural oil production processes to the methods of oil recovery enhancement;

- technical and economic indicators - implemented development system. [28]

Recovery factor is the product of displacement efficiency C_d and sweep efficiency C_s coefficients:

$$RF = C_d * C_s \tag{3}$$

The displacement efficiency is the ratio of the volume of oil displaced from a rock sample during continuous washing to the initial volume in the sample, i.e., at almost 100 % watercut of the produced oil. This value It depends on permeability, void space structure, physical and chemical properties of oil and displacing agent, and there is a close correlation between displacement coefficient and formation permeability.

The oil displacement efficiency C_d is determined by several methods. The most effective, but at the same time the most labor-intensive method of obtaining the results is laboratory research of the oil displacement process using models made of real core samples of productive formations and oil from a particular field. As reservoir reservoirs are characterized by variability of their reservoir properties along the area and the section, C_d values are to be determined on samples uniformly exposing the reservoir or the pay zone with a realistic permeability coefficient variation range. For high-permeability reservoirs the displacement coefficient can reach 0.8-0.90, in a low-permeability reservoir it can be half as much. [28]

Occasionally, no tests are carried out at all, and the value of the oil displacement efficiency is calculated from residual water saturation coefficient values taken from capillary pressure curves and residual oil saturation coefficient values (figure 16). [29]

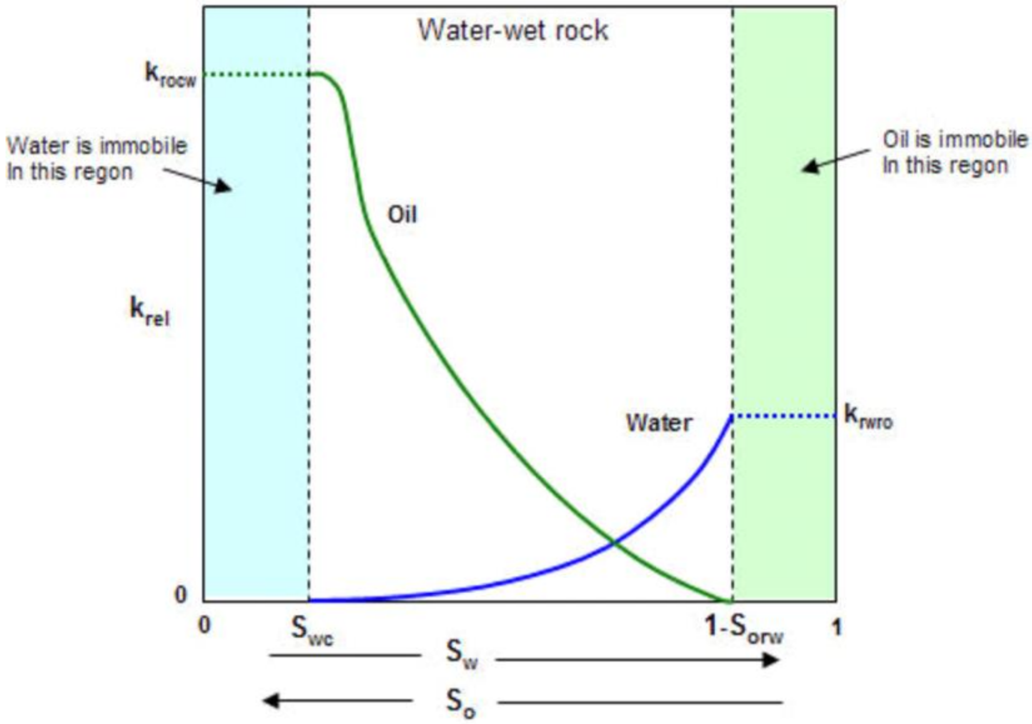

Figure 16 Water-Oil Relative Permeability Curve [30]

It is known that relative phase permeabilities are important data for any 3D hydrodynamic model of productive layer. It is possible to predetermine value of oil displacement efficiency using them, put into 3D hydrodynamic reservoir model. It is known the way of laboratory determination of C_d and phase permeabilities on cores. [31]

It includesthe following operations:

- A core sample extracted from a well is dried and its mass m1 is determined.

- The core is saturated with water under vacuum. The new mass m2 is determined on the basis of weighing.

- The water is displaced from the core with oil. After the stabilized condition the core is weighed again and the mass m^3 is determined. Knowing the values m1, m2, m3 allows, among other things, to calculate the coefficient of residual water saturation S_{wc}.

The S_{wc} value can also be determined by centrifugation method:

- The oil is displaced from core by agent (water, gas). When the core reaches the steady state, it is weighed and the mass m4 is measured. As a result, the value of residual oil saturation S_{orw} ost is obtained.

- The required value of C_d is found by the formula (4). [31]

$$C_d = \frac{1 - S_{orw} - S_{wc}}{1 - S_{wc}} \tag{4}$$

Were
$S_{wc} - connate\ water\ saturation$;
$S_{orw} - residual\ oil\ saturation.$

Sweep efficiency is the ratio of the oil-saturated reservoir volume (reservoir, production unit) covered by the displacement process to the total oil-saturated volume of the reservoir. For a variety of reasons (heterogeneity of productive formations, peculiarities of the development system, bottomholes locations of injection and production wells, etc.) a part of the reservoir volume does not participate in oil displacement, which is taken into account by this coefficient. [28]

For the Triton field, C_d is calculated based on its own data (figure 17) for the first well, and C_s is calculated by analogy with neighbouring fields.

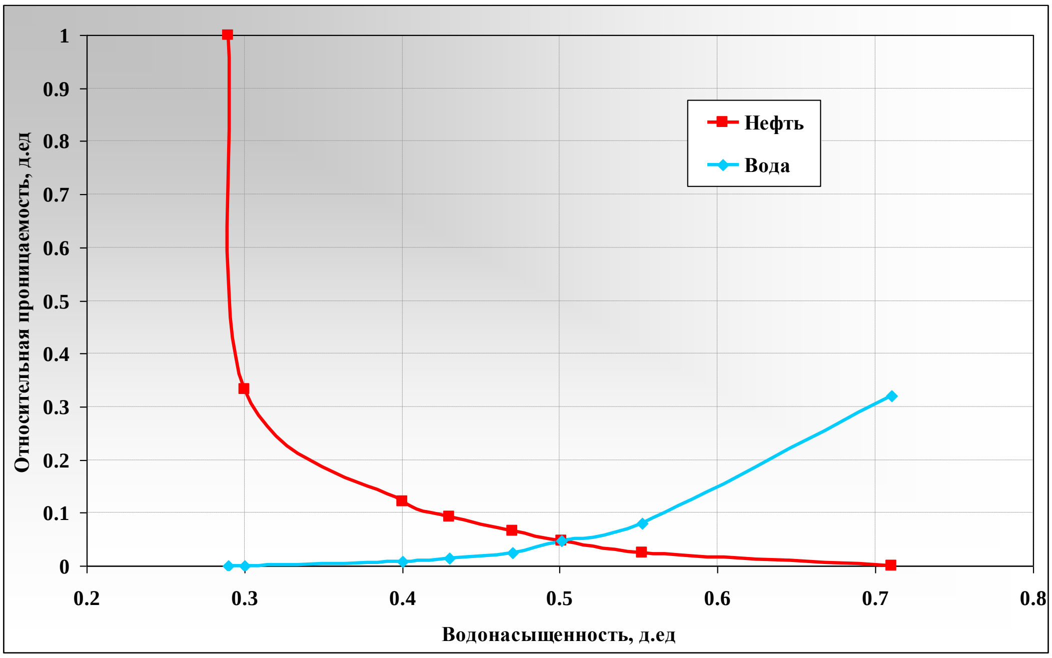

Figure 17 Relative phase permeability (red line – oil, blue line – water, y axis – relative permeability, x axis – water content). [14]

$$C_d = \frac{1 - 0{,}28 - 0{,}27}{1 - 0{,}27} = 0{,}61$$

For the analysis of possible coverage ratios, materials from fields located offshore Sakhalin near the Triton field were considered. As analogues, the practice of developing the Chayvo and Arkutun-Daginskoye fields, for which technical and technological solutions have been developed and are currently being implemented, was considered (table 6). [32] [33]

Table 6 Triton field analog characteristics

layer	Depth, m	layer thickness, m	Porosity, %	Permeability, mD	NGT (net to gross)	Cs, sweep efficiency	Wells type
Triton field							
Uppernutovsky	1465	63	33	229.8	0.6	0.592	
	1545	2	33	177.2	1.0	0.400	
	1566	14	30	24.6	0.8	0.592	
	1606	23	31	67.6	0.4	0.592	
	1728	2	31	51.6	1.0	0.400	
	1747	23	30	96.3	0.6	0.592	
	1814	40	29	11.0	0.4	0.592	
Arkutun-Dagi field							
Lowernutowsky	1605	170	26	308	0.11	0.24	Directioinal
	1650		24	518	0.06	0.20	
	1697		24	287	0.43	0.52	Horizomtal
	1775	255	24	288	0.38	0.20	Directional
	1830		24	263	0.16	0.21	
	1840		25	500	0.16	0.30	
	1801		22	174	0.24	0.39	
	1880		22	144	0.12	0.41	
	1970		22	158	0.17	0.34	
	2030		23	291	0.12	0.17	
	2085		23	104	0.13	0.35	
Chayvo field							
Lowernutowsky	1959		25	1768	0.54	0.62	Horizontal
	2230		22	317	0.47	0.32	
	2438		21	177	0.48	0.63	
	2517		20	106	0.42	0.62	
	2641		19	54	0.26	0.67	
	2689		20	122	0.40	0.67	

Because there are no reservoirs with proven productivity in the Uppernutovsky Triton field, the sweep efficiency for reservoirs V-0, V-2, V-3, VI-1, and VI-2 was calculated in [26] using the Dykstra-Parsons analytical method, which reflects reservoir heterogeneity. The geological basis for the calculation was a model of the listed layers obtained by drilling the first exploratory well. The calculations in [26] resulted in $C_s = 0{,}592$. It is recommended to develop the deposits of these horizons with horizontal wells, as in the above-mentioned Chayvo field, the average sweep efficiency for which is comparable with the calculated in [26] value.

The Arkutun-Daginskoye field is expected to be developed with directional wells involving horizontal completion in increased thickness areas. The application of directional wells is driven by the need to combine several thin and discontinuous reservoirs into a single production zone. This approach allows to achieve an average sweep efficiency of 0.3. [26]

The fields are developed using water injection to maintain reservoir pressure. Based on the peer fields the same recovery regime is proposed for the Triton field.

The reservoirs with approximately the same permeability, porosity, and reservoir pressure, and those containing oil with similar physical and chemical properties, can be classified as the one development zone. It should be stressed that nature itself does not create development zones - they are identified by the engineers developing the field. During the development process, zones may be combined or separated. A development zone may include one or more reservoirs or layers in the same field. The main features of a development target are the presence of commercial oil reserves and the specific, inherent group of wells by which it is developed. [28]

Assuming injection of each formation V-0, V-2, V-3, VI-1, and VI-2 by the independent wells network with horizontal completion C_s is taken equal to 0,592. It is possible to involve layers V-1 and V-4 into development by transit well network and with additional horizontal wellbores drilled in development wells. Such approach to development of productive V-1 and V-4 reservoirs allows to increase C_s up to 0.4. [26]

4.2 Wells placement

The location of oil wells in the structure is typically selected based on the shape of the reservoir, the geological structure of the field, the characteristics of the reservoirs and the possibility of movement of bottom water during the development of the reservoir. The waterflooding system is determined by the relative positioning of production and injection well faces. Wells are placed in a regular or irregular grid. Depending on the reservoir pressure maintenance scheme, waterfloods are possible in the out-contour, peripheral or pattern waterflooding. [34]

Out-contour water injection is characterized by injection of water into the reservoir through a well, which is placed along the perimeter of the reservoir, behind the outer perimeter of the oil-bearing zone. Production wells are placed inside the reservoir perimeter in rows parallel to the perimeter. The most favorable targets for flooding are reservoirs comprised of homogenous sands or sandstones with good permeability and not complicated by tectonic faults. Flooding in limestone reservoirs may not always be successful, as some of the reservoirs are not connected to the surrounding area through ductwork and fractures. [34]

In a peripheral waterflood, water is injected directly into the oil-saturated part of the formation to maintain or restore the reservoir energy balance. In Russia, the following types of waterfloods are used: waterflooding of oil reservoirs into separate areas or blocks of separate development, and pattern flooding. [34]

In medium and small size reservoirs, cross-cutting by rows of injection wells into blocks (block flooding) with no more than 3-5 rows of production wells between two injection rows is used. Five-row systems have proven effective for high productivity, while three-row and single-row systems for medium and low productivity. [34]

Typical well placement systems are presented in figure 18. The filling indicates the area of cells of periodicity of flooding elements; circles—production wells (producers); triangles—injection wells (injectors). [36]

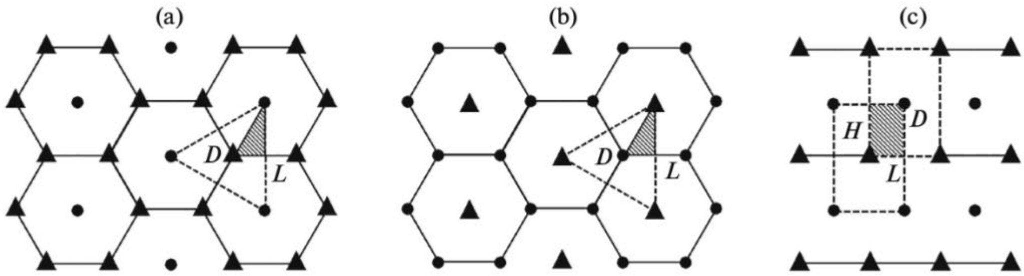

Figure 18 Well placement patterns by schemes A, B, and C [36]

Up to date 5 spot well placement systems are often favored because they allow for a more uniform impact on the reservoir. It is also worth bearing in mind that as the field is drilled out, new information about the reservoir comes in and changes can be made to the engineering design, including the well placement system. With insufficient geological data of the reservoir, we will take the 5-spot development system as the baseline for calculating the production forecast.

4.3 Simultaneous development of production zones

Separate development. This is used in a multi-layer field where each production zone is operated by a separate grid of wells. This requires many wells and leads to high capital expenditures. It is used to develop high yielding targets with large recoverable oil reserves. [37]

Co-development. This system involves combining two or more reservoirs into a single production asset and producing with a single production and injection well network. Each well simultaneously operates two reservoirs combined into one production zone. It has the advantage of ensuring high current production levels for a given number of wells. However, there is mostly unregulated reservoir development, and it is difficult to determine the amount of oil produced from each reservoir, the remaining recoverable reserves, the flow rates and the inject capacity of the wells from each reservoir separately. It is used for reservoirs with the same geological structure and similar permeability and filtration properties. [37]

Dual completion development. It is used when two reservoirs are combined into one production zone, the production wells are equipped with units for simultaneous separate exploitation, the injection wells are equipped with units for simultaneous separate water injection. [37]

For the Triton field, it is proposed to use a split production system with a transfer from one development site to another after the reserves have been depleted.

4.4 Sequential object development systems

Top-down development, in which the underlying asset is exploited after the overlying asset. This system is currently considered unsustainable because it delays exploration and development of the underlying targets, increases drilling and metal consumption for casing. [38]

Bottom-up development, which starts with the lower (reference, basic) unit and then moves on to the upper return units. If there are many reservoirs, the most productive, studied reservoirs with sufficiently large oil reserves are selected as the basis, while the remaining reservoirs are selected as return reservoirs. [38]

As it is recommended in [38] bottom-up development is suggested for the Triton field development.

4.5 Production forecast

The reservoir performance data is characterizing the process of oil field (reservoir) development. It includes annual cumulative production of oil, liquid, gas; annual cumulative injection of agent (water); water cut of produced fluid; oil stock of producing and injection wells; compensation for fluid withdrawal by water injection; Oil recovery factor; oil and fluid flow rates, drilling rate, etc.

Let’s review the methodology of calculating the main performance data of oil field (reservoir) development. [39]

Annual oil production (q_t, tonnes/year) - oil production from all the producing wells in one year. The production of oil for the perspective period is determined with the use of different methods and computer programs. In the development of deposits at the final stages (with declining oil production) annual oil production (qt) can be determined by the formula:

$$q_t = q_0 * e^{-\frac{q_0}{Q_{res}}t} \tag{5}$$

where t is a serial number of the calculation year (t = 1, 2, 3, 4, 5, ..., 10); q_0 - amplitude oil production in the 10th year; e = 2.718 - the base of the natural logarithm; Q_{res} - the residual recoverable oil reserves; [39]

Annual percent of recovery from the reservoir t_{rec} - ratio of annual production (q_t) to initial recoverable reserves (Q_{rec}), %:

$$t_{rec} = q_t / Q_{rec} \tag{6}$$

Annual percent of recovery from the reservoir $t_{rec\ annual}$ % of residual (current) recoverable reserves - ratio of annual production (q_t) to residual recoverable reserves ($Q_{rec\ res}$) - residual recoverable oil reserves at the beginning of calculation (the difference between initial recoverable reserves and cumulative oil production at the beginning of the calculation year):

$$t_{rec\ annual} = q_t / Q_{rec\ res} \tag{7}$$

Cumulative oil production since the beginning of development (Q_c) - sum of annual oil production by the end of the year, thousand tonnes:

$$Q_c = q_{t1} + q_{t2} + .. + q_{t(n-1)} + q_{tn} \tag{8}$$

Oil production from initial recoverable reserves coefficient C_q is the ratio of accumulated oil production to initial recoverable reserves, %:

$$C_q = Q_c / Q_{rec} \tag{8}$$

Oil recovery factor (ORF) is the ratio of accumulated oil production to initial geological or balance oil reserves:

$$ORF = Q_c / Q_{geological} \tag{9}$$

Production of liquid since the beginning of development Q_l - the sum of annual liquid production for the current year, thousand tonnes:

$$Q_{cl} = q_{tl1} + q_{tl2} + .. + q_{tl(n-1)} + q_{tln} \tag{10}$$

Average annual water-cut W (share of water in well production) ratio of annual water production (q_w) to annual liquid production (q_l), %:

$$W = q_w / q_l \tag{11}$$

4.6 Justification of well rates

Calculated flow rates for oil-saturated objects are from 30 to 230 m^3/day on the basis of [26], which can be considered as commercial oil inflows. It should be noted that calculations are made for vertical wells, but at application of modern technologies, development with use of horizontal, multilateral wells, etc., flow rates can allow to achieve higher production rates.

The first Intelligent multilateral TAML5 wells on the V. Filanovsky Field are a great example of how new technologies can contribute to CAPEX optimization, and thanks to a higher PI (productivity index), achieving higher well flow rates. Multilateral well geometry combined with an ability to monitor and control each leg separately helps to optimize flow patterns, prolongs well life, and contributes to a higher cumulative production. [40]

Drilling multilateral smart wells - is a convenient technology that can be applied to increase oil production levels in various fields. Especially in offshore projects, once the first phase of drilling is complete, drilling lateral wells while maintaining the main well bore is the best way to maintain production at minimum cost. [40]

When designing a field development, it is recommended that wells be drilled so that a lateral well with a TAML3 or TAML5 junction (figure 19) can be drilled in the future.

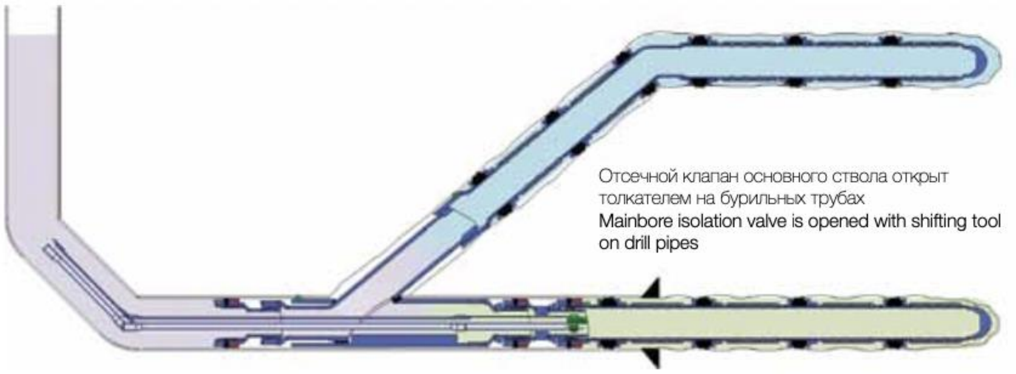

Figure 19 TAML 5 completion [40]

Multilateral intelligent wells allow for faster production ramp-up at the start of the field, lower capital costs associated with drilling the upper the top wells sections. Downhole pressure and temperature sensors and multi-position valves help to control gas breakthrough. In addition, the ability to control flow from each wellbore separately optimizes well performance, by finding a balance between current flow rates and total cumulative production from the field. [40]

The technology of drilling intelligent boreholes was successfully applied at the V.Filanovskogo field. The actual flow rate of a double borehole is 20-60% higher than that of a single borehole with a comparable operating mode. It is also revealed that the double bore well is operated with higher bottomhole pressure (and hence lower pressure drop) than the average single-bore well.

Based on the information above, it can be assumed that at the Triton field the expected flow rates can be 500-800 m^3/day using modern construction and completion technologies.

4.7 Piston and non-piston displacement

Let's consider piston oil displacement with water using a simple example (figure 20).

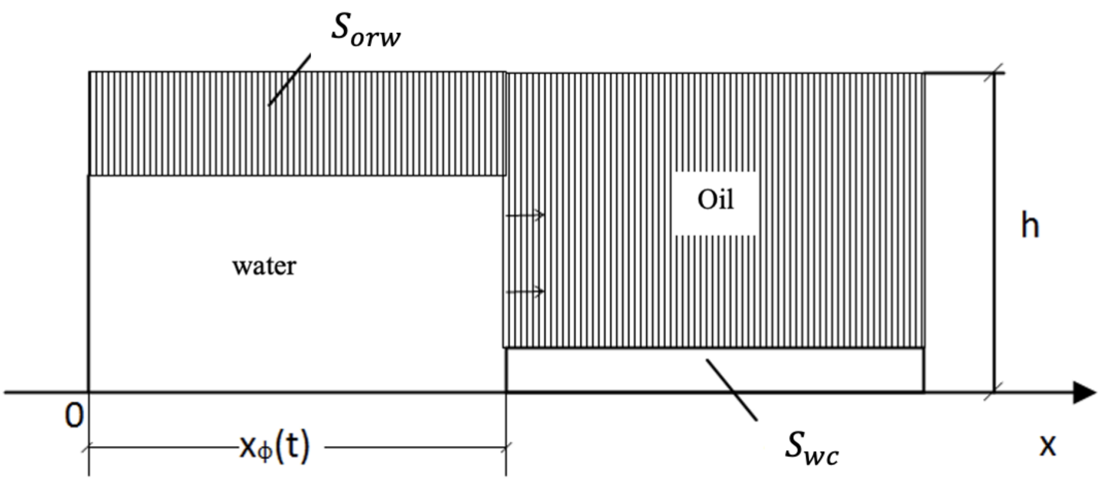

Figure 20 Piston displacement [43]

$x_{\phi}(t) -$ *oil displacement front with water;*
$S_{wc} -$ *coefficient of residual water;*
$S_{orw} -$ *coefficient of residual oil;*
$h -$ *reservoir thickness;*
$S_{orw} = 1 - S_{wc\ lim}$,
$S_{wc\ lim} -$
limit value of water saturation coefficient, at which oil filtration stops
;

The displacement front moves from the injection wells to the production wells, displacing oil. Behind the displacement front only water moves, oil does not move, its quantity is determined by the coefficient $S_{orw} = 1 - S_{wc\ lim}$ (figure 20). Only oil moves ahead of the displacement front, the amount of immobilized water is characterized by the S_{wc} parameter. The water saturation at and behind the displacement front is constant and equal to $S_{wc\ lim}$. [41]

When the displacement front reaches the production well, the production is completely watered out. Thus, water cut is equal to 1 and water saturation is less than 1. Piston displacement can only occur in homogeneous, highly permeable reservoirs or in highly permeable reservoir strata. It is used for approximate calculation of development indicators. [41]

In non-piston displacement, a two-phase oil-water filtration zone is formed behind the displacement front, as it is shown in figure 21. [41]

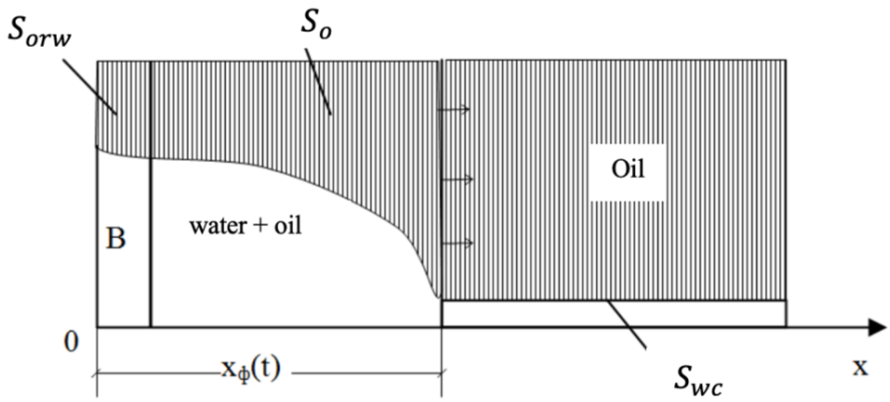

Figure 21 non piston displacement profile [43]

In contrast to piston displacement, joint filtration of two oil and water phases occurs behind the displacement front. Due to heterogeneity of the reservoir and chaotic distribution of different pore channels, the Jamen effect appears. The oil is displaced by water. At the interface between the phases of interaction between the particles - meniscuses and the walls of the pore channel, there are additional resistances - capillary pressures, which must be overcome by the external pressure of water pumped into the reservoir. [42]

When the production wells reach the displacement front, the production starts to water out gradually, and unlike piston displacement, the well operation continues, as oil saturation in non-piston displacement at the displacement front is less than the limit $S_{wc\ lim}$. [41]

The function F(s) is called the Buckley-Leverett function, which describes non-piston oil displacement by water under known dependences of relative phase permeabilities on water saturation:

$$F(S) = \frac{k'_w(S)}{k'_w(S) + \mu_0 * k'_o(S)} \qquad (12)$$

Where:

$F(S) -$ Buckley $-$ Leverett function;

$k'_w(S) - relative\ water\ phase\ permeability$;

$k'_0(S) - relative\ oil\ phase\ permeability$;

$\mu_0 = \frac{\mu_w}{\mu_{oil}} - relative\ \ dynamic\ viscosity.$

The physical meaning of the Buckley-Leverett function characterizes the fraction of water in the filtration fluid flow in an arbitrary section of the two-phase filtration zone. [42]

Thus, the water saturation coefficient characterizes the fraction of water in the pore space of the formation, not necessarily moving. The water saturation coefficient is determined at the surface after separation of the production into water and oil and corresponds to the fraction of water in the produced fluid. [42]

4.8 Calculating Production forecast for the Triton field

Using formulas from previous sections, let’s calculate the production forecast for V1-1 layer:

Dynamic viscosity ratio:

$$\mu_0 = \frac{\mu_w}{\mu_{oil}} = \frac{1}{1{,}2} = 0{,}83$$

For the calculations phase permeability curve (figure 17) is used. Using the phase permeability graph, for each point determine the relative phase permeability of oil $k'_0(S)$, the relative phase permeability of water $k'_w(S)$ and water saturation S.

Let's calculate Buckley-Leverett function using formula 12 for 1 point:

$$F(S) = \frac{k'_w(S)}{k'_w(S) + \mu_0 * k'_o(S)} = \frac{0}{0 + 0{,}83 * 1} = 0$$

Making calculations for the remaining points and get the following table:

Table 7 relative phase permeability and corresponding saturation data for the Triton field [14]

	S_w	S_o	k'_o	k'_w	$F(S)$
1	0,38	0,62	1	0	0,00
2	0,4	0,6	0,35	0,01	0,03
3	0,47	0,53	0,1	0,03	0,26
4	0,52	0,48	0,05	0,06	0,59

5	0,56	0,44	0,03	0,09	0,78
6	0,72	0,28	0	0,32	1,00

Using the obtained data, plot the dependence of F(S) on S (figure 22):

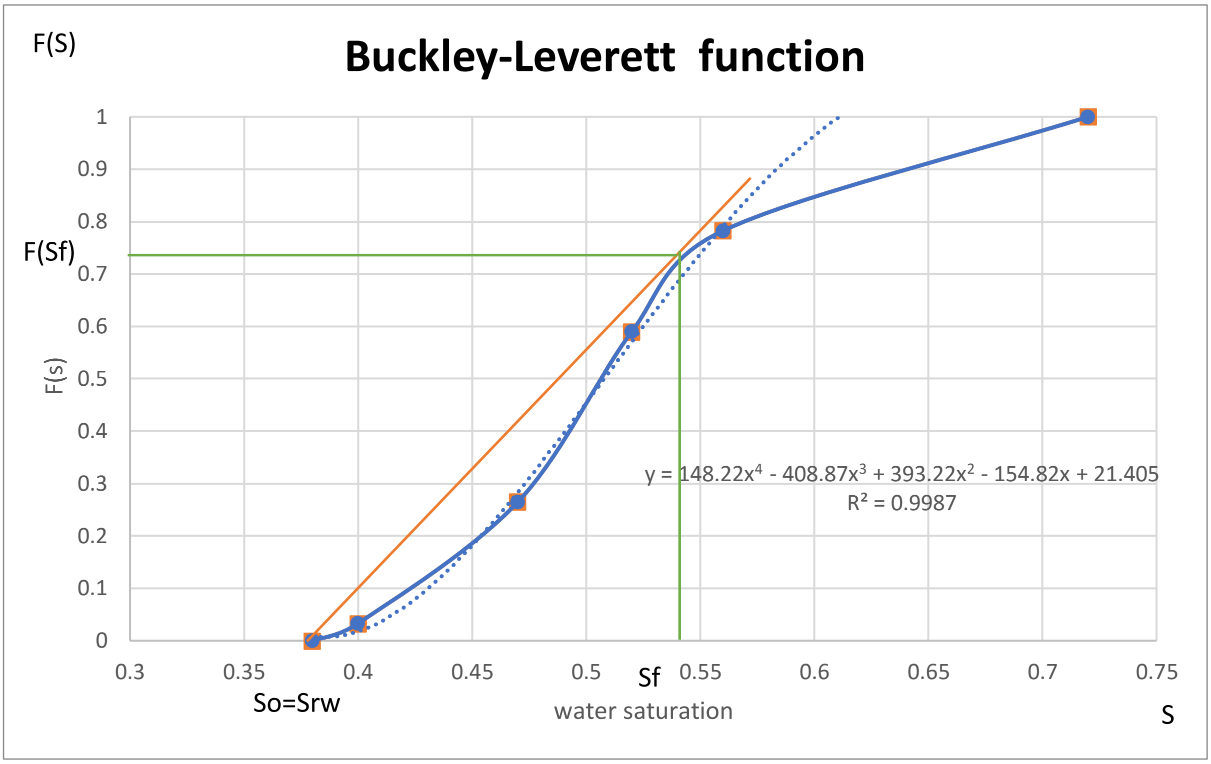

Figure 22 Buckley-Leverett function for the V1-1 layer

Calculate the derivative of the Buckley-Leverett function F'(Sf) by the formula: [43]

$$F'(S_f) = \frac{F(S_f) - F(S_0)}{S_f - S_0} = \frac{0,72 - 0}{0,53 - 0,38} = 4,8$$

Drainage reserve volume can be calculated: [43]

$$V_d = F * h * m * C_s \tag{13}$$

The waterless time is determined by the formula: [43]

$$t_{wl} = \frac{V_d}{n * q * 365 * F'(S_f) * C_d} \tag{14}$$

Substituting formula 13 into 14 and we get:

$$t_{wl} = \frac{F * h * m * C_s}{n * q * 365 * F'(S_f) * C_d} = \frac{3000m^2 * 9000\text{m} * 12{,}9 * 0{,}3 * 0{,}592}{650\frac{m^3}{day} * 365 \ * 0{,}95 * 4{,}8}$$
$$= 10\ years$$

Oil production in waterless period: [43]

$$q = q_0 \cdot n \cdot 365 \cdot C_s \tag{15}$$

Using formulas (5), (7), (9), (10), (11) and (15), we obtain production data for V1-1 layer (table 8).

Table 8 V1-1 Triton field layer production data

year	Oil produced for a year, thousand m^3	Cumulative oil production, thousand m^3	Liquid produced for a year, thousand m^3	Cumulative produced liquid, thousand m^3	Water produced for a year, thousand m^3	Cumulative water production, thousand m^3	Water-cut, %	ORF, %	Number of wells
1	561	561	561	561	0	0	0	0,9	2
2	1121	1682	1121	1682	0	0	0	2,8	4
3	1682	3364	1682	3364	0	0	0	5,7	6
4	1873	5237	2243	5606	369	369	16,47	8,8	8
5	1956	7193	2803	8410	847	1217	30,23	12,1	10
6	1634	8826	2803	11213	1170	2387	41,73	14,9	10
…	…	…	…	…	…	…	…	…	…
26	45	16883	2803	67277	2759	50394	98,41	28,46	10
27	37	16920	2803	70080	2766	53160	98,67	28,52	10

The moment of the end of oil production will be the 27th year, when the water cut of produced oil will exceed 98.5%. Let's present some results of calculation of technological indicators in graphical form (Figure 23). Full calculations are shown in Appendix 2 as well as the calculation results for reservoirs V1-2 and V-0.

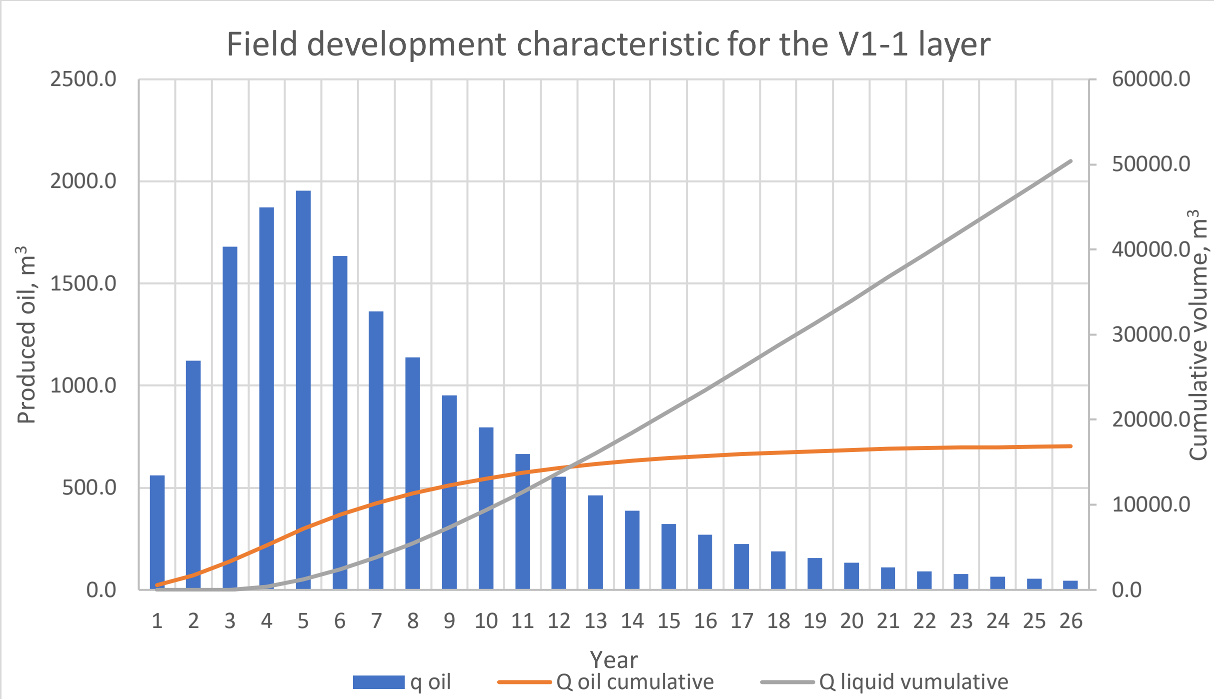

Figure 23 Field development characteristics for the V1-1 layer

It will take 27 years to develop the V1-1 formation, by the end of the 27th year the water cut will exceed 98.5%, and the final ORF will be 28.52%, which is comparable with the previously calculated value of 30%. The development of the V1-2 reservoir will take 11 years and the V-0 reservoir will take 17 years, with final EOR values of 17.8% and 26.8% respectively.

Chapter summary

In this chapter, the basic principles of an offshore oil field development system were reviewed and analysed.

The relative phase permeability curve was analysed to estimate the waterflood displacement ratio. Then, several peer fields were considered and, based on their characteristics, an assumption was made about the coverage factor; its value was assumed to be 0,59. These preliminary estimates made it possible to estimate the oil recovery factor.

Next, the case of intelligent dual bore wells in the Filanovsky field was considered. Based on this case study, assumptions were made about the potential flow rates that could be achieved by using this technology to develop the Triton field.

Piston and non-piston oil displacement systems were also considered. Using non-piston displacement theory, reservoir performance was evaluated for V1-1, V1-2 and V-0, which together account for 86.6% of the total reserves. Having calculated and analysed the result, it was determined that the development period of reservoir V1-1 using 10 production wells will be 27 years and the oil recovery factor is expected to be 28.52 by the end of development. The V1-2 and V-0 reservoirs are proposed to be developed sequentially using 6 production wells. The total development time of the two reservoirs will be 28 years.

In summary, this chapter analysed and evaluated various parameters and factors associated with the Triton field development system on the Okhotsk Sea shelf. The results and assumptions obtained may serve as a basis for further design and development of this field, considering optimal technical and economic performance.

5. Selection concept for the Triton field development

5.1 Features of offshore field development

The development of hydrocarbon resources of the World Ocean has been carried out for about 100 years. At the first stages in the 20-40's of the 20th century, offshore drilling was conducted in the coastal part and was essentially a continuation of onshore field development, the productive strata of which extended beyond the coastline. Since directional drilling technologies were absent in those years, vertical wells were constructed either from artificial islands or from specially constructed supports and overpasses. [44]

By the beginning of the XXI century the offshore oil and gas production has formed a separate, rapidly developing branch of the world fuel and energy complex which nowadays distinguishes 2 trends of prospective development:

1) Development of fields in ultra-deep-water areas of the World Ocean;

2) Development of fields in the areas of freezing seas, including the Arctic shelf. [44]

The latter direction is the most relevant for Russian companies, since the main part of hydrocarbon resources on the Russian shelf is concentrated on the Arctic shelf, as well as on the shelves of the Sea of Okhotsk and the Caspian Sea, natural and climatic conditions of which are favorable for ice formation.

As the development of offshore oil and gas production in Russia, this direction of the fuel and energy complex became a separate industry, the activity of which has its own features that distinguish it from onshore oil and gas production.

Let us note these peculiarities:

- The location of the field is often outside the territorial waters of the Russian Federation. In this case there are disputable issues on the delimitation of maritime space and ownership of shelf territories, as well as border and customs restrictions on the delivery of personnel, equipment and cargo;

- Seasonality of field works;

- Special requirements for engineering surveys;

- Necessity of using special floating equipment for drilling, surveying, construction and installation works and field operation;

- Availability of marine equipment as part of field facilities requires special requirements to the composition and depth of design documentation, as well as to the frequency of technical inspections (surveys), including special docks.

- Necessity of research and development (R&D) at the stage of design and survey works, which are necessary to justify the adopted technical solutions. Currently, during the creation of capital construction facilities in the Russian Federation, no research and development work is provided for at the stage of design and survey work;

- Complicated logistics of delivery of people, machinery, equipment and materials;

- The need to attract highly qualified highly specialized specialists to conduct research and development, manage complex technologies and equipment in the extreme natural and climatic conditions of the Arctic region;

- High capital intensity and, accordingly, high investment costs of offshore field development projects;

- Specifics of the legal framework regulating economic and financial relations of project participants;

- Availability of special information related to national security including, geological, hydrographic, oceanographic and other;

- High level of risks of attracting investments influenced by the probability of discovering a field with promising reserve volumes, availability of infrastructure, etc;

- Additional difficulties in acquisition of initial geological data in comparison with onshore fields connected with limited drilling season on the shelf and high cost of building offshore exploration wells;

- Absence of a stage of experimental-industrial exploitation in the development of the offshore field;

- Organic connection between the type of offshore field development and its development strategy;

Considering that up to 85% of the Russian shelf area is located in the Arctic and subarctic zones, the following, so-called Arctic factors have a great influence on the choice of basic technical solutions: [45]

- Annual and perennial ice;
- Icebergs;
- Frost heave and ground subsidence during freezing and thawing;
- Erosion;
- Ice;
- Permafrosts;
- Short duration of construction and installation season;
- Long distances to onshore supply bases;
- Polar nights;
- Frequent magnetic storms and other natural phenomena affecting radio communication and stability of navigation devices.

These factors are often decisive in choosing the type of field development and therefore its development, as well as the list of technical solutions that are necessary to ensure reliable operation of the field development facilities in this region.

As is known, the development of an oil, gas or gas condensate field is a complex of measures and activities aimed at extracting the maximum quantity of oil, gas, condensate from the deposit and obtaining high profits with minimum capital investments. Along with the factors common for onshore and offshore fields, determining the strategy of implementation of the mentioned set of measures and measures, development of offshore fields has specific features connected, as it was mentioned above, with presence of new "sea" factors connected with presence of water surface above the field. [45]

5.2 Selection criteria for offshore field development

The presence of water surface over the offshore field determines the specifics of its development. Therefore, unlike onshore fields, the type of offshore field development is determined not only by the relative location and functions of field facilities (centralized or decentralized) or the type of production (cluster or individual) and gathering systems (beam, ring, etc.), but also by the location of production (wellheads), gathering and preparation systems relative to the water surface.

Taking this into account, the following types of offshore field development can be distinguished:

- above-ground;
- above-water;
- underwater;
- combined.

Sometimes in the literature the first two types are considered as similar. Such consideration was true at the initial stages of development of offshore oil and gas production in the first half of the twentieth century. As the offshore oil and gas industry developed, the two types began to differ in terms of the requirements of:

- to technologies and equipment for preparation of hydrocarbons for transportation, water treatment systems for RPM purposes in terms of their performance, layout, reliability and maintainability in offshore conditions;

- safety systems of technological processes, emergency and rescue support of the field facilities;

- Regulatory support of design, construction, and operation of oil-field facilities.

In a more detailed consideration of each of the listed types of facilities these differences will be specified.

Traditionally the selection of field development system is performed at pre-investment stage of field development project or in investment justification by means of technical and economic comparison of different field development options. This considers a number of factors (criteria), which can be combined into several groups. [47]

Geological group includes the following factors:

- geological features of the occurrence of productive horizons;
- Physical properties of rocks;
- the area of the deposit;
- type of deposit.

Group of situational factors:

- sea depth;
- distance to shore;
- Availability of developed infrastructure on the coast;
- location of end users;
- natural and climatic conditions.

A group of technological factors:

- composition of the extracted products;
- selected field development system (depletion, pressure maintenance, etc.);
- Availability of required technologies and technical means for implementation of selected development system.

Economic:

- price of produced hydrocarbons;
- capital investments for construction of facilities
- operational costs;
- taxation regime.

As already noted, the system of offshore field development along with the features inherent to the onshore field (centralized, decentralized, beam, etc.), has several fundamental features, typical only for offshore projects. [46]

These features influence the choice of technologies, equipment, and materials for the organization of production, collection, preparation, and transportation of hydrocarbon raw materials in offshore field conditions and, ultimately, determine the technical and economic performance of offshore field development. [47]

The costs of creating the system of gathering and facilities for the preparation of hydrocarbons in an offshore field constitute more than 70% of all capital investments for its development. The cost of individual oil and gas production platforms reaches several billion dollars. The cost of laying a modern deep-water pipeline is $2-3 million per km.

Manufacturing, installation, operation, and maintenance of a subsea production complex requires the use of new knowledge-intensive high-precision technologies and equipment, which differ significantly from their onshore counterparts both in terms of their mass and dimensions characteristics and their cost. [48]

Therefore, the choice of optimal placement of hydraulic structures over the area of the field, their method of placement (above-ground, above-water, underwater), purpose (production, technological, drilling, storage tankers, multifunctional) largely predetermine both the efficiency of development and optimization of capital and operating costs for the development of the field.

5.3 Field development concepts

An offshore fixed platform is an offshore oil and gas production facility consisting of a topside structure and a support base, fixed on the ground for the entire period of use and an offshore oil and gas field development facility. The average operational period of the fixed at the field is 25 years. [49]

All offshore drilling rigs (platforms) are divided into three main categories:

- stationary - permanent bases, trestles, artificial islands;
- floating (semi-submersible) drilling rigs;
- mobile - drilling ships, barges and other floating devices. [50]

The main problem when designing structures for oil and gas shelf development is that the cost of such structures increases significantly, by several times, with an increase in the depth of the reservoir. Therefore, the main task for the designer is to find an optimal ratio of such indicators as reliability and efficiency of technical means for the operation of fixed platforms in areas with severe ice conditions. [51]

Let's define the factors that need to be paid attention to when designing:

1) Year-round field operation. This factor makes it necessary to design the platform in such a way that it will remain reliable under changing environmental conditions;

2) Durability;

3) Uniqueness of natural and climatic conditions for the field in question. Requires an individual approach in choosing the option of field development.

Hence, when designing the structure for work in the northern regions, the main value of the impact on the structure is the action of the horizontal forces of the moving ice. Average wind pressure on the structure is taken as approximately 2 kPa, waves - from 96 to 144 kPa, ice load is 2.88 MPa and more. [52]

Due to the predominance of the ice load in relation to other loads (wave and wind), the preferred type of ice structures for such areas are monopod structures (i.e., those platforms with one massive support, also called monopods), which better withstand the advancing ice fields.

All structures according to the method of resistance to ice pressure can be conventionally classified into one of three classes:

- Installed on the seabed and equipped with a massive support part (foundation), on which the ice load is applied;

- floating platforms with platform body and tensioning devices or anchor system taking up ice pressure;

- island-type structures, the stability of which is ensured by an embankment of sand or gravel.

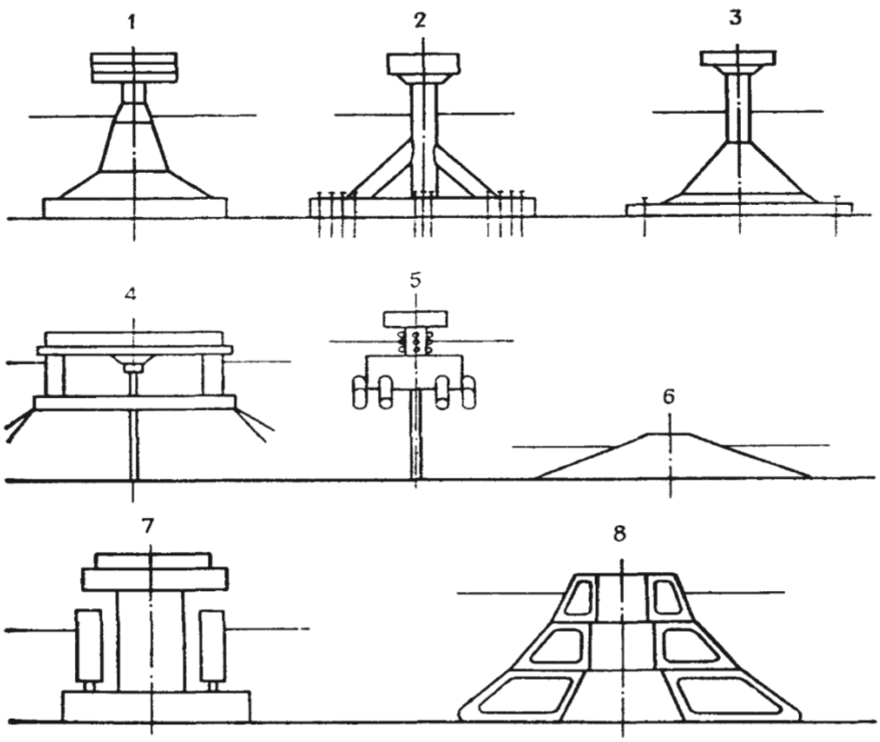

Figure 24 Schemes of structures for operation in various ice conditions [52]

Figure 24 shows diagrams of different types of structures designed for operation in different ice conditions.

In the moderate subarctic ice zone, metal fixed platforms of monopod 2 type are used (Fig. 24, option 2), which are anchored to the seabed with piles.

Floating platforms are not designed for significant ice load, but they are used for exploratory drilling and production in deep waters (Fig. 24, option 4). [52]

Island-type structures have found their application in shallow water areas of the Arctic shelf and are mainly designed for exploratory drilling but removing the wave protection from the island (e.g., sandbags) will lead to its destruction (the island practically disappears under the influence of waves). As the depth of the sea increases, the volume of bulk material at a constant angle of slope increases in an almost cubic relationship. That is why the construction of reusable island constructions allows for considerable saving of construction material. At present, the preference is given to the caisson structures of island-type structures. Concrete blocks, steel ring structures with or without a rigid platform can be used as caissons. For deeper waters, there are designs of individual ring caissons (Figure 23, option 8). For example, Exxon has developed a concrete conical structure design for sea depths of 18-36 m. Underwater ice floes pushing on the structure move up the conical surface and break. In order to apply these structures in deeper waters, Exxon proposed a bottom structure that supports the conical structure, which makes it possible to apply it in depths of up to 60 m.

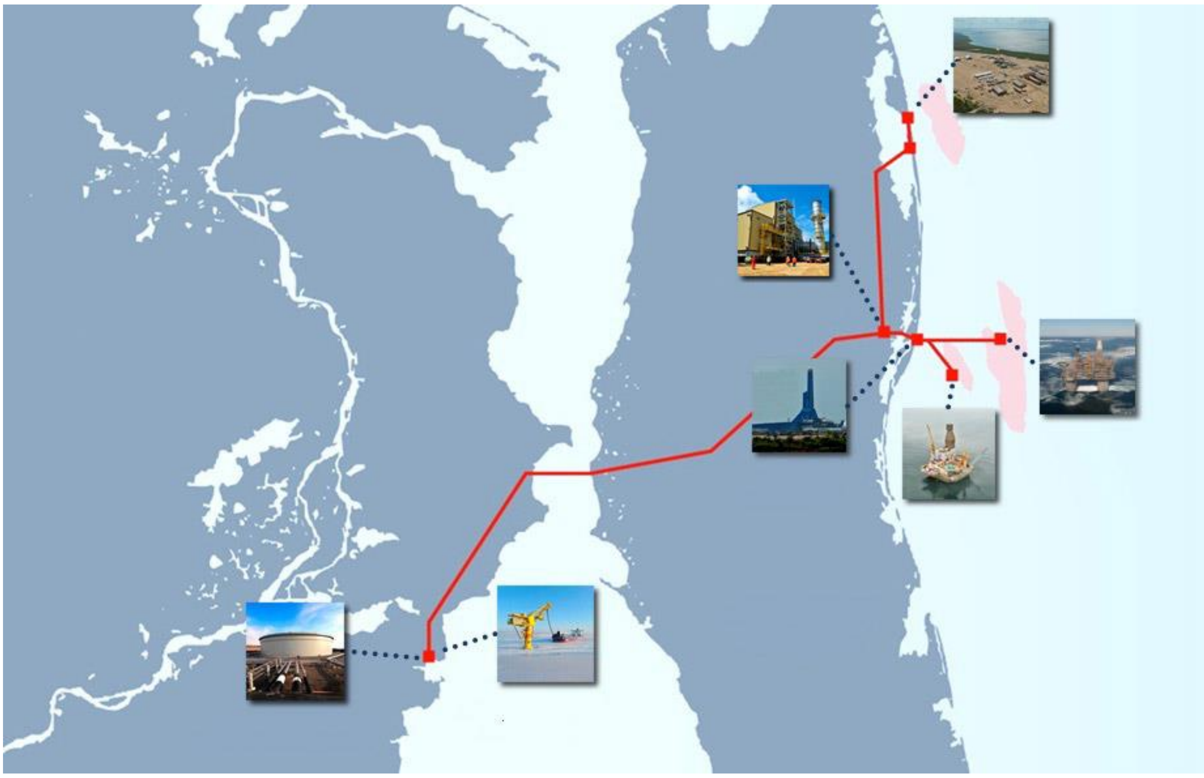

Figure 25 Geographic location of Sakhalin-1 projects [53]

One of the most famous oil and gas development projects of the Okhotsk Sea shelf are Sakhalin 1, 2. "Sakhalin-1 (Figure 25) is an oil and gas project on Sakhalin Island under the terms of a production sharing agreement. The project involves oil and gas development on the northeastern shelf of Sakhalin Island. The project involves the development of the Chaivo, Odoptu-Sea and Arkutun-Dagi fields, with estimated recoverable reserves of 2.3 billion barrels of oil (307 million tons) and 485 billion cubic meters of natural gas.

Sakhalin-2 is an oil and gas project on Sakhalin Island under a production sharing agreement. The project involves the development of two offshore fields: Piltun-Astokhskoye (primarily an oil field with associated gas) and Lunskoye (primarily a gas field with associated gas condensate and oil rim). Total reserves are 182.4 million tons of oil and 633.6 billion m^3 of gas.

5.4 The Orlan platform

The Orlan platform (Figure 26) is a steel-concrete gravity-type structure that houses the drilling and accommodation modules. The platform is used to develop the southwestern part of the Chaivo field. The Chaivo field is located 12 km off the northeastern coast of Sakhalin Island. Sakhalin. Oil and gas produced are delivered to the Onshore Processing Facility (OPF), where products are treated and stabilized for shipment. The oil is transported via a 226 km pipeline crossing Sakhalin and the Tatar Strait to Khabarovsk Krai on the Russian mainland for temporary storage at the De-Kastri terminal. From the De-Kastri terminal, oil flows through an underwater pipeline about 6 km long to the world's largest tanker loading facility, the Single Point Outlet Pier (SPO), where it is loaded into specially designed double-hulled tankers for delivery to customers in the world market. Natural gas is transported through a network of pipelines owned and operated by other companies for sale to buyers in the Russian Far East. [54]

The platform refers to CIDS (CIDS – concrete island drilling system), which is also a mobile offshore drilling unit (MODU - mobile drilling offshore). The platform is designed for offshore drilling in harsh Arctic conditions at depths of 10.7-16.8 m.

Eagle's steel-concrete foundation can easily withstand the onslaught of ice and giant hummocks reaching the height of a six-story building. The weight of the platform is about 70,000 tons. The length of the construction is 96 m, its width - 89,9 m, the total height of the base - 30 m. "Orlan" is able to withstand extremely low temperatures and seismicity up to 8 points, resist a wave up to 13 m high, ice and hummocks up to 6 m high. The power capacity of 14 MW and up to 750 tons of heavy drilling rig with a 2,300 horse-power drive will allow "Orlan" to achieve maximum oil production of 23,000 tons per day, ensuring operation of 20 wells, each of which may deviate up to 13 km along the horizon. [55]

The platform consists of four main components: a steel base, a concrete middle section, and two steel deck sections that house the platform's new world-class drilling rig, process modules, and living quarters. [55]

The installation area of the Orlan platform with the drilling and accommodation modules has a sea depth of 15 m.

Figure 26 Orlan plpatform [55]

5.5 The Berkut platform

Hydrocarbons are produced in the Arkutun-Dagi field from the Berkut gravity platform, which is located about 25 kilometers offshore in the difficult subarctic conditions of the Sea of Okhotsk, where winter temperatures can drop to -44°C, waves reach 18 meters high with wind speeds up to 140 km/hour, and sea ice is up to 2 meters thick. Sea depth in the Arkutun-Dagi field varies from 30 to 40 m. That is why the offshore ice-resistant drilling platform is designed with such a safety margin to ensure year-round operation despite the difficult climatic conditions. [56]

Oil and gas are transported via a new field pipeline to the existing Chayvo onshore processing facility and then through existing pipelines for sale.

In addition, because Sakhalin is in an area of high seismic activity, the Sakhalin-1 operator has equipped the platform with pendulum-type friction mounts to make the structure seismically stable. The platform consists of two parts: a gravity base and the upper structure, where drilling and production equipment and living quarters are located. [56]

The Berkut platform (Figure 27) is designed specifically for operation in harsh subarctic conditions and will be able to withstand waves up to 18 meters high, pressure from ice fields up to two meters thick, and temperatures down to -44 C°.

The gravity base is a rectangular concrete caisson on which 4 concrete columns are set to accommodate the upper structure. - Caisson length - more than 133 m -width -100 m -height with the columns-about 55 m. The weight of the base of the gravity type - 160 thousand tons. [57]

The upper structure is a huge 6-level structure with integrated technological, drilling, residential modules, and other structures. Each level is comparable in size to a standard soccer field. The Berkut upper structure and drilling rig are among the largest and most powerful in the industry. The platform has equipment for wellhead pressure boosting and gas lift gas injection, which allows for maximum oil recovery. The "Berkut" is equipped with a powerful drilling rig designed for work in harsh winter conditions, capable of drilling and carrying out the most complex operations of injecting wells with a step-out of more than 7 km (4.4 miles) from the vertical. There is a total of 45 drill slots on the rig. The rig is capable of moving in all directions between drill holes. The Berkut platform rig allows drillers to use advanced technologies, including a smart well system, dual-horizon well injection, and the installation of multi-horizon gravel packs. [57]

Figure 27 Berkut platform [57]

5.6 The Molikpaq platform

The Molikpaq offshore production platform (Figure 28) is a converted drilling rig previously used in Arctic waters off the coast of Canada. In 1998, the platform was towed from the Beaufort Sea in the Canadian Arctic across the Pacific Ocean to South Korea, where it was refitted for the Sakhalin II project. It was then towed from Korea to Russia and installed on a steel base made by the Amur Shipyard to allow the platform to be used in deeper waters offshore Sakhalin Island. The platform could be used in deeper waters off Sakhalin. The base was filled with sand, which ensured that the structure was firmly fixed on the seabed. [58]

The Molikpaq platform was installed in the Astokh area of the Piltun-Astokh (PA-A) field in the Sea of Okhotsk in September 1998, 16 km offshore, with a sea depth of 30 m at the installation site.

"Molikpaq" consists of a caisson, the center of which is filled with sand to ensure effective anchoring of the platform on the seabed. The main working areas are enclosed, with temperature control and ventilation. The equipment located outdoors is equipped with protection against icing and low temperatures. Living quarters are designed for 132 permanent and 32 seasonal workers. The Molikpaq platform used an extended-reach deviated drilling method with a maximum horizontal deviation of up to 6 km and a maximum well depth of up to 6650 m. [58]

The Molikpaq platform is located 16 km off the coast of northeastern Sakhalin Island. Sakhalin.

The Molikpaq platform is 120 m wide.

The weight of the Molikpaq platform is over 37,500 tons.

More than 150 people live and work on the platform.

Base: 111 m x 111 m.

Weight: 37,523 tons.

Drilling rig height: 101 m.

Top structures: 73 m x 73 m.

Helicopter deck height: 49 m.

Drilling windows: 32 drilling windows.

Operational wells: 13 oil production wells, one gas injection well, four water injection wells, and one drill cuttings injection well.

The Molikpaq platform has a capacity of 90,000 barrels (14,300 m^3) of oil and 2.1 million cubic meters of associated gas per day. Previously, the platform operated only during the summer months; year-round production from Molikpaq began in 2008. [59]

After the minerals are extracted, they are sent via oil - and gas pipelines to the LNG plant in Prigorodnoye (figure 29). The plant itself is divided into two zones (gas and oil) by the so-called green belt.

Figure 28 the Molikpaq platform [59]

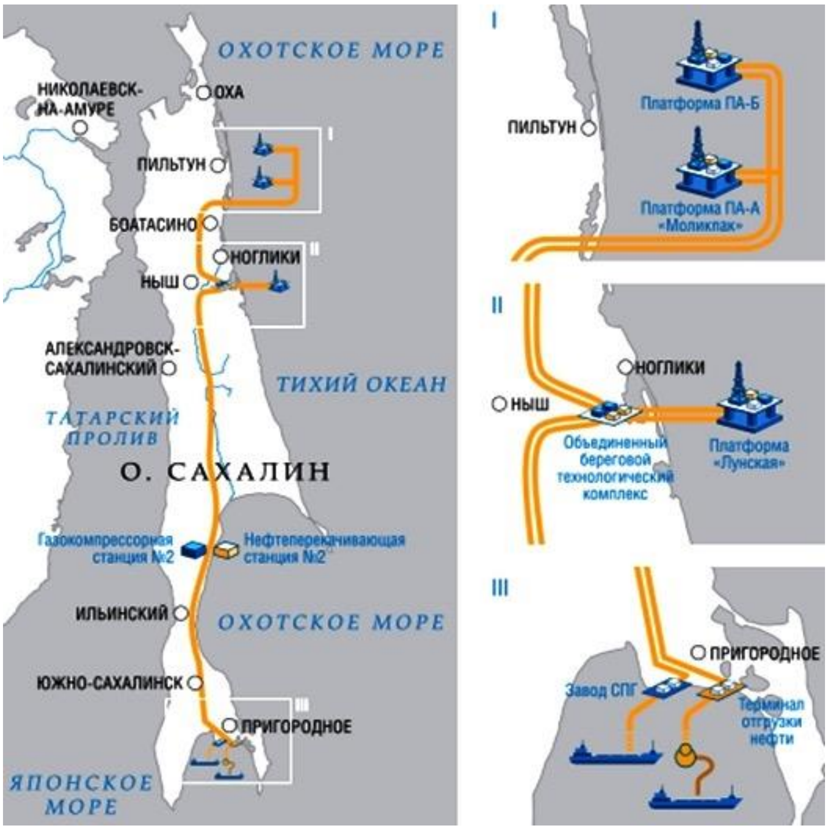

Figure 29 Sakhalin-2 logistic chain [59]

5.7 The Piltun-Astokhskaya-B (PA-B) platform

The hydrocarbons are supplied via the Trans-Sakhalin pipeline system to the LNG plant and the Prigorodnoye oil export terminal.

The base of the platform is a reinforced concrete gravity base with four supports, on which the platform topsides with process facilities are located. The southeast pillar is used as a well site, the northeast pillar is designed for offshore pipeline/pipeline risers with a large radius rounding, and the remaining two pillars serve to install pumps and reservoirs. The topside complex was built in South Korea. The platform topsides contain drilling and liquid hydrocarbon separation equipment, a chemical storage facility, and an accommodation module. The main working areas are enclosed, with temperature control and ventilation. The equipment located outdoors is equipped with ice protection.

The PA-B platform (Figure 30) is designed for year-round operation under harsh climatic, wave, ice and seismic loads. [60]

The platform is installed about 12 km off the northeastern coast of Sakhalin Island. Sakhalin offshore at a depth of 32 m. The concrete base is of gravity type with four supports.

The PA-B platform height is 121 m from the seabed to the top of the deck, i.e., it is equivalent to the height of a 30-storey house.

The platform is equipped with equipment for drilling, hydrocarbon distribution, liquids/water, and chemical storage.

Personnel accommodation: 100 permanent and 40 temporary employees. Oil from the PA-B platform is transported through a system of offshore and onshore pipelines to an oil export terminal in southern Sakhalin. [60]

Foundation:

Height: 53 m.

Mass: 90,000 tons

Dimensions: 94 m x 91.5 m x 11.5 m Support height: 56 m

Top structure:

Flare tube height: 98.6 m Weight: 28,000 tons

Drilling windows: 45

PA-B has a capacity of more than 70,000 barrels (11,100 m^3) of oil and 92 million standard cubic feet (2.9 million m^3) of associated gas per day.

Figure 30 The PA-B platform [60]

5.8 The Lunskaya platform

The Lunskoye oil and gas condensate field is located on the shelf of Northern Sakhalin, 12-15 km east of the island shoreline. The sea depth in the field is 42-47 m.

Lunskoye-A platform is a drilling and production platform installed 15 kilometers off the northeastern coast of Sakhalin Island as part of the Sakhalin-2 project.

The Lunskoye-A (Lun-A) platform (Figure 31) was installed in the Sea of Okhotsk, 15 km off the coast at a depth of 48 m. The Lun-A platform is equipped with minimal technological equipment. It is designed for year-round production and produces most of the gas for the liquefied natural gas (LNG) plant. Primary gas processing takes place at the Onshore Processing Facility, after which the gas is transported to the LNG plant. [61]

The base of the platform is a reinforced concrete gravity base with four supports that house the platform topsides with process equipment and facilities. The southeast pillar is used as a well site, the northeast pillar is designed for offshore pipeline/pipeline risers with a large radius, and the remaining two pillars will be used for installation of pumps and oil transfer tanks.

The platform topsides were built in South Korea. The platform topsides contain drilling and liquid hydrocarbon separation equipment, a chemical storage facility, and an accommodation module. For safety reasons, all process and drilling equipment is located on the opposite end of the platform from the living module. The main working areas are enclosed, with temperature control and ventilation. The equipment located outdoors is equipped with icing and low temperature protection. [61]

Lun-A is used to drill extended reach deviated wells with a maximum horizontal deviation up to 6 km and a maximum true vertical depth of 2920 m.

Personnel accommodation: 126 employees, but up to 140 people live on the platform.

Foundation:

Height: 69.6 m.

Mass: 103,000 tons

Base slab: 88 m x 105 m x 13.5 m Support height: 56 m

Support diameter: 20 m

Upper structure:

Mass: 21,800 t

Flare pipe height: 105 m

Estimated capacity of Lun-A platform is more than 50 million m^3 of gas and approximately 8,000 m^3 (50,000 barrels) of associated condensate and oil per day. [61]

Figure 31 The Lunskaya platform [61]

5.9 The Johan-Castberg field

Johan Kastberg is a site in the Barents Sea, 100 km north-west of the Snow-White field. Water depth is 370 meters The project consists of three fields Skrugard, Havis and Drivis, confirmed between 2011 and 2013. The discoveries will be developed together, and a development and exploitation plan was approved in June 2018. A floating production, storage and offloading unit is planned with additional subsea solutions, including 18 horizontal production wells and 12 injection wells (Figure 32). The reservoirs contain oil with gas caps in three separate deposits. The producing formations are located at depths ranging from 1,350 to 1,900 meters. The field will be developed by maintaining reservoir pressure through gas and water injection. Oil will be offloaded into shuttle tankers and delivered to market. The depth of the subsea production complex is 380 meters. The distance to the shore is about 240km. The reserves of the project are estimated at 70 million tons of oil. [63]

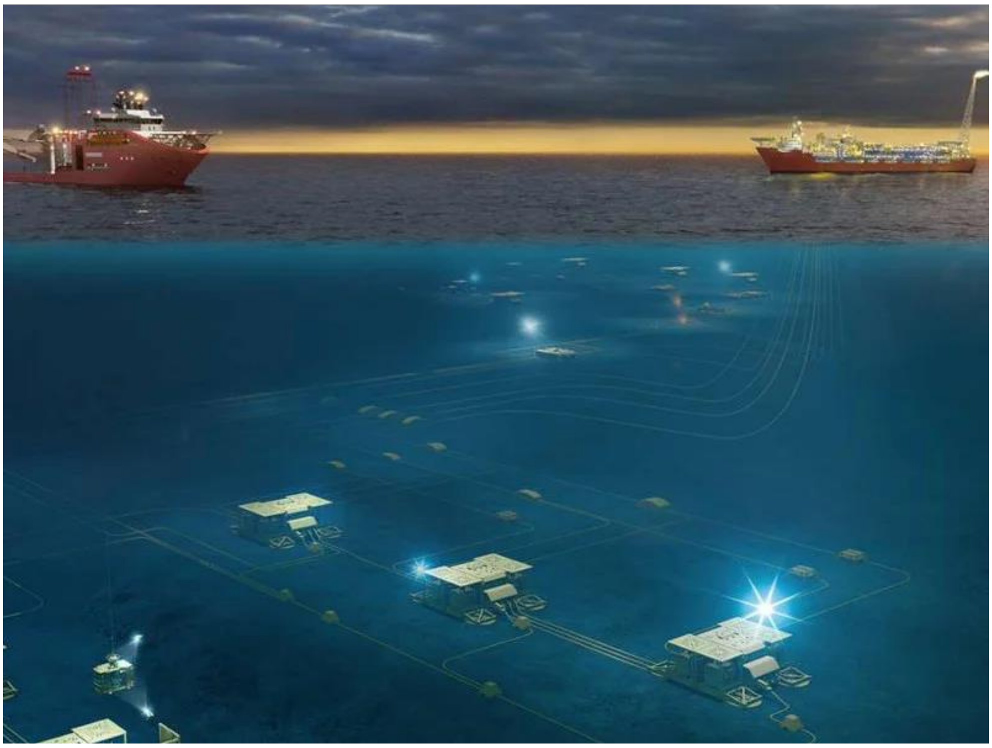

Figure 32 The concept of the Johan Kastberg field development project. [63]

5.10 Yuzhno-Kirinskoye field

Kirinskoye gas condensate field - located in the Kirinskiy block area and belongs to the Sakhalin-3 project on the Sakhalin Island shelf (figure 33). The field was discovered in 1992. Commercial gas production and operation of the field started in 2013.[61] Located 28 km offshore, east of Sakhalin Island. Sakhalin. The sea depth in the area of Kirinskoye field is 91 m [63]. The operator of the project is Gazprom. At present the Kirinskoye gas condensate field holds 137 billion cubic meters of gas and up to 15.9 million tons of gas condensate.

SPS wight is about 400 tons was installed on the seabed, each complex combines 2-4 production wells. The use of production complexes is a new technology which is used in the development of the Kirinskoye field for the first time in Russia.

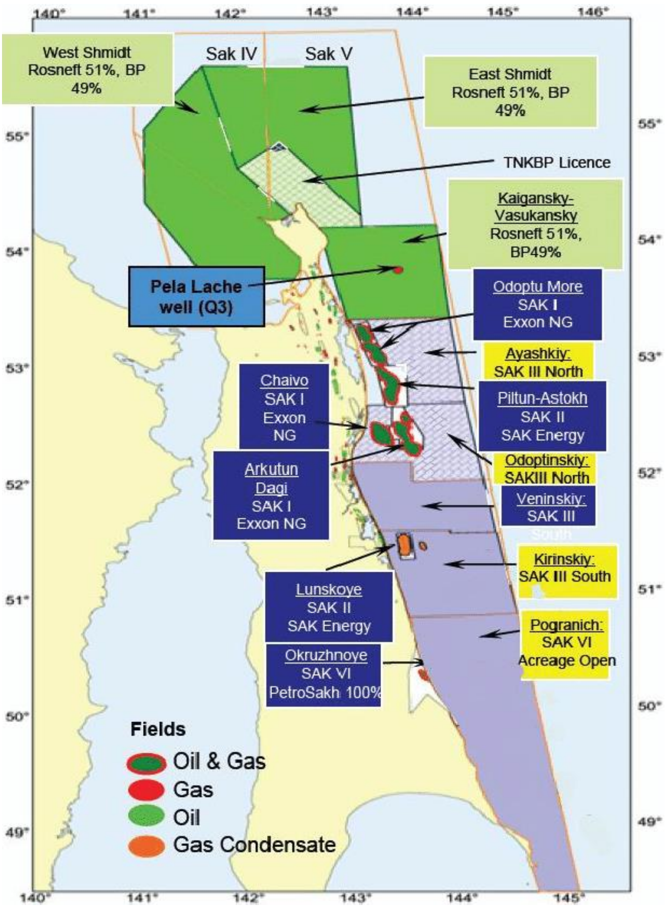

Figure 33 Map showing block areas and primary fields of the Sakhalin projects.[64]

Ice is the most dangerous environment load. The environmental and climatic conditions of this territory are very similar to those of the Arctic. Ice covers the sea for an average 7 months of the year, the beginning of freezing is November, the end of the period is May. The average thickness of ice in a harsh winter reaches 1-2 meters high. The territory of the Okhotsk Sea is characterized by 18,1m - H_{max}, 100-year max of the wave height and 2m – H_s, significant wave height. [66]

SPS located on the seabed of the Sea of Okhotsk (figure 34) without platforms or other above-water structures makes it possible to produce gas under the ice, in difficult climatic conditions, excluding the influence of natural phenomena. This allows us to avoid many of the risks inherent to operations in unfavorable natural and climatic conditions.

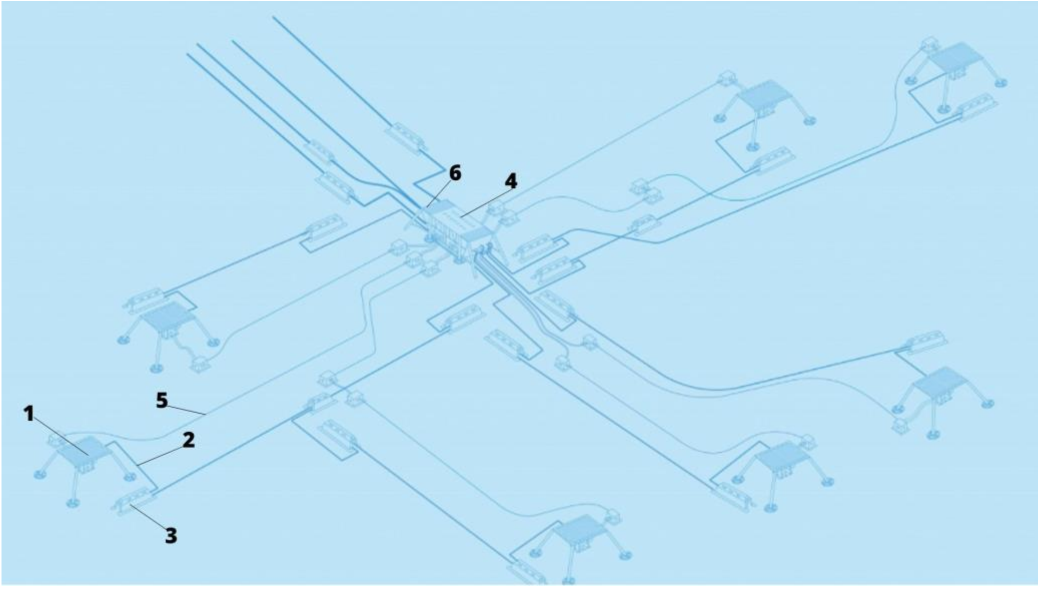

Figure 34 SPS Layout in the Kirinskoye Field [67]

SPS comprises of [67]:

HXT (horizontal X-mas tree with protection equipment) – 1;

- Gathering pipeline – 2;
- Terminal unit – 3, the purpose is to connect the outmost wells under water to a line that is connected to the manifold;
- Manifold – 4, distributes gas, monethylene glycol (MEG), chemicals and control signals to the subsea production facility.
- Intrafield umbilical – 5, serves as the source of the signal
- Outlet – 6, to which the pipe, electro-hydraulic umbilical and special pipeline through which MEG supplies are connected.

5.11 Fram Oil Field Concept

The Fram field is in the North Sea, 65 km off the coast of Kollsnes, at a depth of 360 meters. The field is located next to the largest oil and gas field – Troll field, which consists of two parts: Troll West (oil field) and Troll East (gas field). The scheme of the connection between the fields is shown in Figure 35. [68]

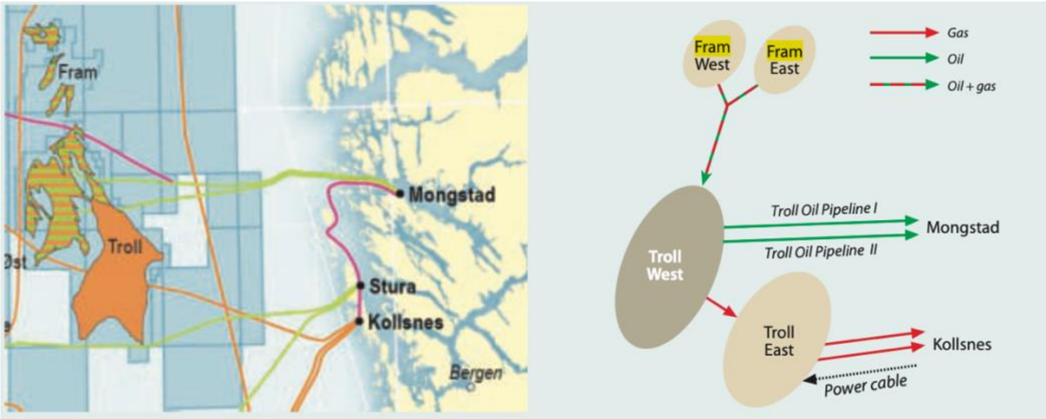

Figure 35 Infrastructure of the Troll site [69]

The development system of the Troll field is divided into three stages:

1) Commissioning of the Troll A platform of the Troll East gas field

2) Commissioning of the Troll B and Troll C platforms, start of oil production

3) Consideration of gas production at Troll West

The Fram field consists of two parts: West and East, and is located at 20km distance from the Troll C. It was technically decided that the oil from the East and West Fram field would be piped to the Troll C platform, where oil would be processed and further transported to shore. Of the disadvantages, it should be noted that the period of oil production in the Fram field depends on the production cycle of Troll C [69]. Figure 36 [70] shows the Fram West development that consists of two subsea templates with five wells, which are connected to the Troll C platform.

In winter the waters on the surface of the North Sea average 6 degrees, and in summer the temperature rises to 17 degrees. During the installation of the advanced guide system on the Trol C platform in [71] weather limits of Hs<1.5m and Tp<10sec were adopted. Consequently, there is no ice in the North Sea. The winter season is characterized by the strongest winds. Average month speeds are 5-6 m/s.

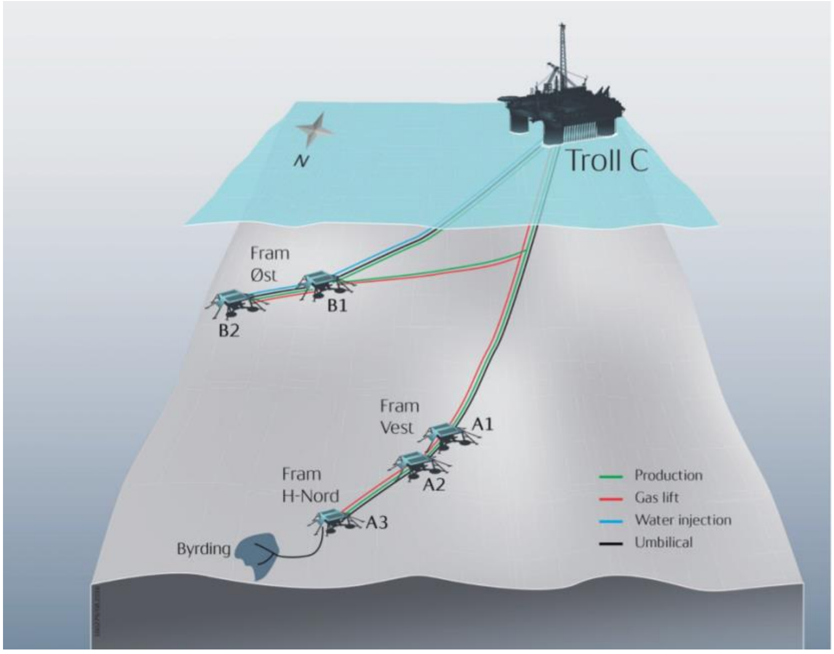

Figure 36 Subsea Layout of Farm field [70]

5.12 Skarv oil and gas field

Skarv is an oil and gas field located in the Norwegian Sea (its northern part). The first oil production started in 2013. The field is located at a depth of 350-450 m and at 200 km distance from the shore.

There are a total of 17 wells in the field. Thirteen of them are production wells (7 oil producing and 6 gas producing wells) and four injection wells. The concept of field development is the joint application of five subsea templates and floating, production, storage, and offloading vessel (FPSO), which is shown in figure 35. The oil offloading system consists of transferring products to shuttle tankers, which deliver the products to refining (figure 37) [72].

Figure 37 The Skarv FPSO [72]

As the vessel potentially could move, the station keeping system must ensure that its excursions remain within the design limits of its risers and dynamic umbilicals. In the event that excursions are not maintained within riser design limits, the risers may fail, and subsequent containment may be lost. The control system in addition to the mooring lines, thus, additional barrier provides greater reliability. The design was made in such a way as to ensure that the ship would remain stationary even if the two mooring lines failed. In calm weather conditions, the heading control system is used for personnel comfort as it is used to minimize vessel movement.

In paper [73] 1, 10 and 100 year extreme 1-hour wind speeds and wave conditions (H_s, T_p) were considered, results are shown in table 9 and table 10 respectively. For wave conditions JONSWAP spectrum was applied. The FPSO vessel is moored in one of the worlds harshest marine environments.

Table 9 Extreme 1-hour average wind speed [73]

Parameter	Unit	Value		
Return period	years	1	10	100
Wind speed	m/s	29,7	33,5	36,9

Table 10 Extreme wave conditions [73]

Return Period, years	Hs, m	Tp, s
1	11	14,6
10	13,7	16,1
100	16,3	17,4
10000	21,4	19,6

The layout of the Sakrv field development is shown in figure 38. [74]

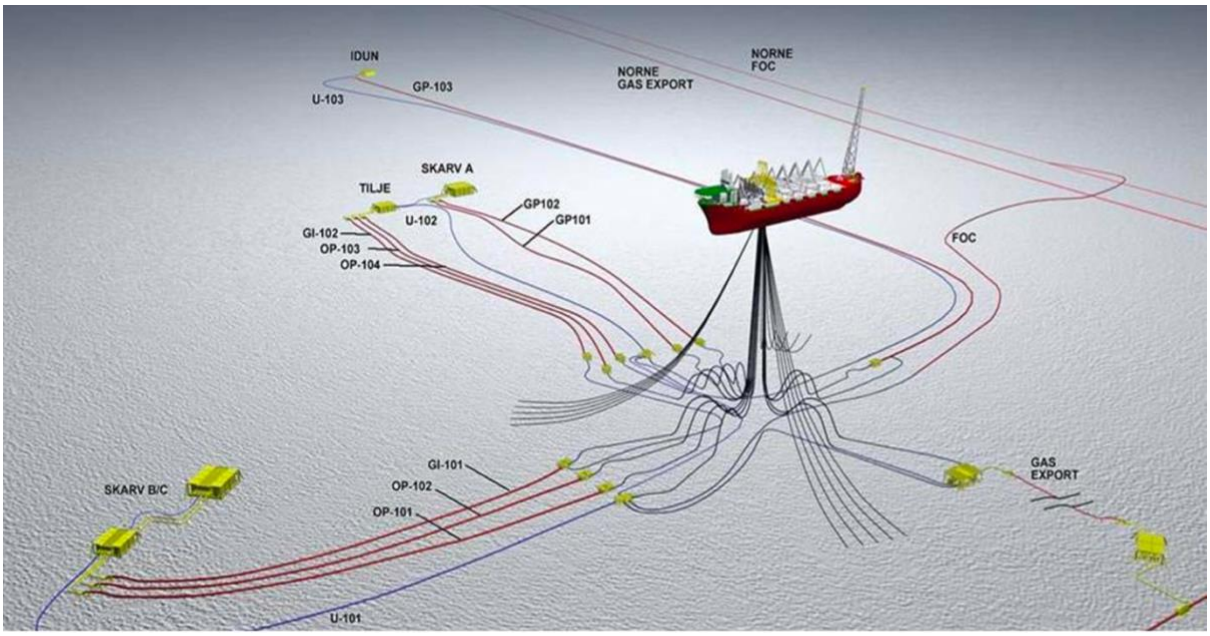

Figure 38 Subsea layout of Skarv field [74]

U – umbilical
GI/GP – gas injector/gas producer
OP – oil producer
FOC – fiber optic cable

5.13 The Triton field concept suggestion

Also, the concept of using SPS paired with FPSO was approved [74] in 2018 for the development of the Johan Castberg field. In the project, 18 production wells and 12 injection wells are approved, which are proposed to be equipped with subsea production equipment.

Basin on the information represented in this section, the strong and weak points are marked in the table 11.

Table 11 Comparison of the different subsea installation concepts

Concept	Strength	Weakness	Application	Comments for the Triton field
SPS and onshore production facility	No impact of severe environment, cost free from water depth	remoteness from the shore, lack of boosting equipment	shallow/deep water	Will there be enough energy to transport the oil to shore?
SPS and FPSO	Mature technology, high capacity for oil storage	Limited resistance to severe conditions	shallow/deep water	The need for FPSO integrity in ice conditions
SPS and platform	Mobility, the ability to produce from neighboring fields	Limited resistance to severe conditions	shallow/deep water	Cost effectivness

The choice of the Triton field development option is proposed using the analogy method. Appendix 3 contains a comparative table of existing offshore field development options.

The proposed comparative table shows three possible offshore field development options: an offshore fixed gravity-based platform, an underwater production facility and the use of a floating unit for oil production, storage, and offloading.

Given the conditions and features of the Triton field in the Sea of Okhotsk, subsea production complex may be the most suitable development option.

It is also worth considering that the reservoir pressure is close to the hydrostatic pressure. Wellhead pressures will be low to achieve target flow rates, indicating the need for subsea multiphase pumps. The maximum achievable SPS connection distance in an oil field using multiphase pumps is 35 km. Connection tests above 50 km encounter problems with pump power, losses, and noise, which prevent normal flow.

The development of a subsea production facility is a promising concept, which has already been used successfully in Norwegian offshore fields such as Johan Kastberg. The use of an SPS with transport of the produced oil to the Molikpaq platform (PA-A), whose upgrade is proposed, for transport via the Trans-Sakhalin pipeline system (Figure 39) appears to be an effective solution for the Triton field.

It is proposed to transport the produced oil to the Molikpaq platform by pipeline, from where the product will be transported to the onshore treatment facility als. It is then proposed to transport the treated product to the Prigorodnoye Oil Export Terminal (OET).

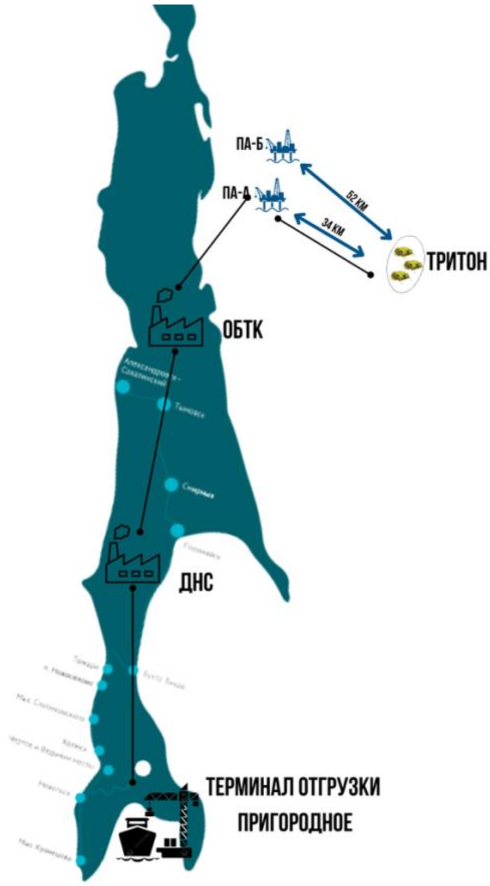

Figure 39 Suggested logistic for the Triton field oil products

The suggested concept shall include integrated template structures (IST) that contains Xmas trees and should further be connected to manifold to transport HC. According to the research carried out and the results obtained in [76], the use of 4 slots integrated template structures is recommended as the optional scenario. An important technical point is the selection of the necessary IST installation facilities (vessel, wire, crane etc.) and the determination of the feasibility of a lifting operation to install the module at the sea condition. This issue and the calculation of the maximum possible sea state at which the module can be safely launched is described in detail in appendix 4. Based on the results of the calculations presented in appendix 4, for the selected vessel and template it is determined that at significant wave height values not exceeding 3 m, the descent operation will be safe. For significant wave heights exceeding 3 m, it is recommended to postpone the operation and wait for favorable conditions. These calculations are important for the entire project as they help to avoid accidents, save lives, protect the environment, and preserve the integrity of the equipment. Any complication could lead to a delay in the project phase, which in turn would have an impact on the delay in the start of first oil production.

Chapter summary

As a result of the analysis and justification of various options for developing the Triton field offshore the Sea of Okhotsk, it was found that the use of an underwater production complex is the preferred solution.

This choice is driven by several factors. Firstly, the economic component plays an important role. An underwater production complex has lower construction and operating costs, which significantly affects the total cost of the project. This reduces investment risks and increases the financial efficiency of the project.

Secondly, the subsea production complex provides greater safety and reliability. In the Sea of Okhotsk with its severe weather conditions and seismic activity, use of the subsea production system makes it possible to minimize the risk of emergencies and ensure continuous production.

In addition, the use of the subsea production complex makes it possible to reduce the negative impact on the environment. More efficient use of resources, absence of air emissions and lower risk of oil spills contribute to sustainable operation of the field and reduction of environmental impact.

Thus, the selection of an underwater production facility for the Triton field development in the Sea of Okhotsk is optimal considering technical, safety and environmental factors. This solution will ensure efficient and sustainable oil and gas production, reduce risks, and ensure long-term profitability of the project.

Conclusion

The research carried out on the selection of the Triton field development and the definition of the development system for the Okhotsk shelf included an analysis of the natural and climatic conditions, the geological characteristics of the field, and the principles of offshore field development. The analysis of these factors led to conclusions and recommendations that are crucial for the development of the field and ensuring safe and efficient oil and gas production.

The first chapter dealt with the stages of oil and gas field development projects. The main stages were identified and described, and this Master's thesis relates to the project planning stage and includes the review of existing field development concepts, development concept suggestion, the determination of the required number of production and injection wells, the number of templates, well drilling rates and engineering design.

In the second chapter, it was noted that the natural and climatic conditions of the Okhotsk Sea, such as strong winds, storms, tsunamis, and ice, can significantly affect the operation of oil platforms and vessels. These conditions pose risks to infrastructure and complicate oil production operations. It is recommended that these conditions are considered when selecting field development options and that appropriate technical solutions are applied to ensure safety and minimise risks.

The third chapter focused on the geological characteristics of the Triton field. The processes of hydrocarbon formation and accumulation were examined, and an assessment of the geological reserves of oil and gas was made. The results of the analysis demonstrated the perspectivity and significance of the Triton field and categorised it as a major reserve. These results provide a basis for making informed decisions on development and project planning.

In the chapter dedicated to the offshore oilfield development system, key principles and parameters of reservoir development were analysed. Using the non-piston displacement theory, the technological performance indicators for the

V1-1, V1-2 and V-0 reservoirs were evaluated. The calculations and analyses showed that the development period for the V1-1 reservoir, using 10 producing wells, would be 27 years with an expected ultimate recovery factor of 28.52. For the V1-2 and V-0 reservoirs, the development period was determined to be 28 years. Thus, this chapter has provided an analysis and evaluation of various parameters and factors associated with the Triton field development system on the shelf of the Okhotsk Sea. The results and assumptions obtained can serve as a basis for further design and development of the field.

The fifth chapter examined various options for the field development system, including the use of a subsea production complex. An analysis of technical, safety and environmental factors indicated that the subsea production system was the preferred development solution. This choice is justified by its low construction and operating costs, by ensuring safety and reliability of operations, and by minimising negative environmental impacts in the event of emergencies. It is proposed that produced products from the Triton field be transported via a subsea pipeline to the Molikpaq platform, which is located 34 km from the field. Then the products are delivered to the onshore processing terminal, from where they are transported through a system of pipelines to the oil loading terminal in Prigorodnoye. It has been revealed that the recommended option for the field development is the use of a 4-slot template. However, it is worth noting that when recommending the modification of the template, it is worth considering the possibility of a marine operation to install it. This issue is considered separately in Appendix 4.

Appendix 4 highlights the important issue of defining the Okhotsk Sea limit states in which marine operations are permitted. This issue is important because it can complicate the field development process, which is the focus of this study. Therefore, given the assumptions made, it was determined that it was not advisable to conduct offshore operations in sea conditions of greater than H_s=3m for the recommended template, wire and installation vessel, which was used to install the templates in the Kirinskoye gas condensate field. This reasoning avoids and reduces the risks of loss of personnel, damage to the environment and loss of equipment.

Economic analysis plays a crucial role in determining the financial feasibility and profitability of a project. It involves assessing various factors such as capital costs, operating expenses, revenue projections, and market conditions. However, without a fixed investment date, it becomes difficult to estimate the specific economic indicators and perform a comprehensive evaluation.

Once an approximate project start date is established, it would become possible to carry out a more detailed economic analysis. This would involve examining the current market conditions, studying historical price trends, and considering relevant economic indicators. By incorporating these factors into the analysis, it would be possible to assess the project's financial viability and determine whether it is economically feasible to proceed.

It is important to emphasize that conducting an economic analysis is a complex and rigorous process that requires accurate data, reliable forecasts, and comprehensive market research. Given the fluctuations in oil prices and the uncertainties associated with economic conditions, it is essential to approach the analysis with caution and to update it regularly as new information becomes available.

Overall, based on the conducted research, *where a technically feasible development solution has been identified,* it can be concluded that the development of the Triton field on the Okhotsk Sea shelf is promising. Considering the natural and climatic conditions, applying advanced technologies and extraction methods, and strictly adhering to safety measures and economic factors, high efficiency and project sustainability can be achieved.

Reference list

1. Gudmestad, O.T., Løset, S., Alhimenko, A.I., Shkhinek, K.N., Tørum, A., Jensen, A.: "Engineering aspects related to Arctic offshore developments," LAN, St Petersburg, 2007.
2. "Sakhalin Indigenous people settlements," URL: http://simdp.com/eng.php?id=22&pid=21 [Last access 1st June].
3. Geonedra, "Triton field description", https://geonedra.ru/2018/triton-oil-fiedld/ [Last access 1st June].
4. Chief Directorate of the Hydrometeorological Service under the USSR Council of Ministers,"Handbook on the climate of the USSR humidity of air, atmospheric precipitations, snow cover," 1970, Edition no. 34. Sakhalin region. "Справочник по климату СССР. Выпуск 34. Сахалинская область. Влажность воздуха, атмосферные осадки, снежный покров."
5. Russian ministry of Emergency Situations, "Characteristics of the Sakhalin region", URL: https://65.mchs.gov.ru/glavnoe-upravlenie/harakteristika-subekta [Last access 1st June].
6. Sakhalin energy, "Reconstruction of the well stock at the Astokh area of the Piltun-Astokhskoye oil and gas condensate field (Group 6)." Environmental impact assessment, "Реконструкция фонда скважин на Астохском участке Пильтун-Астохского нефтегазоконденсатного месторождения (группа 6)" ОЦЕНКА ВОЗДЕЙСТВИЯ НА ОКРУЖАЮЩУЮ СРЕДУ
7. Novinenko, E.G. "Peculiarities of the thermal regime of the Okhotsk Sea", Russian Fishery Industry Repository, 2007, "Особенности термического режима охотского моря"
8. Andreev, A. G. "Mesoscale Circulation of Waters in the Region of the East Sakhalin Current (the Sea of Okhotsk).", Izvestiya, Atmospheric and Oceanic Physics, Volume 56, Issue 12, p.1628-1637
9. Gazenko O.Yu., Sarapulov V.N., Khakhaev I.A. "Hydrodynamic analog of water and ice circulation adaptation on condition of the sea of Okhotsk.", ISSN 1991-5497. World of science, culture, education journal, no. 4 (41) 2013
10. Dashko N.A. "Peculiarities of the winter wind regime in the Sea of Okhotsk," Proceedings of the USSR Hydrometeorological Center, 216, 110-119.
11. "Hydrometeorology of the Sea of Okhotsk," Unified state system on the situation in the world's oceans, URL: http://www.esimo.ru/atlas/Oxot/3_wavesheight_waterarea_recurrence_0.html [Last access 1st June].

12. Pisarev, S.V., Tsvetsinsky, A.S., Onishchenko, D.A. "Stratified Ice on the Sea of Okhotsk Shelf - Problem of Identification and Potential Threat to Offshore Structures", FSBI "GOIN," Gazprom VNIIGAZ LLC.
13. Petrov A.G., Stasiuk E.I. "Icing of ships in the Okhotsk sea," State Institution "Far Eastern Regional Hydrometeorological Research Institute" (FERHRI), (GU "DVNIGMI"), Обледенение судов в Охотском море," Петров А.Г., Стасюк Е.И.
14. Gazpromneft , company's internal document: "The Triton field description".
15. Rosgeologiya, Sevmorneftegeofizika, Росгеология, Севморнефтегеофизика, URL: http://smng.com/(ru) [Last access 1st June].
16. Kharakhinov V.V. "Tectonics of the Okhotomorskaya oil and gas bearing province." D. dissertation of Doctor of Geological and Mineralogical Sciences, SakhalinNIPIMorneft, 1998. "Харахинов В.В. Тектоника Охотоморской нефтегазоносной провинции. Дис. д-ра геол.-минер. наук. Оха-на-Сахалине: СахалинНИПИМорнефть, 1998."
17. Shein V.S., Ignatova V.A. "Geodynamics and oil and gas potential of sedimentary basins of the Far East," Moscow, Publ. of VNIGNI, 2007.
18. Gaynanshin R.N., Logvinenko N.V., Zhukovskaya E.A., Snachev M.V., , Litvin V.V., Tanygin I.A., "Shelf of Sakhalin Island- new horizonts", "Oil economy" journal.
19. Otis R.M., Schneidermann N. "A Process for Evaluating Exploration Prospects," AAPG Bulletin (1997) 81 (7): 1087–1109.
20. Delfiner P. "Modeling dependencies between geologic risks in multiple targets," 9P, SPE 63200, 2000.
21. Demidkina, S. "Probabilistic assessment of oil and gas reserves in the 'EVA - Risk Analysis' software." Gubkin Russian State University of Oil and Gas., Демидкина С. Вероятностная оценка запасов нефти и газа в программе «EVA - анализ рисков» РГУ нефти и газа им. И.М. Губкина, факультет геологии
22. Caldwell R.H., and Heather, D.I. "How to Evaluate Hard-to-Evaluate Reserves." Journal of Petroleum Technology 43 (1991): 998–1003.
23. Holmes A.; Illowsky B.; Dean S.. "Introductory Business Statistics." OpenStax, Senior contributing authors. The University of Oklahoma, DeAnza College.
24. Kosova R.; Shehu V.; Naço A.; Xhafaj E.; Stana A.; Ymeri A.. "Monte Carlo simulation for estimating geologic oil reserves, a case study from Kuçova oilfield in Albania.", Muzeul Olteniei Craiova. Oltenia. Studii şi comunicări. Ştiinţele Naturii. Tom. 31, No. 2/2015 ISSN 1454-6914
25. Rasheed, R.; Kulkarni A. "Reserve Estimation Using Volumetric Method." International Research Journal of Engineering and Technology (IRJET) 03, no. 10 (Oct 2016).

26. Gainanshin R.N.; Zhukovskaya E.N.; Snachev, M.V. "Forecasting discoveries of hydrocarbon deposits in the North Sakhalin petroleum region based on statistical analysis.", editorial staff publishing house “Oil industry”, 5th edition, 2019.
27. Ministry of Natural Resources of the Russian Federation. "ORDER of November 1, 2005, N 298 on approval of the classification of oil and gas reserves and inferred resources."
28. Yushkov R.; Khizhnyak G.P.; Ilyushin P.Y. "Oil and gas field development." IPublishing House of Perm National Research Polytechnic University, 2013.
29. Mikhailov N.N. "Physics of oil and gas reservoirs (physics of oil and gas reservoir systems): Volume 1: Textbook.", Foundation: Textbooks and training manuals, Publisher: MAX Press, 2008., Михайлов Н.Н. Физика нефтяного и газового пласта (Физика нефтегазовых пластовых систем)., Фонд: Учебники и учебные пособия, Издательство: МАКС Пресс, 2008.
30. Amix J.W.; Bass D.M.,. Whiting R.,L., "Petroleum Reservoir Engineering: Physical Properties." The Agricultural and Mechanical College of Texas., McGraw-Hill Book Company, Inc. (June 1, 1960)
31. S&P Global Commodity Insights, Relative permeability, URL: https://www.ihsenergy.ca/support/documentation_ca/Harmony/content/html_files/reference_material/general_concepts/relative_permeability.htm
32. Kovalev I.B. Master's thesis. "Geological structure, reservoir properties, and fluid characteristics of the Nutovsky horizon of the Chayvo oil-gas-condensate field (Sakhalin region).", Tomsk Polytechnic university.
33. Bogdanchikov S.M.; Astafiev V.N.; Bojarshin E.K. "Exploration and Development of Oil and Gas Field on the Shelf of Sakhalin.", The Proceedings of The Fifth (1995) International OFFSHORE AND POLAR ENGINEERING CONFERENCE, volume 1, 1995.
34. Boyko V.S. "Development and Exploitation of Oil Fields: Textbook for Universities." Moscow, Nedra publisher, 1990.
35. Vladimirov I.V.; Almukhametova E.M. "Efficient Allocation of Production Well Rows and Injection Wells in Highly Viscous Oil Deposits with Extended Zones of Reservoir Deconsolidation.", journal: Problems of collection, treatment and transport of oil and oil products, volume 3, 2019 , И.В. Владимиров Э.М. Альмухаметова Эффективное размещение рядов добывающих и нагнетательных скважин в нефтяных залежах высоковязкой нефти с протяженными зонами разуплотнения коллектора
36. Potashev K.; Mazo A. "Mathematical Modeling of Oil Reservoir Waterflooding Using Fixed Streamtube at Various Values of Viscosity Ratio.", Georesursy 22(4):70-78, 2020

37. Khisamov R.S. "Features of geological structure and development of multilayer oil fields." Kazan: Publishing House "Monitoring," 1996.
38. Boyko V.S. "Development and Operation of Oil Fields.", Nedra publisher, Moscow, 1990,
39. Lysenko V.D. "Designing Development of Oil Fields." Nedra publisher, Moscow, 1987.
40. GolenkinM.Yu.; Latypov A.; Shestov S.; Bulygin, I.; Khakmedov A. "First Intelligent Multilateral TAML5 Wells on the V. Filanovsky Field.", Rogtec journal, 2018.
41. Tumen state university, student textbook, URL: https://www.tyuiu.ru/media/files/2015/01_19/uchebnoe-posobie.pdf [Last access 1st June].
42. Zhibin Zh., Jiexiang W., Jing Zh., Research on the overall optimization method of well pattern in water drive reservoirs, Journal of Petroleum Exploration and Production Technology 7(2), 2016.
43. Zheltov Y. P., Strizhov I. N., Zolotukhin A. B., Zaitsev V. M., Oil field development tasks, textbook, Nedra publishing, Moscow, 1985, Ю. П. Желтов, И. Н. Стрижов, А. Б. Золотухин, В. М. Зайцев, сборник задач по разработке нефтяных месторождений, учебное пособие
44. Ovcharenko D.M., Chukhareva N.V. Development of technical solutions for the construction of underwater gas pipelines in the Arctic shelf // Abstracts of the conference. - Tomsk: National Research Tomsk Polytechnic University, 2022., Овчаренко Д.М., Чухарева Н.В. Разработка технических решений по сооружению подводных газопроводов в условиях арктического шельфа // Тезисы доклада на конференции. - Томск: Национальный исследовательский Томский политехнический университет, 2022..
45. Gudmestad, O.T., Løset, S., Alhimenko, A.I., Shkhinek, K.N., Tørum, A., Jensen, A. Engineering aspects related to Arctic offshore developments. LAN publisher, St Petersburg, 2007.
46. Borodin A.S., Glushkov V.V., Zavyalov D.V., Markelov S.M. Technological features of offshore field development. // Offshore oil and gas technologies. - volume 4, 2014. , Бородин А.С., Глушков В.В., Завьялов Д.В., Маркелов С.М. Технологические особенности обустройства морских месторождений. // Морские нефтегазовые технологии.
47. Shiller A.M., Semenov M.G. Development of oil and gas fields on the shelf. // Nedra publisher, Moscow, 2004, Шиллер А.М., Семенов М.Г. Разработка нефтяных и газовых месторождений на шельфе. // Москва: Недра, 2004.
48. Government of the Russian Federation, Rules for the Development and Exploitation of Oil and Gas Fields on the Shelf of the Russian Federation, approved by Decree No. 1555 of the Government of the Russian

Federation, dated November 21, 2019., Правила обустройства и эксплуатации нефтегазовых месторождений на шельфе Российской Федерации, утвержденные постановлением Правительства РФ от 21 ноября 2019 г. № 1555.
49. Ilyina S.V. "Problems in selecting the type of marine stationary platform for operation in ice conditions" / S.V. Ilyina. - Proceedings of the First International Scientific Conference "Technical Sciences in Russia and Abroad" (Moscow, May 2011), Moscow., Ильина, С. В. "Проблемы при выборе типа морской стационарной платформы для работы в ледовых условиях" / С. В. Ильина. — Материалы I Междунар. науч. конф. "Технические науки в России и за рубежом" (г. Москва, май 2011 г.), Москва.
50. Borisov R.V., Makarov V.G., Makrov V.V., Nikitin V.S., Portnoy A.S., Simonenko A.S., Sokolov V.F., Stepanov I.V., Timofeev O.Ya. Part I. Offshore drilling rigs: Textbook.". - SPb.: Shipbuilding, 2003., Борисов Р.В., Макаров В.Г., Макров В.В., Никитин В.С., Портной А.С., Симоненко А.С., Соколов В.Ф., Степанов И.В., Тимофеев О.Я. "Морские инженерные сооружения. Ч.I. Морские буровые установки: Учебник." – СПб.: Судостроение, 2003 г.
51. Arctic bases of economical construction" (Skenska firm, Sweden) - Oil, gas and petrochemistry abroad. № 3, 1985, Арктические основания экономичной конструкции" (фирма «Скенска», Швеция) – Нефть, газ и нефтехимия за рубежом. №3, 1985.
52. Potapov V.M. "Features of Creating Floating Drilling Rigs for Operation in Conditions of Northern and Far-Eastern Seas" / Shipbuilding Technology № 9, 1990., Потапов В.М. "Особенности создания плавучих буровых установок для эксплуатации в условиях северных и дальневосточных морей" / Технология судостроения No 9, 1990 г.
53. Prima media, Sakhalin area, URL: https://primamedia.ru/news/555205/
54. Gazpromnet, materials from the official website of the project developer: "Construction of the Orlan Platform at the Chayvo Field (Sakhalin Island), Материалы официального сайта компании-разработчика проекта: "Строительство платформы «Орлан» на Чайвинском месторождении (остров Сахалин)", URL: https://www.gazprom-neft.ru/press-center/project-works/development-of-fields/4214467/ [Last access 1st June].
55. Godblesky R. O. "Construction of the Orlan platform at the Chayvo field on Sakhalin Island." Proceedings of the International Scientific and Practical Conference "New Technologies in Construction and Design," 7(3), 2019, Годблесский, Р. О.. "Строительство платформы «Орлан» на Чайвинском месторождении острова Сахалин". Труды Международной научно-практической конференции «Новые технологии в строительстве и проектировании», 7(3), 2019.

56. Slatnick S. C., Fenz D. M., Sheppard R. E., Turner J. W. "Seismic Challenges and Structural Solutions on the Berkut Platform." Paper presented at the SPE Arctic and Extreme Environments Technical Conference and Exhibition, Moscow, Russia, october, 2013, URL: https://doi.org/10.2118/166913-MS [Last access 1st June].
57. Neftegazru, Berkut offshore ice-resistant platform, Oil and Gas Business, Neftegaz.RU journal, № 10, 2014, Морская ледостойкая платформа «Беркут», Нефтегазовое дело, «Neftegaz.RU» №10, 2014.
58. Sakhalin Energy, Molikpaq offshore production platform, Морская добывающая платформа Моликпак, Сахалин Энерджи, URL: https://www.sakhalinenergy.ru/ru/company/assets/molikpaq/ [Last access 1st June].
59. Khanakhmedov N.B. Explanatory note on the discipline "Features of well construction on the shelf and in the Arctic", Offshore fixed platform "Molikpaq", Engineering School of Natural Resources (ISNR), Tomsk, 2022, Ханахмедов Н.Б-о. Пояснительная записка по дисциплине «Особенности строительства скважин на шельфе и в Арктике», Морская стационарная платформа «Моликпак», Инженерная школа природных ресурсов (ИШПР)
60. Sakhalin Energy, PA-B offshore production platform , Морская добывающая платформа ПА-Б, Сахалин Энерджи, URL: https://www.sakhalinenergy.ru/en/company/assets/pab/ [Last access 1st June].
61. Sakhalin Energy, Lunskoye offshore production platform, Морская добывающая платформа Лунское, Сахалин Энерджи, URL: https://www.sakhalinenergy.ru/en/company/assets/lunskoe/ [Last access 1st June].
62. Offshore technology, Johan Castberg Field Development Project, Barents Sea, August 23, 2019, URL: https://www.offshore-technology.com/projects/skrugard-field-development-project-norway/
63. Wikipedia, The Kirinskoye gas condensate field, Киринское газоконденсатное месторождение, URL: https://ru.wikipedia.org/wiki/Киринское_газоконденсатное_месторождение [Last access 1st June].
64. Jaehong K., Petroleum geology of the Sea of Okhotsk region, the Russian Far East, Research Gate, December, 2010.
65. Safonova E. "Everything is ready for 'Sakhalin-3,' heading to Shtokman", Rbk daily, 2011, URL: https://web.archive.org/web/20110701072537/http://www.rbcdaily.ru/2011/06/30/tek/562949980550418 [Last access 1st June].
66. Russian Maritime Register of Shipping, Reference data for the wind mode of the Barents, Okhotsk and Caspian Sea. Saint-Petersburg: Report.

67. Gazprom, Subsea Production System at the Kirinskoye gas condensate field, URL: https://sahalin-shelf-dobycha.gazprom.ru/about/technologies/pdk/
68. Norwegian Petroleum Directorate, Fram field, URL: https://factpages.npd.no/en/field/pageview/all/1578840 [Last access 1st June].
69. Industrial Heritage Plan, Oil and gas Fields in Norway, URL: https://www.norskolje.museum.no [Last access 1st June].
70. Equinor, Completes acquisition Byrding interest, URL: https://www.equinor.com/news/archive/completes-acquisition-byrding-interest [Last access 1st June].
71. Hjermann B. K., "Fram Vest project – Subsea tie-back to a floating production unit." Paper presented at Offshore Technology Conference, OTC 16532, 2004.
72. Aker BP., Skarv project. URL: https://akerbp.com/en/asset/skarv-2/ [Last access 1st June].
73. Naciri M., Heimsnes T. E., Newport A., le Mée R., "Feedback on the Design and Operation of the Skarv FPSO Mooring System." Paper presented at Offshore Technology Conference, OTC-27743-MS.
74. Sangesland S., Bergsaker T., "Subsea Well Intervention in the North Sea, Learning from Mistakes and Experience." Earth Sciences and Petroleum Engineering, June, 2012.
75. Pribytkov E.A.; Zolotukhin A.B.; Gudmestad O.T., Optimization of Integrated Template Structures for Arctic Subsea-Production Systems, Oil & Gas Fac 3 (04): 47–53.
76. Volkov A.V., Gudmestad O.T., SPS installation and calculating loads on it, University of Stavanger, Marine operations course project, autumn, 2022.
77. Wikipedia, Akademik Chersky, URL: https://ru.wikipedia.org/wiki/%D0%90%D0%BA%D0%B0%D0%B4%D0%B5%D0%BC%D0%B8%D0%BA_%D0%A7%D0%B5%D1%80%D1%81%D0%BA%D0%B8%D0%B9 [Last access 1st June].
78. DNV·GL, Recommended practice: Modelling and analysis of marine operations, DNV-RP-H103
79. OrcaFlex technical specification, version 11.3
80. Marine operations course lecture materials, University of Stavanger, autumn, 2022.
81. Ab Aziz M.Yu., Muhamad N.H., Ardiyansyah S., Analysis of hydrodynamic force acting on commercialized rowing blades using computational fluid dynamics, AIP Conference Proceedings 1831(1):020017, April 2017

Appendix 1 Geological reserves estimation program

Handwritten code for a program for modelling the distribution of probability oil reserves:

Import of the necessary libraries :

```
[1]: from scipy.stats import *
     import numpy as np
     import seaborn as sns
     import matplotlib.pyplot as plt
```

Oil calculations

```
[2]: #iterations is the number of times you wish to run the simulation. The higher the better. Remember that higher numbers
     iterations = 1000

     Area = norm(25134,3000).rvs(iterations) # oil and gas area
     Thickness = norm(13.4,1).rvs(iterations) # thickness of the oil interval
     Por = norm(.36,.03).rvs(iterations) #reservoir porosity
     Sw = 0.49 #initial water saturation
     ro = 818 #oil density
     Bo = 1.144 #conversion factor

     stoiip = Area * Thickness * Por * (1 - Sw) * ro / Bo / 1000
```

```
[3]: #plot1
     plot1=sns.distplot(stoiip,
                        kde=True,
                        norm_hist=True,
                        #color='skyblue',
                        #hist_kws={"linewidth": 15,'alpha':1}
                       )
     plot1.set(xlabel='Normal Distribution', ylabel='Frequency')
     plt.figure()

     #plot2
     plot2=sns.distplot(stoiip,
                        hist_kws=dict(cumulative=True),
     kde_kws=dict(cumulative=True))

     plot2.set(xlabel='STOIIP thousand tonnes', ylabel='probability')
     plot2.axhline(y=0.9, label='P10', color="red")
     plot2.axhline(y=0.5, label='P50', color="red")
     plot2.axhline(y=0.1, label='P90', color="red")

     plt.show()
```

```
/Users/aleksandrvolkov/opt/anaconda3/lib/python3.9/site-packages/seaborn/distributions.py:2619: FutureWarning: `distp
lot` is a deprecated function and will be removed in a future version. Please adapt your code to use either `displot`
(a figure-level function with similar flexibility) or `histplot` (an axes-level function for histograms).
  warnings.warn(msg, FutureWarning)
/Users/aleksandrvolkov/opt/anaconda3/lib/python3.9/site-packages/seaborn/distributions.py:2619: FutureWarning: `distp
lot` is a deprecated function and will be removed in a future version. Please adapt your code to use either `displot`
(a figure-level function with similar flexibility) or `histplot` (an axes-level function for histograms).
  warnings.warn(msg, FutureWarning)
```

Obtained calculations results:

```
[4]: #to calculate the P90, P50 and P10 values (90%, 50% and 10% probabilities to have the specified volume):

     stoiip_sorted=np.sort(stoiip)
     x10=int(iterations/10*9)
     x50=int(iterations/2)
     x90=int(iterations/10)

     p10=stoiip_sorted[x10]
     p50=stoiip_sorted[x50]
     p90=stoiip_sorted[x90]

     print("P10 value is: ", p10, "thousand tonnes")
     print("P50 value is: ", p50, "thousand tonnes")
     print("P90 value is: ", p90, "thousand tonnes")

     P10 value is:  54058.884550767616 thousand tonnes
     P50 value is:  43353.50243248271 thousand tonnes
     P90 value is:  34911.7684220618 thousand tonnes
```

Appendix 2 Production profiles

Table 12 V1-1 reservoir production characteristics calculation result

Year	q_{oil}, m^3	$Q_{oil\ cumulative}$, m^3	Q_{liquid}, m^3	$Q_{cumulative\ liquid}$, m^3	q_{water}, m^3	$Q_{cumulative\ water}$, m^3	Watercut, %	ORF, %	Total wells
1	560640	560640	560640	560640	0	0	0	0,94496726	2
2	1121280	1681920	1121280	1681920	0	0	0	2,83490178	4
3	1681920	3363840	1681920	3363840	0	0	0	5,66980356	6
4	1873144	5236984	2242560	5606400	369416	369416	16,47	8,82701557	8
5	1955726	7192710	2803200	8409600	847474	1216890	30,23	12,123422	10
6	1633560	8826270	2803200	11212800	1169640	2386530	41,73	14,8768121	10
7	1364464	10190734	2803200	14016000	1438736	3825266	51,32	17,1766368	10
8	1139696	11330430	2803200	16819200	1663504	5488770	59,34	19,0976119	10
9	951954	12282384	2803200	19622400	1851246	7340016	66,04	20,7021452	10
10	795139	13077523	2803200	22425600	2008061	9348077	71,63	22,042364	10
11	664156	13741679	2803200	25228800	2139044	11487121	76,31	23,1618089	10
12	554750	14296428	2803200	28032000	2248450	13735572	80,21	24,0968479	10
13	463366	14759794	2803200	30835200	2339834	16075406	83,47	24,877858	10
14	387036	15146830	2803200	33638400	2416164	18491570	86,19	25,5302126	10
15	323279	15470109	2803200	36441600	2479921	20971491	88,47	26,0751049	10
16	270026	15740135	2803200	39244800	2533174	23504665	90,37	26,5302372	10
17	225544	15965679	2803200	42048000	2577656	26082321	91,95	26,9103957	10
18	188390	16154070	2803200	44851200	2614810	28697130	93,28	27,2279307	10

19	157357	16311427	2803200	47654400	2645843	31342973	94,39	27,4931583	10
20	131436	16442862	2803200	50457600	2671764	34014738	95,31	27,714695	10
21	109784	16552647	2803200	53260800	2693416	36708153	96,08	27,899738	10
22	91699	16644346	2803200	56064000	2711501	39419654	96,73	28,0542989	10
23	76594	16720940	2803200	58867200	2726606	42146260	97,27	28,183399	10
24	63977	16784917	2803200	61670400	2739223	44885483	97,72	28,2912325	10
25	53438	16838354	2803200	64473600	2749762	47635246	98,09	28,3813026	10
26	44635	16882989	2803200	67276800	2758565	50393811	98,41	28,4565354	10
27	37282	16920271	2803200	70080000	2765918	53159729	98,67	28,5193752	10
28	31141	16951412	2803200	72883200	2772059	55931788	98,89	28,5718634	10
29	26011	16977423	2803200	75686400	2777189	58708977	99,07	28,6157052	10
30	21726	16999149	2803200	78489600	2781474	61490451	99,22	28,652325	10
31	18147	17017296	2803200	81292800	2785053	64275504	99,35	28,6829124	10
32	15158	17032454	2803200	84096000	2788042	67063546	99,46	28,7084611	10
33	12661	17045115	2803200	86899200	2790539	69854085	99,55	28,7298012	10
34	10575	17055690	2803200	89702400	2792625	72646710	99,62	28,747626	10
35	8833	17064524	2803200	92505600	2794367	75441076	99,68	28,7625145	10
36	7378	17071902	2803200	95308800	2795822	78236898	99,74	28,7749504	10
37	6163	17078064	2803200	98112000	2797037	81033936	99,78	28,7853377	10
38	5148	17083212	2803200	100915200	2798052	83831988	99,82	28,794014	10
39	4300	17087512	2803200	103718400	2798900	86630888	99,85	28,801261	10
40	3591	17091103	2803200	106521600	2799609	89430497	99,87	28,8073142	10

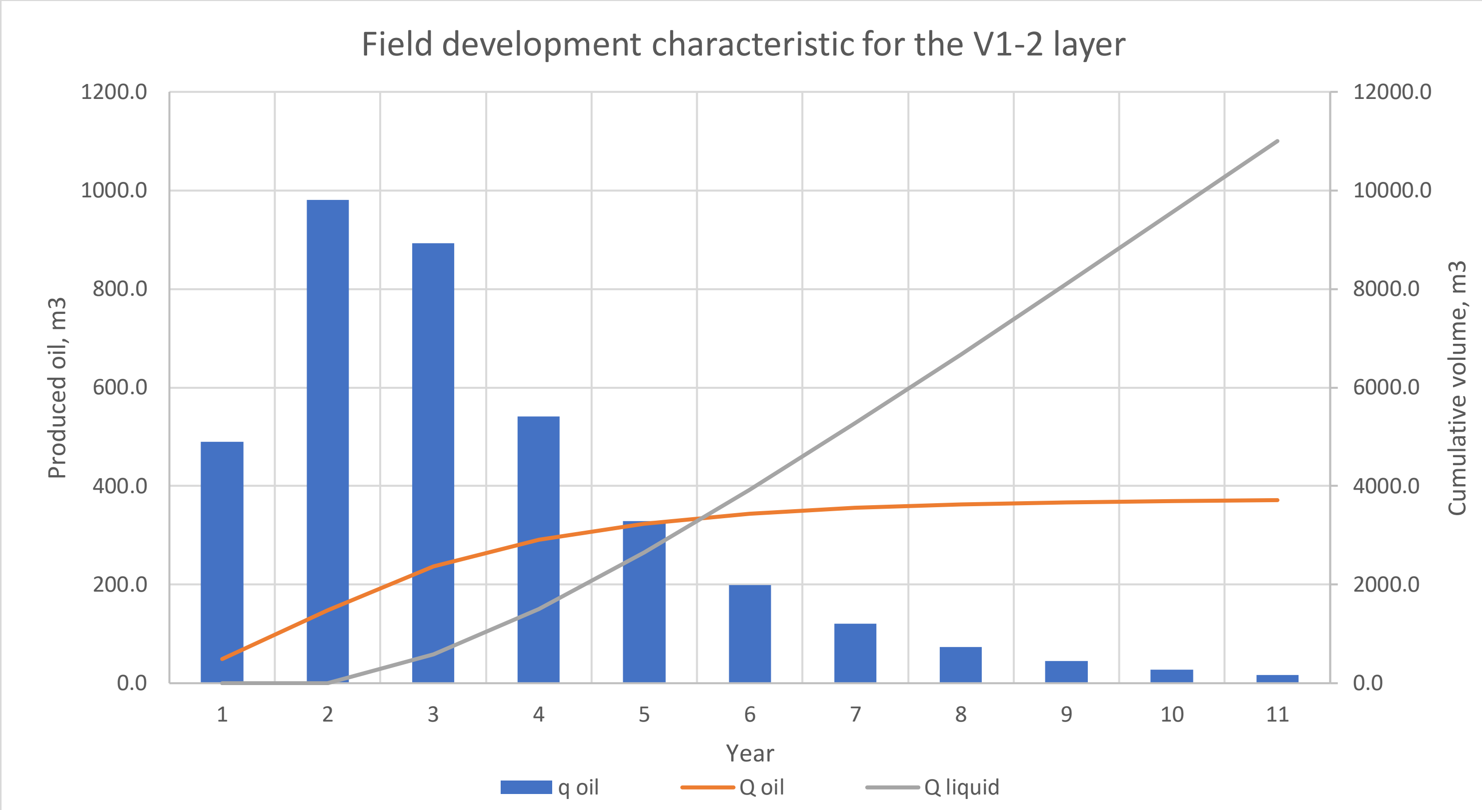

Figure 40 Field development characteristic for the V1-2 layer

Table 13 V1-2 reservoir production characteristics calculation result

Year	q_{oil}, m^3	$Q_{oil\ cumulative}$, m^3	Q_{liquid}, m^3	$Q_{cumulative\ liquid}$, m^3	q_{water}, m^3	$Q_{cumulative\ water}$, m^3	Watercut, %	ORF, %	Total wells
1	490560	490560	490560	490560	0	0	0	3,53855528	2
2	981120	1471680	981120	1471680	0	0	0	10,6156659	4
3	892619	2364299	1471680	2943360	579061	579061	0,393469	17,0543927	6
4	541401	2905700	1471680	4415040	930279	1509340	63,21	20,9596779	6
5	328376	3234076	1471680	5886720	1143304	2652644	77,69	23,3283531	6
6	199170	3433246	1471680	7358400	1272510	3925154	86,47	24,7650273	6
7	120803	3554049	1471680	8830080	1350877	5276031	91,79	25,6364142	6
8	73271	3627320	1471680	10301760	1398409	6674440	95,02	26,1649371	6
9	44441	3671761	1471680	11773440	1427239	8101679	96,98	26,4855024	6
10	26955	3698715	1471680	13245120	1444725	9546405	98,17	26,6799351	6
11	16349	3715064	1471680	14716800	1455331	11001736	98,89	26,7978645	6

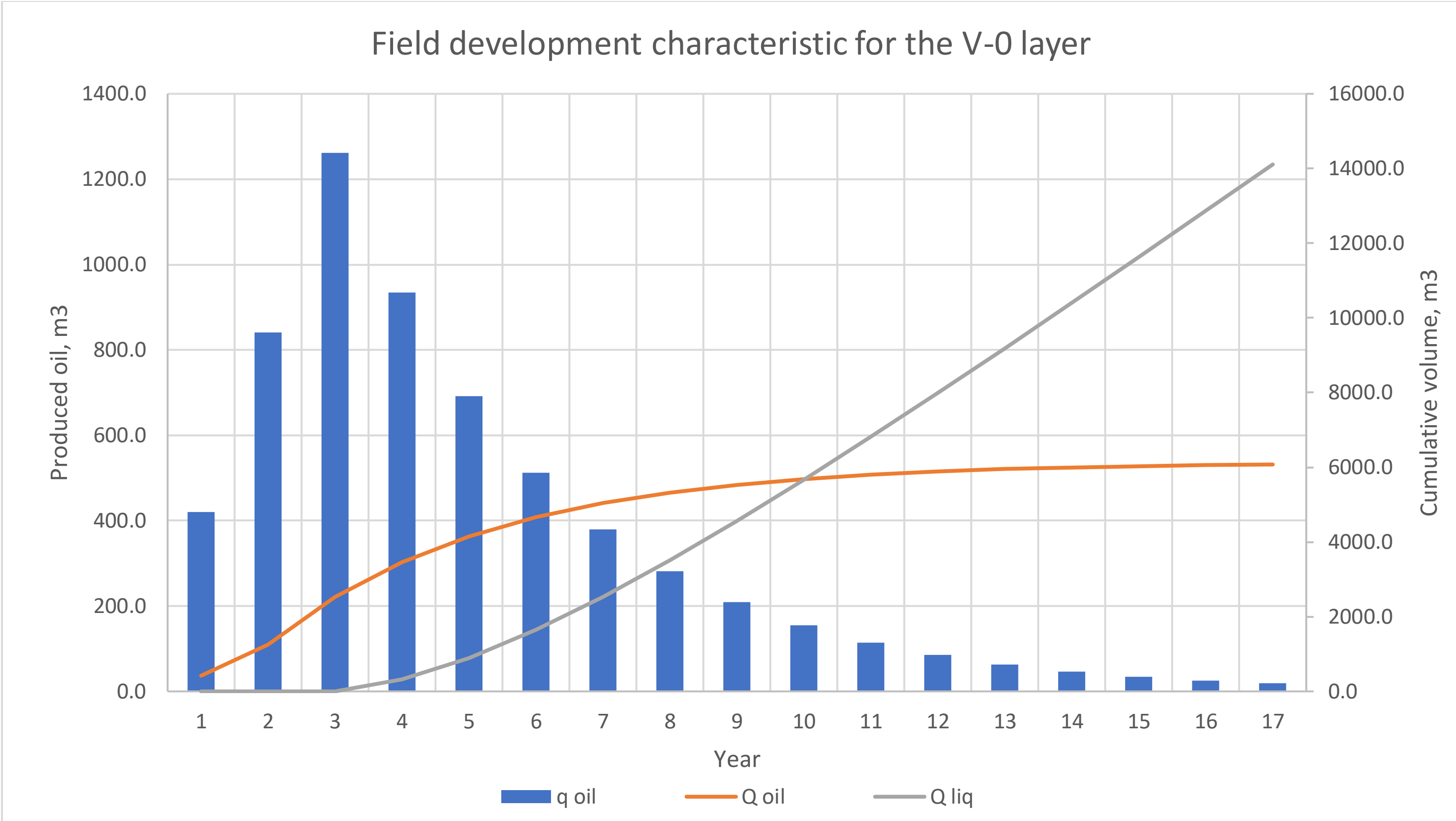

Figure 41 Field development characteristic for the V-0 layer

Table 14 V-0 reservoir production characteristics calculation result

Year	q_{oil}, m^3	$Q_{oil\ cumulative}$, m^3	Q_{liquid}, m^3	$Q_{cumulative\ liquid}$, m^3	q_{water}, m^3	$Q_{cumulative\ water}$, m^3	Watercut, %	ORF, %	Total wells
1	420480	420480	420480	420480	0	0	0	1,23139967	2
2	840960	1261440	840960	1261440	0	0	0	3,69419902	4
3	1261440	2522880	1261440	2522880	0	0	0	7,38839804	6
4	934498	3457378	1261440	3784320	326942	326942	25,92	10,125128	6
5	692293	4149671	1261440	5045760	569147	896089	45,12	12,1525474	6
6	512863	4662534	1261440	6307200	748577	1644666	59,34	13,6544966	6
7	379938	5042472	1261440	7568640	881502	2526168	69,88	14,767168	6
8	281465	5323938	1261440	8830080	979975	3506142	77,69	15,5914552	6
9	208515	5532452	1261440	10091520	1052925	4559068	83,47	16,2021022	6
10	154471	5686924	1261440	11352960	1106969	5666036	87,75	16,6544806	6
11	114435	5801359	1261440	12614400	1147005	6813041	90,93	16,9896108	6
12	84776	5886135	1261440	13875840	1176664	7989705	93,28	17,2378813	6
13	62803	5948938	1261440	15137280	1198637	9188342	95,02	17,4218047	6
14	46526	5995464	1261440	16398720	1214914	10403256	96,31	17,5580584	6
15	34467	6029931	1261440	17660160	1226973	11630229	97,27	17,6589977	6
16	25534	6055465	1261440	18921600	1235906	12866135	97,98	17,7337754	6
17	18916	6074381	1261440	20183040	1242524	14108659	98,50	17,789172	6

Appendix 3 Comparative table of existing concepts

Table 15 Comparative table of development concepts

Platform	Ice conditions	Structure type	Field characteristics	Water depth, m	Distance to shore	Type of hydrocarbon transportation	Mass of the structure, thousand tonnes	Oil volume, mln tonnes	Wells, total	Well length, km	Type of reservoir	Permeability, 10-12 m2
Orlan	one-year ice	Steel-concrete structure of gravity type. The platform consists of four main components: a steel base, a concrete middle section and two steel deck sections. The length of the structure is 96 m, its width is 89.9 m, and the total height of the base is 30 m. The platform belongs to the CIDS type of drilling rig (CIDS - steel-concrete drilling rig on an artificial base). Gravity platform, fountain armature on the platform	Chayvo-Sea field 17.1 million tons of oil and condensate and 9.9 billion m^3 of gas	15	12 km. off the north-eastern coast of Sakhalin Island. Sakhalin	Oil and gas are delivered to the Onshore Processing Facility, Oil is transported by pipeline (226 km)	70	152	20	up to 13	porous type, 23-28%	0,24-0,3
Berkut	one-year ice	The platform consists of 2 parts: the gravity base and the upper structure. The gravity base is a rectangular concrete caisson on which 4 concrete columns are installed to accommodate the upper structure. - Caisson length - over 133 m - width - 100 m - height with columns - about 55 m The upper structure is a huge 6-level structure with integrated technological, drilling, accommodation modules and other structures. Gravity platform, fountain valves on the platform	The Arkutun-Dagi field. Chayvo, Odoptu-Sea and Arkutun-Dagi, with estimated recoverable reserves of 2.3 billion barrels of oil (307 million tons) and 485 billion m^3 of natural gas.	30-40	About 25 km from the coastline, in northeastern Sakhalin, east of Chayvo.	Oil and gas are transported through a new field pipeline to the Chayvo Onshore Processing Facility,	160	114,5	45	up to 7	porous type, 16-30%	0,021–0,84
Piltun-Astokhskaya	one-year ice	consists of a caisson, the center of which is filled with sand, ensuring effective anchoring of the platform on the seabed. The main working areas are enclosed, with temperature control and ventilation. The equipment located outdoors is equipped with icing and low-temperature protection. Base: 111 m x 111 m	Piltun-. Astokhskoye (mainly oil field with associated gas) contains gas - 102.8 billion m^3; oil - 125.2	30	The Piltun-Astokhanskaya-A (Molikpaq) platform is installed at the Astokh area of the Piltun-Astokhskoye	through oil and gas pipelines to the LNG plant in Prigorodnoye. The plant itself is divided into	54	-	13	-	-	-

		Upper structures: 73 m x 73 m. Drilling tower height: 101 m Gravity platform, fountain fittings and separation on the platform	million tons; condensate - 8.3 million tons.		field 16 km offshore	two zones (gas and oil) by the so-called so-called green belt.						
Piltun-Astokhskaya-B		The platform base is a reinforced concrete base of gravity type with four supports, on which the platform topsides with technological facilities are located. The southeast pillar is used as a well site, the northeast pillar is designed for offshore pipeline/pipeline risers with a large radius, and the remaining two pillars are used to install pumps and reservoirs. The platform's upper structures house drilling and liquid hydrocarbon separation equipment, chemical storage, and an accommodation module. Foundation: Height: 53 m Mass: 90,000 tons Dimensions: 94 m x 91.5 m x 11.5 m Support height: 56 m Top structures: Flare tube height: 98.6 m Weight: 28,000 tons	Piltun area of the Piltun-Astokhskoye field	32	The platform is set about 12 km off the north-eastern coast of Sakhalin	-	118	-	-	-	-	-
Lunskaya	one-year ice	The base of the platform is a reinforced concrete base of gravity type with four supports on which the platform topsides with technological equipment and facilities are located. The southeast pillar is used as a well site, the northeast pillar is designed for offshore pipeline/pipeline risers with a large radius rounding, and the remaining two pillars will serve to install pumps and oil transfer tanks. Base: Height: 69.6 m. Weight: 103,000 t Foundation slab: 88 m x 105 m x 13.5 m Support height: 56 m Pillar diameter: 20 m Superstructures	Lunskoye gas field. First-class gas reservoir with a thin oil rim: initial geological reserves of 18.6 trillion cubic feet of gas; balance reserves of marketable oil of 931 million barrels. (130 million tons)	48	Lunskoye-A platform - installed 15 kilometers off the north-eastern coast of Sakhalin Island n	-	124,8	124,4	15	up to 6	-	-

		Mass: 21,800 t Flare pipe height: 105 m Gravity platform, wellheads and primary separation on the platform.										

Appendix 4 Limit Hs calculation

The issue of determining suitable weather conditions was addressed by me as part of a project in the Marine Operations course, the results of which I presented in the 3rd semester of my Master's degree. This section provides a summary of the research carried out. To date, the application of SPS is a technology that allows minimising the capital costs of field development processes. It is suggested to apply this concept to the Triton field development. In general, the field development process is complex and requires a special approach and consideration at each stage. It is important to consider that the subsea template has to be installed on the seabed during marine operations. This type of work is always associated with high risks and uncertainties. Personnel, the environment, the vessel, and the equipment to be installed are the main objects of attention during lifting operations. In order to minimise the risk of loss or damage, it is important to be able to calculate the limit weather conditions in which marine operations can be safely carried out. If the limit conditions are exceeded, the wire on which the IST is lowered may break and the template itself may be damaged by a sudden impact with the waves.

This appendix discusses the limiting approach, which identifies the maximum significant wave height under which a safe installation can be carried out for a given vessel, wire, and template.

Vessel characteristics

The study [76] determined that the recommended vessel is the Akademik Chersky, a crane-laying vessel (KMTUS), which combines the functions of a crane ship and a pipe-laying vessel. It is owned by the Samara Thermal Energy Property Fund. This vessel was used in the installation of an underwater production complex at the Kirinskoye gas condensate field. Launched in China in 2007 at the Jiangsu Hantong Shipyard in Tongzhou, commissioned by the Nigerian-Dutch Sea Trucks Group Limited. The design was developed by the Norwegian company Vik-Sandvik. The vessel was originally named Jascon-18. In June 2011, Jascon-18 arrived at the Kwong-Soon shipyard in Singapore for completion. In December 2015, the ship was purchased by the Singapore branch of the Russian company Mezhregiontruboprovodstroy (MRTS). The company obtained a $1 billion loan from Gazprombank, guaranteed by Gazprom, to purchase the vessel. In January 2016, the ship was seized in Singapore at the request of the shipyard for non-payment of the full construction cost. After the dispute was resolved, the vessel was transferred to Gazprom Fleet LLC in June 2016. [77]

Figure 42 Akademik Chersky installation vessel [77]

Academic Chersky vessel characteristics were used to perform calculations in ORCAFLEX software:

Table 16 Vessel parameters [77]

Vessel characteristics	
Vessel length, m	103
Mass, Te	9017,95
Beam	16
COG x, m	2,53
COG y, m	0
COG z, m	-1,974

For the analysis we need to specify crane tip height placement and remoteness from the vessels board. The last one parameter is determined as a half of templates width, while the crane tip height is set at 19 m height relative zero X and Y axis positions. This data is given in the table 18:

Table 17 Vessel dimensions [77]

Vessel characteristics	
L_1,m	53
L_2,m	50
S,m	12,34
H,m	13,32
R, m	13,5

Where:

L1 – the distance from the back of the vessel to its center, m

L2 – the distance from the front of the vessel to its center, m
S – crane tip height placement (relatively to vessels deck), m
H – vessels height, m
R – distance from the vessels board to the templates center, m

For given RAO vessels data (figure 43) is being exported using ORCAFLEX software. According to the recommendation [78] , vessel heading should be added (22,5° – our case).

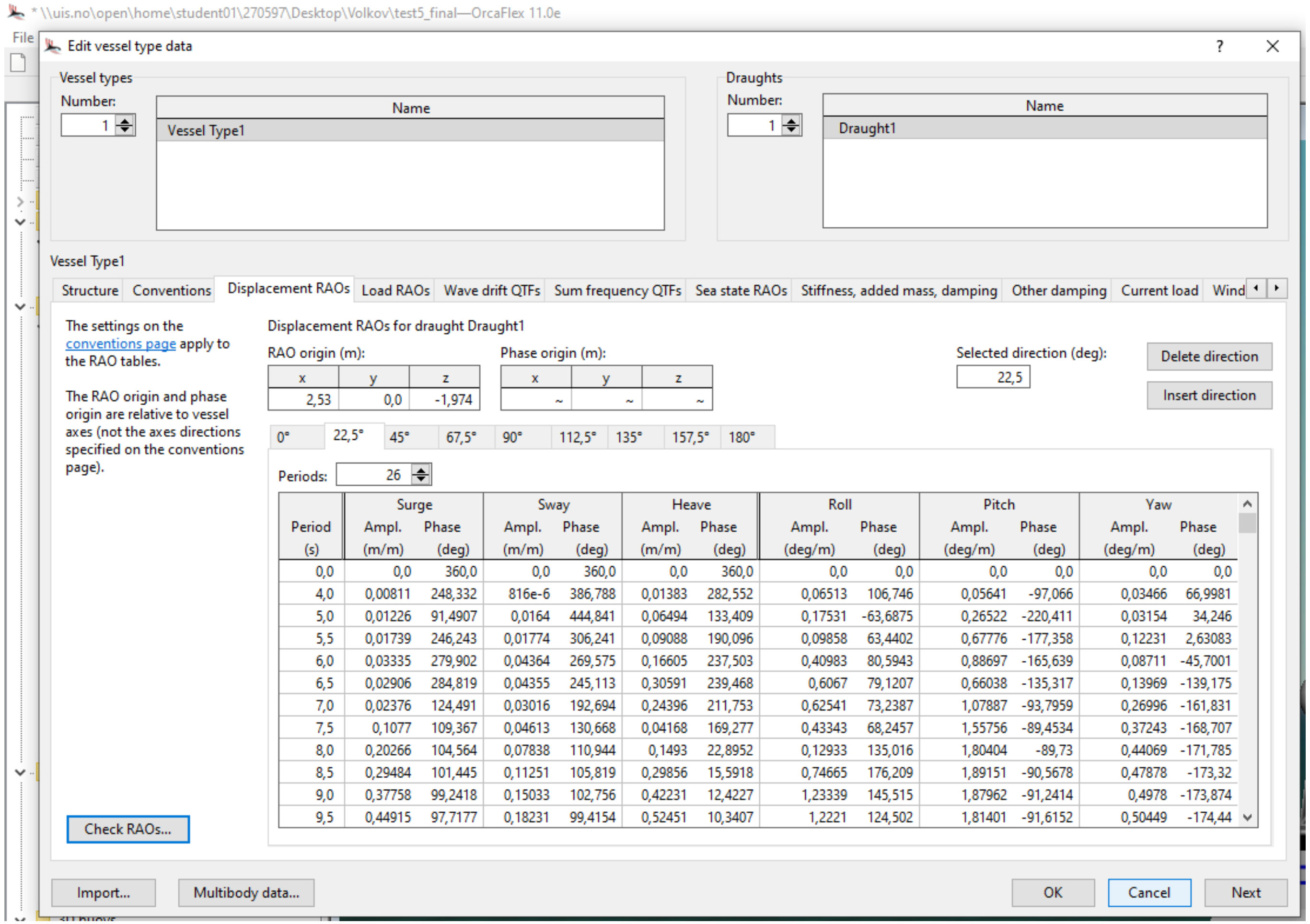

Figure 43 Vessels RAO data generated from ORCAFLEX software [76]

We assume that the crane is fixed at the vessel, so crane motions will coincide with the of the vessels one. On this basis, lets calculate and analyze the crane tip transfer function.

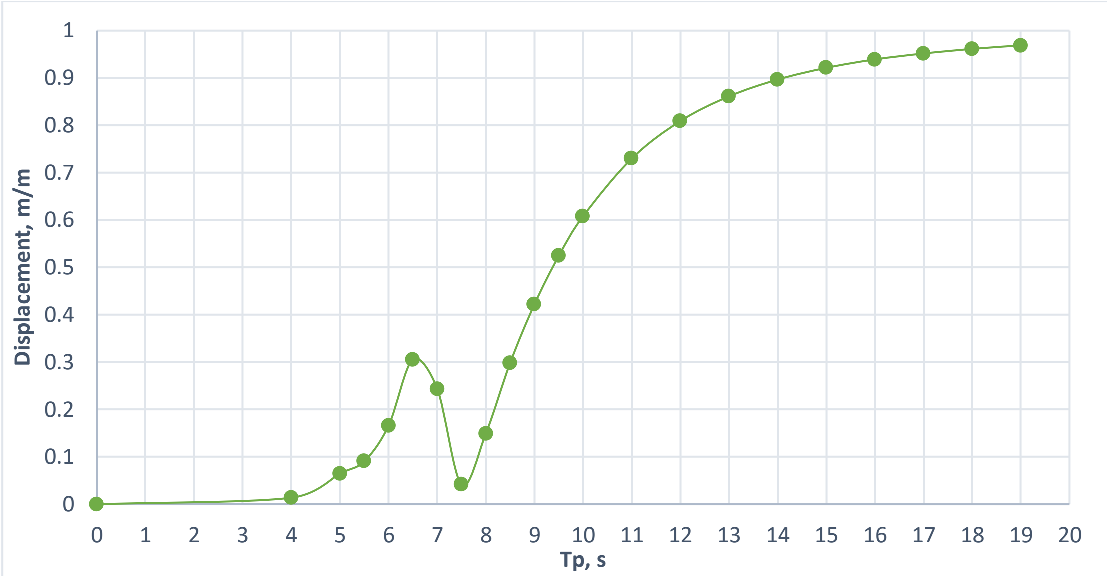

Figure 44 Vessel displacement values for the different T_p [76]

That figure 44 shows how vessel will react to the different waves. From the graph we can conclude that waves with peak period of 5,5 – 7,5 s or less can cause most severe motions and following large loadings, all that can result in large slamming forces. From ORCAFLEX T_p periods corresponding to the certain T_z values could be found:

Table 18 Calculated wave period for corresponding zero up-crossing period [76]

T_z, s	T_p, s
4	5,4
5	6,8
6	8,1

7	9,5
8	10,8
9	12,2
10	13,5
11	14,9
12	16,2
13	17,6

From that table 19 we can conclude that most likely largest crane tip loading could occur at 4–6s zero up-crossing periods that relevant for 5–8 s peak periods range. That is why forces analysis for these period ranges should be provided.

Subsea template

The subsea template model was created in ORCAFLEX software, pipe elements were modeled using lines elements, crane wire connected with four bridles on which template is suspended. The connection between the bridles and the wire is made with 3D buoy. The suction anchors and roof are modeled using 6D buoys elements. Obtained scheme of the modeled is presented in the fig. 45:

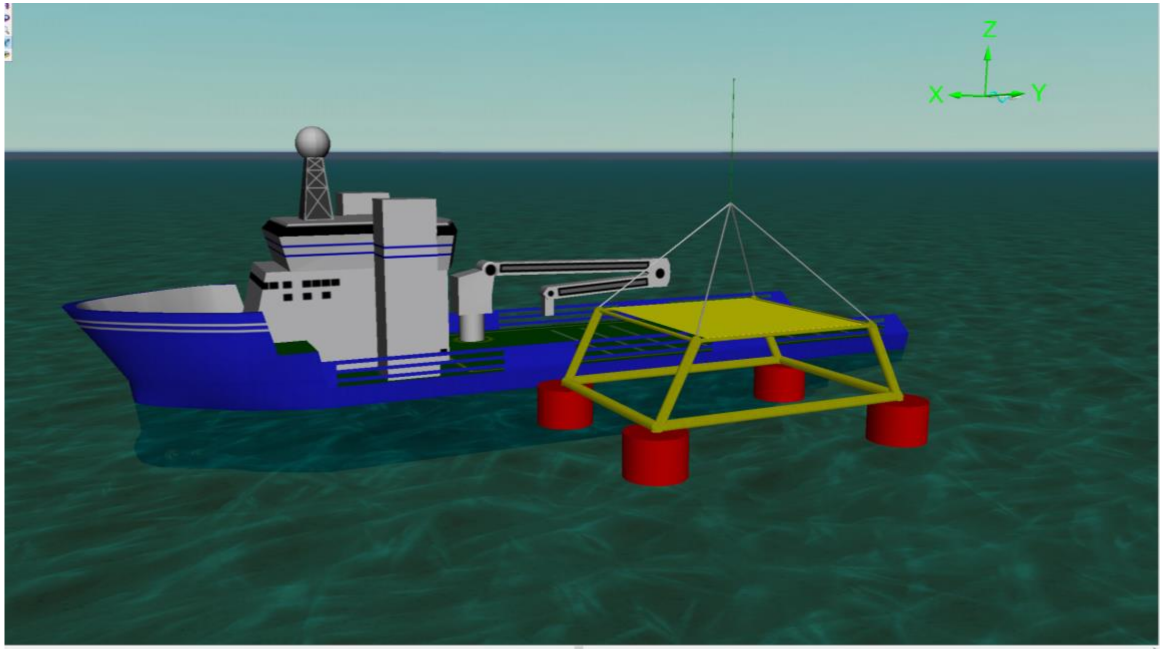

Figure 45 Template layout (the figure is taken from ORCAFLEX software) [76]

The roof and suction anchors are connected with 6D Main buoy, which is suspended by bridles. The frame of the template is represented by steel pipes. Two types of pipes were used in the model: steel tube 1 and steel tube 2. Four steel tube 2 pipes are the base for the roof, which lies on these pipes, the remaining 8 pipes are described by the characteristics of steel tube 1. All characteristics of pipe, roof and anchors material are presented tables 20-23: [79]

Table 19 Steel tube 1 sizes [76]

Steel tube 1	
number of pipes	8
inclined	4
horizontal	4
Length, inclined, m	7,07
Length, horizontal, m	14
D out,m	0,5
D inner,m	0,49
steel density , te/m3	7,85

Table 20 Steel tube 2 sizes [76]

Steel tube 2	
number of pipes:	4
Length, m	10
D out,m	0,2
D inner,m	0,19
steel density , te/m3	7,85

Table 21 Roof (hatch) sizes [76]

Roof	
Width, m	9
Lenth, m	10
Area, m2	90
height, m	0,01
mass, te	7,06

Table 22 Suction anchors sizes [76]

Suction Anchors	
Number of anchors	4
Height, m	2
D out, m	3
D in, m	2,9
Steel density, te/m^3	7,85

Numerical modeling and analysis
Model set up

There are exist several tasks while lifting operation analysis. First one is to provide simulation to determine necessary wire with characteristics that will allow to provide lifting operations in defined sea conditions. In this study we will focus on another task: determining maximum sea parameters (limitations) when safe lifting operations can be provided. Before that convergency study was provided to find optimal time step value. We assume hoisting system capacity is 400Te or 3924 kN. Also, total wire tension should be greater than 10% of static load of the template – 147,15 kN. And we assume that in case wire tension less than that value, we provide safe work and crane – wire system can withstand that load. [80]

Before starting analysis, the model was built and convergency [81] on different time steps and number of elements was checked. Weather input data was taken from whether description part. It should be noted that z coordinate corresponds to the bottom part of the suction anchor, i.e z =0 value means that suction anchors touched water. Wire effective tension was analyzed for different H_s and T_z values.

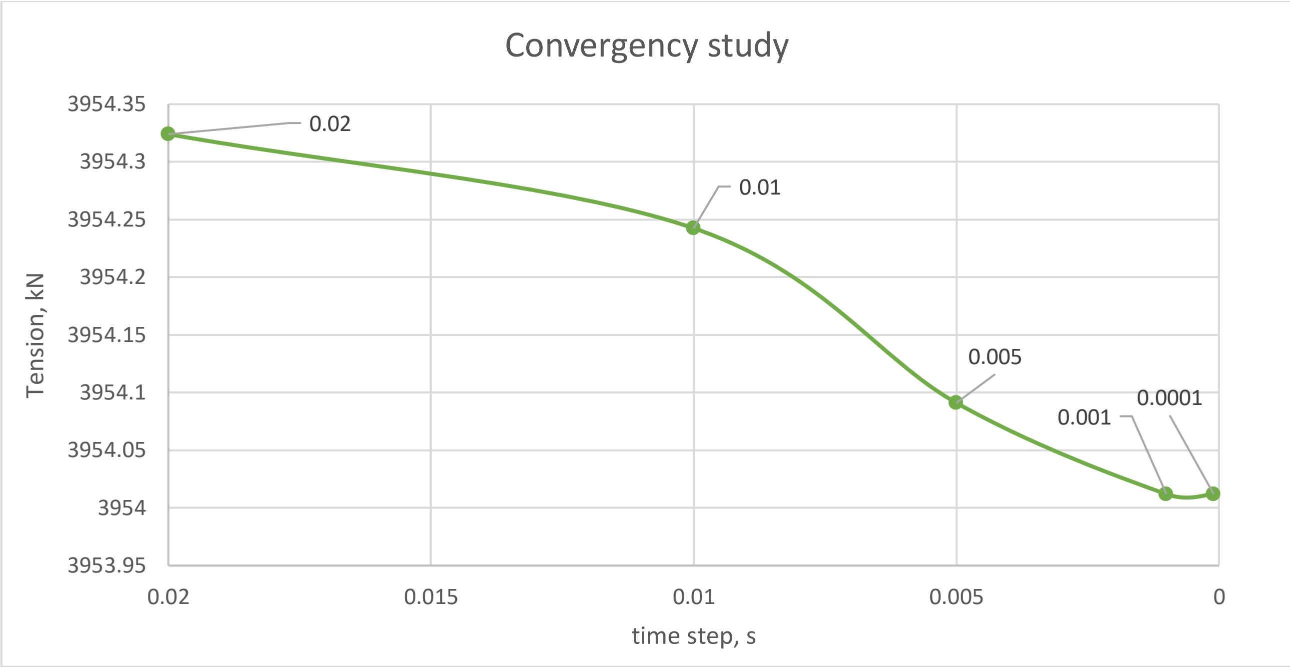

Figure 46 Convergency study on different time steps [76]

The difference between calculated values stops to change from 0,001s time step value (figure 46). For our calculations we use that value, as decreasing time step will not give us more accurate value and with higher time step calculated parameter less accurate value will be obtained. [81]

An example of calculated wire tension is shown on fig. 46.

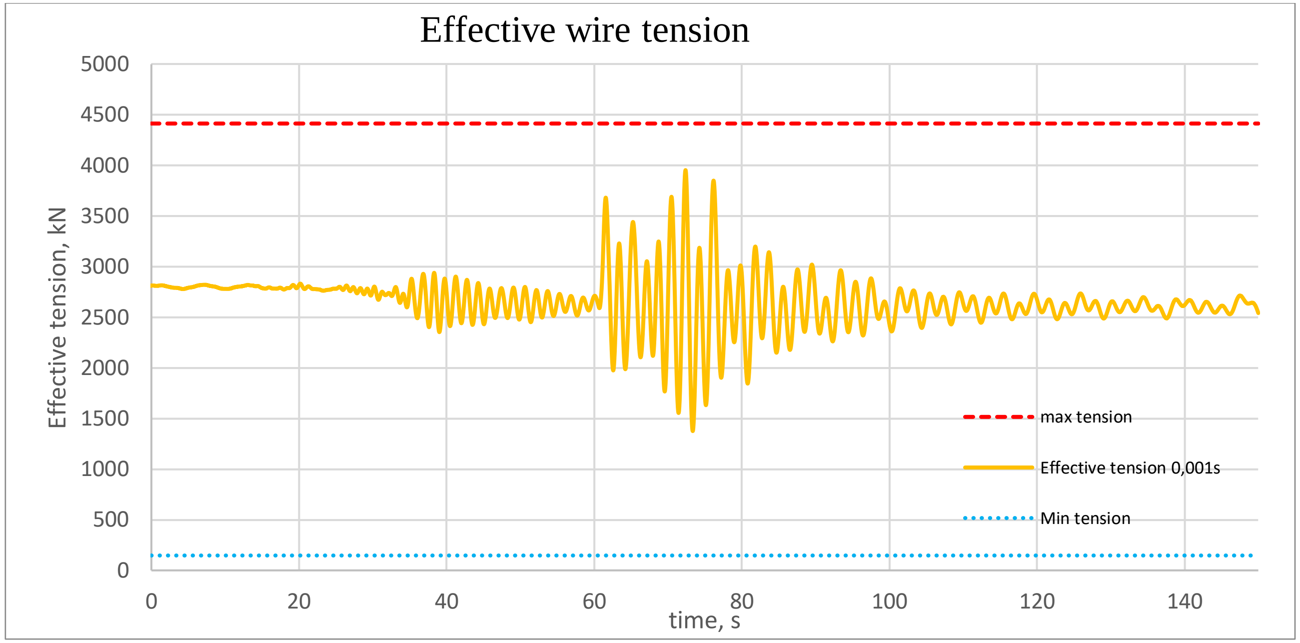

Figure 47 Effective wire tension for Hs=2, Tz = 4 (excel postprocessing) [76]

Minimum and maximum obtained values of effective wire tension are shown in the tables 24-32:

Table 23 Maximum wire tension for Hs = 2s [76]

Hs = 2 s										
Z, m	Tz, s									
	4	5	6	7	8	9	10	11	12	13
2	2821	2857	2849	2839	2832	2830	2817	2830	2831	2836
0	2815	2852	2833	2809	2829	2837	2836	2828	2806	2807
-1	2833	2906	2856	2849	2831	2803	2800	2815	2827	2820
-3	2939	2703	2736	2780	2688	2688	2700	2702	2690	2674
-5	3954	3782	3264	3236	3172	2831	2951	2789	2862	2732
-10	3851	3781	2889	2980	2998	2809	2907	2776	2763	2704
-15	2736	2760	2720	2688	2695	2659	2681	2664	2674	2651

Table 24 Maximum wire tension for Hs = 2,5s [76]

Hs = 2,5										
Z, m	Tz, s									
	4	5	6	7	8	9	10	11	12	13
2	2826	2876	2861	2847	2840	2837	2822	2838	2840	2845
0	2827	2855	2843	2812	2836	2845	2845	2837	2813	2811
-1	2873	2941	2850	2871	2846	2816	2803	2819	2841	2835
-3	3052	2786	2715	2781	2713	2701	2713	2692	2715	2684
-5	4225	4087	3605	3369	3210	2914	2995	2830	2927	2764
-10	4239	3932	3155	3039	3006	2886	2935	2809	2804	2735
-15	2748	2782	2764	2698	2706	2674	2688	2676	2688	2662

Table 25 Maximum wire tension for Hs = 3s [76]

Hs = 3									
Z, m	Tz, s								
	5	6	7	8	9	10	11	12	13
2	2896	2873	2857	2848	2844	2827	2847	2855	2855
0	2900	2852	2816	2843	2851	2855	2847	2820	2820
-1	3038	2903	2891	2863	2828	2807	2827	2852	2852
-3	2938	2827	2802	2736	2727	2731	2701	2717	2717
-5	4279	3808	3518	3249	2988	3007	2865	2800	2800
-10	3735	3348	3100	3019	2934	2940	2834	2763	2763
-15	2809	2805	2709	2722	2682	2689	2688	2671	2671

Table 26 Maximum wire tension for Hs = 3,5s [76]

Hs = 3,5									
Z, m	Tz, s								
	5	6	7	8	9	10	11	12	13
2	2917	2885	2869	2856	2851	2832	2856	2862	2864
0	3037	2882	2821	2849	2859	2865	2860	2826	2832
-1	3200	2919	2908	2881	2841	2811	2835	2877	2869
-3	2990	2849	2821	2759	2753	2760	2713	2733	2738
-5	4481	3965	3537	3345	3066	3007	2904	2994	2831
-10	3746	3509	3092	3038	2973	2929	2861	2861	2791
-15	2841	2839	2723	2740	2689	2701	2702	2711	2680

Further the same analysis for minimum wire tension was provided:

Table 27 Minimum wire tension for Hs = 1,5s [76]

Hs = 1,5 s										
Z, m	Tz, s									
	4	5	6	7	8	9	10	11	12	13
2	2783	2767	2760	2770	2762	2773	2772	2778	2777	2755
0	2778	2756	2769	2763	2766	2793	2796	2778	2781	2759
-1	2751	2735	2742	2738	2751	2754	2758	2755	2751	2753
-3	2432	2571	2578	2531	2601	2632	2600	2598	2619	2599
-5	1551	1697	2294	2187	2195	2498	2366	2515	2432	2438
-10	1755	1437	2384	2344	2242	2419	2342	2450	2496	2473
-15	2479	2488	2539	2536	2531	2557	2544	2558	2563	2548

Table 28 Minimum wire tension for Hs = 2s [76]

Hs = 2 s										
Z, m	Tz, s									
	4	5	6	7	8	9	10	11	12	13
2	2779	2755	2746	2762	2750	2765	2762	2772	2771	2768
0	2774	2729	2757	2751	2757	2792	2794	2772	2774	2778
-1	2737	2696	2718	2715	2741	2743	2750	2748	2739	2776
-3	2354	2553	2565	2511	2575	2615	2588	2597	2610	2636
-5	1376	1588	1858	2094	2134	2474	2319	2475	2369	2497
-10	1633	1196	2139	2294	2200	2378	2293	2397	2461	2521
-15	2481	2470	2519	2520	2525	2548	2534	2545	2551	2566

Table 29 Minimum wire tension for Hs = 2,5s [76]

Hs = 2,5										
Z, m	Tz, s									
	4	5	6	7	8	9	10	11	12	13
2	2774	2742	2731	2755	2737	2757	2753	2764	2765	2762
0	2751	2702	2745	2738	2748	2791	2792	2766	2765	2771
-1	2704	2674	2711	2679	2727	2731	2743	2741	2711	2762
-3	2295	2524	2599	2518	2556	2586	2570	2601	2589	2620
-5	1345	897	1726	1992	2103	2493	2294	2444	2310	2472
-10	1031	1380	2247	2238	2193	2271	2280	2354	2431	2497
-15	2471	2436	2492	2503	2519	2533	2527	2534	2541	2557

Table 30 Minimum wire tension for Hs = 3s [76]

Hs = 3									
Z, m	Tz, s								
	5	6	7	8	9	10	11	12	13
2	2727	2717	2747	2724	2748	2744	2756	2760	2755
0	2655	2731	2725	2739	2789	2790	2761	2756	2759
-1	2552	2653	2642	2712	2719	2734	2733	2702	2753
-3	2298	2522	2511	2558	2567	2546	2582	2611	2599
-5	1215	1665	1870	2051	2426	2288	2416	2279	2438
-10	1577	2025	2164	2188	2203	2286	2317	2411	2473
-15	2400	2463	2484	2510	2523	2522	2523	2534	2548

Table 31 Minimum wire tension for Hs = 3,5s [76]

Hs = 3,5									
Z, m	Tz, s								
	5	6	7	8	9	10	11	12	13
2	2711	2701	2740	2712	2740	2734	2747	2754	2749
0	2480	2712	2710	2729	2786	2787	2757	2745	2745
-1	2350	2647	2621	2697	2708	2725	2716	2698	2750
-3	2272	2484	2494	2553	2547	2514	2579	2606	2586
-5	853	1499	1893	1997	2369	2355	2380	2255	2410
-10	1554	1971	2154	2195	2143	2273	2279	2391	2450
-15	2359	2438	2465	2498	2513	2518	2512	2527	2541

From the presented results it can be concluded that dynamic responses increase with increasing significant wave height value. Tension fluctuations are increasing when suction anchors and roof crosses the water area. At that stage we see correlation between Hs and dynamic response.

Identify limiting conditions for installation

Next, by determining the maximum for each wave height, find the point of intersection with the maximum allowable tension (fig. 48).

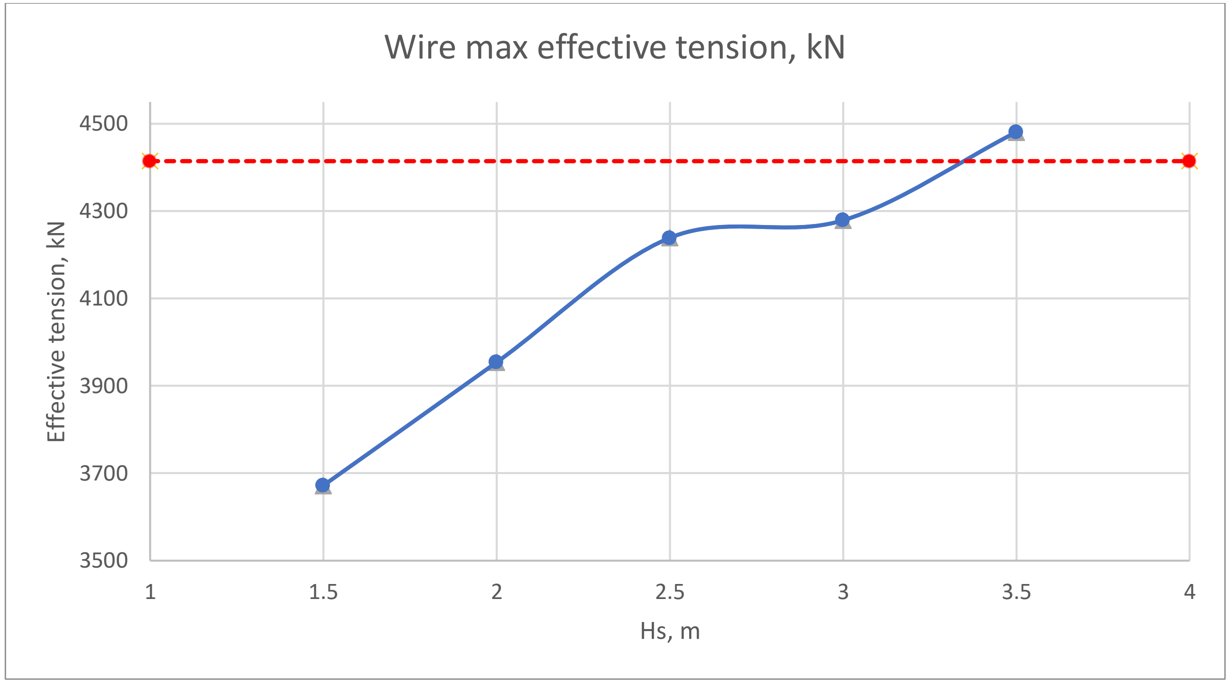

Figure 48 Maximum wire tension for different significant wave heights [76]

Basing on the graph above, it can be concluded that maximum available wave height is 3 m for the lifting operations considered in this study.

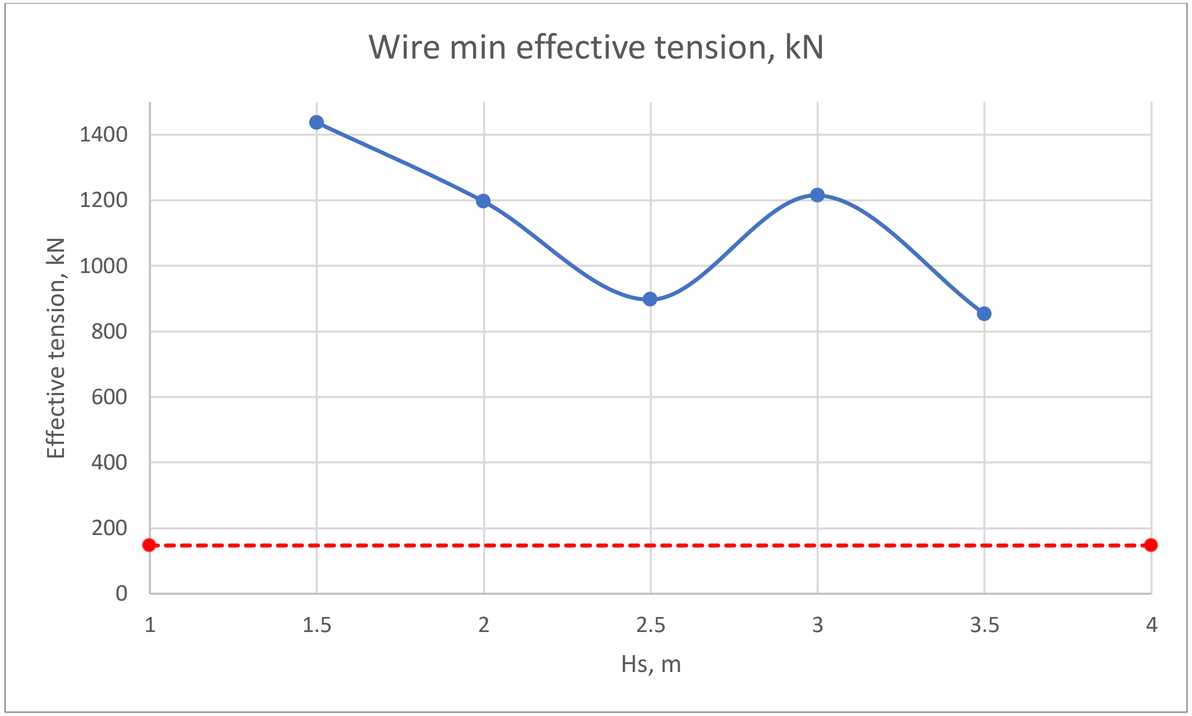

Figure 49 Minimum wire tension for different significant wave heights [76]

As it can be seen from the figure 49, the effective tension of the wire during the lifting operation is always greater than the minimum allowable one. The minimum tension limit has not been reached. That means we have only maximum limit.

Summarizing all the results, we can conclude that maximum allowable wave height at which we can provide safe operation with the given vessel type, wire and template characteristics is H_s=3m.

Appendix summary

This appendix focuses on the crucial task of analysing and identifying critical situations where the template is susceptible to large hydrodynamic forces when crossing the splash zone. Such an analysis plays a key role in ensuring the structural integrity of the template and consequently the safety of lifting operations in the challenging marine environment of the Sea of Okhotsk. By determining the limiting sea states, the company can effectively mitigate the risks and hazards associated with this complex marine operation.

A subsea production system has already been installed offshore in the Sea of Okhotsk. The Sakhalin 3 project is known for being the first to implement this development concept. The severe sea conditions, which can be compared to the conditions of the Arctic region, the presence of ice and currents, confirm the importance of carrying out engineering studies and calculations to determine the allowable conditions in which the vessel with personnel and equipment can successfully and safely carry out the operation.

Th objectives of this study have been successfully achieved and fulfilled. However, it is important to note that the results obtained are approximate, given the assumptions made in the analysis. Nevertheless, it is suggested that the company can rely on these results with confidence, considering the inherent uncertainties of the analysis.